NTNU
Norwegian University of
Science and Technology

Reliability-based Reserve Connections in the Sheringham Shoal Offshore Wind Farm

A Technical-Economical Evaluation of
Increasing the Reliability in an Existing
Offshore Wind Farm

Mari Slettahjell

Master of Energy and Environmental Engineering
Submission date: June 2016
Supervisor: Vijay Vadlamudi, ELKRAFT

Norwegian University of Science and Technology
Department of Electric Power Engineering

Problem Description

This master thesis is developed in cooperation with Statkraft, a leading European company within renewable energy. Statkraft is a significant wind power developer, and has invested in various offshore wind farms in the UK. To improve the power production for these wind farms, the layout of both the turbines and the offshore platforms should be optimized, in addition to the connections between them. In future power systems, reliability will become an important factor, and studies conducted in this area will therefore be of great value.

The aim of this master thesis is to study the benefits of installing reserve connections in the Sheringham Shoal offshore wind farm, located on the east coast of England. Five alternative layouts with reserve connections are introduced and compared with the existing offshore wind farm. A technical-economical evaluation is made on the different alternatives, and the optimal layout is found.

A reliability analysis is conducted in this thesis to find the expected energy delivered to shore in each case. The additional investment cost for the reserve connections will be compared with the potential income generated by the installations, and the profit will be an indicator of how good the investment is. A power flow analysis is conducted to investigate if the reserve connections suggested are feasible, and a sensitivity analysis is carried out to investigate the dependency of the different input parameters.

At the end the optimal layout with or without reserve connections is found, and investment suggestions are made based on the different analyses conducted in this master thesis.

Preface

This master thesis is developed during the 10th semester in the master programme Energy and Environmental Engineering at The Norwegian University of Science and Technology, NTNU. It is written for the Department of Electric Power Engineering in the area of Power Systems.

The purpose of this thesis is to look at the benefits of installing reserve connections in an already existing wind farm. By investing in additional connections between the radials in an offshore wind farm, the system reliability will increase and more power will be delivered to shore during failures in the system. Different alternative layouts are introduced and a technical-economical evaluation is made.

For readers of this master thesis some knowledge in the field of reliability and power systems is recommended, but not necessary. Terms and methodologies will be explained, and examples will be made.

The project is developed in cooperation with the Department of Offshore Wind at Statkraft. I want to thank my supervisors at Statkraft, Sverre S. Gjerde and Karstein Brekke, for all help in developing the project description and collection of data. I also want to thank my supervisor at NTNU, Vijay V. Vadlamudi, for all help and support along the way.

Abstract

Offshore wind has become one of the fastest growing renewable energy sources over the last twenty years. It has the advantage of having great energy generating capabilities, which may be of good value for the energy companies. Due to the constantly increasing power demand, the trend today is towards larger components, more complex control systems and locations further away from shore. As the wind farms are supplying more customers, the need for reliable electrical systems becomes critical. Studies conducted in the area of offshore wind and reliability may therefore be very interesting.

In this master thesis, five layouts with reserve connections have been compared with an existing offshore wind farm, Sheringham Shoal, located on the east coast of England. The wind farm is installed with 88 turbines and has a total capacity of 316.8 MW. It has two export cables connected to different offshore substation platforms, each at 132 kV, and several inter array cables at 33 kV. No reserve connections between the radials are installed, and the benefits of investing in such connections are therefore investigated.

A reliability analysis is conducted to find the expected power delivery for each layout. The Relrad methodology is introduced and discussed, and used to find the energy not delivered to shore and the annual system availability index for the layouts. In reliability analyses done for regular distribution systems, the energy not supplied (ENS) to the load points is found. This index would have to be modified, due to the consideration of the load points in this master thesis, looking at each turbine as a negative load point consuming negative power. To fit the wind system analyzed, the previous index is modified and set to energy not delivered (END) from the load points. In addition to the reliability analysis, a power flow analysis is carried out to investigate if the power flows occurring during failures are manageable. If the power is exceeding the cable capacity, actions have to be taken if the reserve connections are to be installed. To find the most profitable reserve connection investments, an economic analysis is also conducted. The potential income from the saved energy is compared with the additional investment cost,

and a profit for each layout is calculated.

The result shows that for the three first layouts analyzed (Layout 1-3), the expected energy delivered to shore has increased compared with the radial system, and the profits are positive. The two remaining layouts (Layout 4 and 5) have a significant increase in the expected energy delivered to shore compared with all previous layouts, and are much more reliable. Layout 4 however, is discarded as a result of the power flow analysis and Layout 5 has, as for now, a negative profit. The sensitivity analysis shows that the results are very much depending on the failure rates and repair times given to the reliability analysis, in addition to the energy price used in the economic analysis.

Layout 2, with four reserve connections installed, is found to be the best layout of the ones analyzed in this master thesis. In this layout, the reliability has increased and the profits are high, and is proven to be a good alternative for the existing Sheringham Shoal. In addition to investing in reserve connections, a control system should be installed to prevent the power flow from exceeding the cable capacity. The reliability analysis do also show that in future systems, a connection between the two offshore platforms should be considered because of the significant reduction of energy not delivered to shore. If the energy price increases both Layout 1 and 5 becomes more profitable, and are therefore good alternatives to the one suggested in the Sheringham Shoal offshore wind farm.

Sammendrag

Havvind har i løpet av de siste tyve årene utviklet seg til å bli en av de raskest voksende fornybare energikildene. En stor fordel med havvind er at den har betydelig potensiale når det kommer til generering av energi, noe som kan være av stor verdi for de forskjellige energiselskapene. På grunn av et konstant voksende energibehov i verden i dag, går trenden mot større komponenter, mer komplekse kontrollsystemer og beliggenheter lengre ut i havet. Siden vindparkene stadig leverer energi til flere kunder, er behovet for pålitelige kraftsystemer spesielt viktig. Studier gjort på havvind og pålitelighet vil derfor være av stor interesse i framtiden.

I denne masteroppgaven er fem forskjellige kabellayouter med reservekoblinger sammenlignet med en eksisterende havvindpark, Sheringham Shoal, som ligger på østkysten av England. Vindparken er installert med 88 turbiner, og har en total kapasitet på 316.8 MW. Den har to eksportkabler koblet til to forskjellige offshore plattformer, hver av dem på 132 kV, og flere inter array kabler på 33 kV. Det eksisterende systemet har ingen reservekoblinger mellom radialene, og fordelene ved å installere slike koblinger er derfor undersøkt.

For å finne forventet levert effekt til land for hver av layoutene er en pålitelighetsanalyse gjennomført. Relrad-metoden er introdusert og diskutert, og brukt til å finne "energy not delivered" og "annual system availability index". I pålitelighetsanalyser gjort på vanlige distribusjonssystem, er "energy not supplied" (ENS) for hvert lastpunkt funnet. På grunn av lastpunktbetraktningen gjort i denne masteroppgaven, ved å se på turbinene som negative lastpunkt, er denne indeksen modifisert til å passe vindparksystemet i dette prosjektet. Indeksen er derfor endret til "Energy not delivered" (END) fra lastpunktene. I tillegg til pålitelighetsanalysen, er det gjort en lastflytanalyse for å undersøke om lastflyten som oppstår under en feil er håndterbar. Hvis effekten i kablene er høyere enn kapasiteten må tiltak bli iverksatt for at reservekablene skal kunne bli installert. For å finne den mest økonomiske layouten er det også gjennomført en økonomisk analyse. Den potensielle inntekten fra den sparte energien i hver layout er sammenlignet med de ekstra kostnadene for reservekablene, og profitten for hver layout er beregnet.

Resultatene viser at for de tre første layoutene analysert (Layout 1-3), har mengden energi levert til land økt og profitten er positiv. De to siste layoutene (Layout 4 og 5) har en signifikant økning i energien levert til land sammenlignet med alle tidligere layout, og er mye mer pålitelig. Layout 4 er derimot forkastet på bakgrunn av resultatene i lastflytanalysen og Layout 5 har en negativ profitt. Sensitivitetsanalysen viser at resultatene er veldig avhengig av feilratene og reparasjonstidene gitt til pålitelighetsanalysen, i tillegg til kraftprisen brukt i den økonomiske analysen.

Layout 2, med sine fire reservekabler installert, er funnet til å være den beste layouten av systemene analysert i denne masteroppgaven. I denne layouten har påliteligheten økt og profitten er høy, og er et godt alternativ for den eksisterende Sheringham Shoal. I tillegg til investering av reservekabler, bør det også installeres et kontrollsystem for å forhindre at lasten overstiger kapasiteten i kablene. Pålitelighetsanalysen viser også at i framtidige systemer bør det vurderes å installere en kobling mellom de to offshore plattformene, på grunn av den store økningen i energi levert til land. Hvis kraftprisen øker, får både Layout 1 og 5 en mye høyere profitt, og er derfor gode alternativer til layouten foreslått brukt i Sheringham Shoal.

Contents

List of Abbreviations

AC	Alternating Current
DC	Direct Current
EWEA	European Wind Energy Association
OSP	Offshore Substation Platform
PCC	Point of Common Connection
OWF	Offshore Wind Farm
LV	Low Voltage
HV	High Voltage
HVAC	High Voltage Alternating Current
HVDC	High Voltage Direct Current
MV	Medium Voltage
MVAC	Medium Voltage Alternating Current
XLPE	Cross-Linked Poly-Ethylene
LCC	Line Commutated Converter
VSC	Voltage Source Converter
IA	Inter Array
WTG	Wind Turbine Generator
DFIG	Doubly Fed Induction Generator
PMSG	Permanent Magnet Synchronous Generator
CB	Circuit Breaker
DS	Disconnector Switch
RS	Reconfiguration Switch
MTTR	Mean Time To Repair
U	Unavailability
ENS	Energy Not Supplied
END	Energy Not Delivered
ASAI	Annual System Availability Index

List of Figures

List of Tables

Chapter 1

Introduction

Offshore wind has become one of the fastest growing renewable energy technologies over the last twenty years [6]. Since 2008, the UK has been the world leading country in offshore wind, with as much installed capacity as the rest of the world combined. By 2016, there will be around 6 GW capacity installed, and 10 GW by 2020. Offshore wind will then supply 8-10 % of the annual UK electricity [7]. Sheringham Shoal, located on the east coast of England, is supplying around 220,000 homes with clean energy [8] each year, and is used as a Base Case in this project.

Compared with onshore, offshore wind provides larger energy generating capability due to better wind resources. There is a trend towards larger components and more complex systems with future wind farm capacities above 1 GW. At the same time, the need for lower cost is significant, and a reduction in both installation and lifetime costs are desirable. To make offshore wind a good alternative for renewable power production the wind farm layout have to be optimized, and already existing layouts should be improved by installing reserve connections.

Various wind farm topologies have been proposed in studies with the intension of improving the reliability in the system. Earlier studies have investigated both the use of AC and DC, and introduced various topologies, both radial and ring structures. Various factors should be included in the analyses, such as power transfer between turbines, optimal redundancy and power production. For now, there is not an exact answer on how a park layout should be presented and this area is therefore an interesting study.

In this master thesis, the installation of reserve connections is investigated. These investments are done to increase the system reliability, and to facilitate a secure and maintainable power delivery to shore. The existing system in the Sheringham

Shoal offshore wind farm is used as a base case, and five layouts are chosen as alternatives to the already operational wind farm. The alternative layouts all have reserve connections installed, arranged in different structures. Both connections between inter array cables and offshore platforms are investigated. A reliability analysis and an economic analysis is done, in addition to a power flow analysis to see if the reserve connections are feasible. At the end, the most beneficial layout is chosen, having both Sheringham Shoal and a general perspective in mind.

Chapter 2

The Literature Study

Due to many previous studies on the subject of offshore wind and reliability, a literature study was conducted to get an idea of what already have been done in earlier projects and what should be done in this master thesis. Several studies have been especially helpful, and given insight to offshore wind, power system reliability, power flow problems and economics. These studies are introduced in this chapter.

The two master theses *"Impacts of Interconnecting the Wind Farm Projects Within the Dogger Bank Zone"* [9] and *"Optimal redundans i Dogger Bank referansevindpark"* [10], written by S. Veila and K. Vingdal respectively, have been very helpful in the area of power system reliability. In these projects several important principles are discussed, for both offshore wind and reliability. [10] is also used when discussing the importance of load point considerations in Chapter 4 in this master thesis. Other studies used as good sources in the area of offshore wind reliability are *"Comparison of Wind Farm Topologies for Offshore Applications"* [5] written by H. J. Bahirat, B. A. Mork and H. K. Hoidalen and *"Reliability Assessment of DC Wind Farms"* [11] written by H. J. Bahirat, G. H. Kjolle, B. A. Mork and H. K. Hoidalen. Both publications make use of the same methodology for calculating the reliability in offshore wind farms, which also is one of the methodologies considered in Chapter 4 in this thesis. They also give good presentations of important principles used in the reliability calculations. The book *"Reliability Evaluation of Power Systems"* [4] written by R. Billinton and R. N. Allan is also used to get insight in the field of power system reliability. General principles in an offshore wind farm and its various components are introduced in *"Offshore Wind Energy Generation: Control, Protection, and Integration to Electrical Systems"* [1] written by O. Anaya-Lara, D. Champos-Gaona, E. L. Moreno-Goytia and G. P. Adam. To understand the Relrad methodology used in this thesis, lectures at NTNU have

been helpful, especially in the course ET8207 Power System Reliability, in addition to the publication *"Relrad - an Analytical Approach for Distribution System Reliability Assessment"* [12] written by G. Kjolle and K. Sand.

To learn more about power flow and power flow problems the *"Matpower 5.1 User's Manual"* [13] written by R. D Zimmerman and C. E. Murillo-Sánchez is used for both information about basic power flow principles and the methodology used in the Matpower program. The writer of this master thesis also have a lot of knowledge about power flow calculations from various courses at NTNU, such as TET4115 Power System Analysis and ELK-16 Advanced Power Systems. For the cost calculations the methodology presented in *"Reliability Study - Analysis of Electrical Systems within Offshore Wind Parks"* [14], an Elforsk report from 2007, is used due to its simplicity and straight forwardness. Also cost methodologies introduced in *"Optimal Design of an Offshore Wind Farm"* [15] written by M. Nandigam and S. K. Dhali and the methodologies used in the master theses mentioned above were considered, but not implemented.

Much of the data used for the Sheringham Shoal offshore wind farm is obtained from both the LORC Knowledge website [3] and the 4Coffshore website [16]. Typical cable and cost data is also retrieved from internal databases in Statkraft.

Chapter 3

Offshore Wind

In this chapter, the main features of offshore wind is discussed. A general offshore wind system with all its components is introduced, and general principles are explained. The existing offshore wind farm used in this master thesis, Sheringham Shoal, is also presented and the Base Case layout is shown. At the end the Weibull probability distribution is introduced, used to find wind speed probabilities.

3.1 Offshore Wind Energy Systems

Wind energy has become one of the fastest growing renewable energy technologies over the last twenty years [6], going from turbines producing only a couple of tens of kW to several MW per unit. The European Wind Energy Association (EWEA) predict a doubled installed total wind power capacity in the EU by 2030 [17], and with these large investments in new installments, the need for reliable and secure electrical systems becomes critical.

With several restrictions preventing the construction of new wind farms onshore, offshore wind farms have become more attractive. Today, the trend is towards larger turbines, more complex power electronics and locations further away from shore, making the power production more exposed than onshore wind farms. Therefore, new technologies are constantly under research and are being developed, making the installations more reliable and cost effective.

Of the 8,759 MW installed in the world in 2014, over 90 % of the capacity was located in northern Europe, in the North, Baltic and Irish Seas [18]. The reason for this is the good conditions for offshore wind in this area, namely large wind resources and suitable water depths. A schematic of the typical components in an

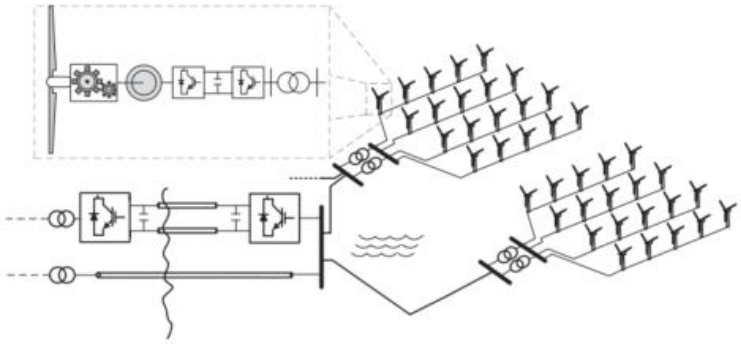

Figure 3.1: The offshore wind energy system [1].

offshore wind farm is illustrated in Figure 3.1, and each part of the system will be introduced and discussed in this section.

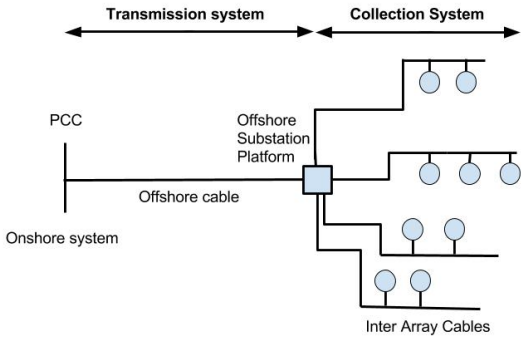

Figure 3.2: The transmission and the collection system in an offshore wind farm.

A typical electrical offshore wind system is divided into two sections, as shown in Figure 3.2, the transmission and the collection system. In the transmission system, the power coming from the wind turbines is transferred from an offshore substation platform (OSP) to a point of common connection (PCC) onshore. The power is carried through large high voltage (HV) offshore submarine cables, at a voltage level ranging from 130-400 kV [19]. Many offshore wind farms (OWFs) are built with HVAC connections to shore, transferring the power through three XLPE submarine cables, as illustrated in Figure 3.3. However, as the distance to shore increases the electrical losses also increase and the transmission gets limited due to the reactive power being generated in the cables, which is increasing with the cable length and the square of the voltage [19]. To have enough transferring capability to carry the power through long distances, reactive power compensation units have to be installed, which is difficult and may be expensive when using submarine cables.

Also, in offshore applications, compensation can only be installed at the end of each line, which will have limited effect on the transmission.

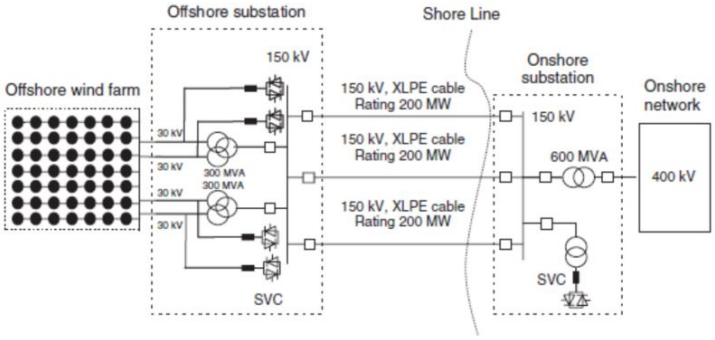

Figure 3.3: Basic configuration of an offshore wind farm with a HVAC connection to shore [2].

Another solution more suited for future wind farms is therefore the use of HVDC cables, installed with either Line Commutated Converter (LCC) or Voltage Source Converter (VSC). The HVDC LCC solution has been used for power transmission for a long time, but may not be suitable for offshore applications due to its large size and poor performance when connected to a weak AC grid [19]. The HVDC VSC solution however is more compact and suitable for offshore wind farms, and is not dependent on the distance to shore as the HVAC cables are. It consists of two converter stations (offshore and onshore) and two polymeric extruded cables [19], and is illustrated in Figure 3.4 . This system is more voltage and frequency stable compared to the LCC solution, due to independent control of reactive and active power, and is the most attractive transmission technology for future offshore wind farms. In Figure 3.5, an overview of the different choices of transmission technologies are shown. As the figure illustrates: HVDC is used for longer distances, while HVAC is limited by distance and voltage level.

In the collection system, also called the inter-array system (IA system), power is transferred from each individual wind turbine to the OSP. The typical voltage level is 25 - 40 kV [20], but a 66 kV voltage level is proposed in several studies. The work done in [21] shows that higher voltage levels in the inter-array system will lead to cost reductions and a higher yield, and are solutions that should be included in future systems. The power in the collection system is typically transferred through medium voltage (MV) AC cables, but DC transmission is also possible. The DC collection grid has several advantages, such as increased efficiency and reduction of size and weight of components [22], but the technology is still not sufficiently developed, and no OWF is built with a DC collection grid at this time. The grid can have various layouts, and an optimal solution should be found with

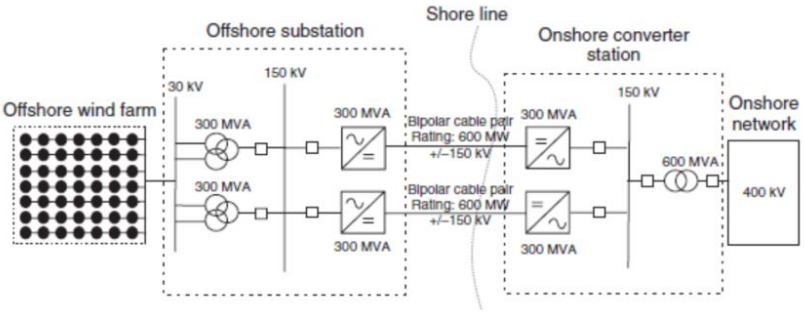

Figure 3.4: Basic configuration of an offshore wind farm with a HVDC VSC connection to shore [2].

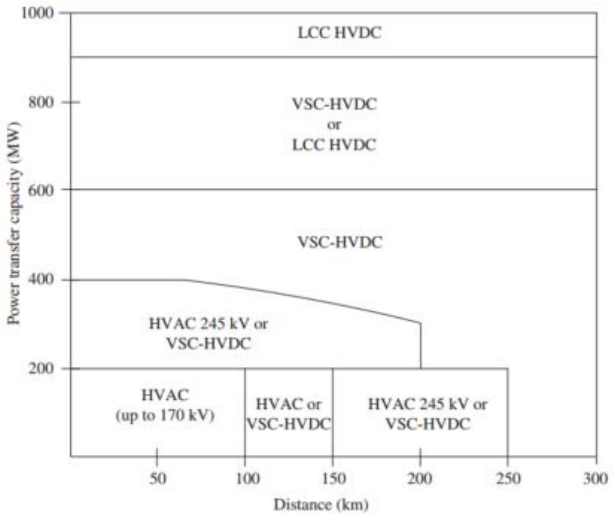

Figure 3.5: An overview of the different transmission technologies used for various distances [1].

respect to available technology, cost and reliability. The radial IA system is the one commonly used, mainly due to the simplicity of the system, and is the one used in Figure 3.1. When planning an OWF, alternative systems with higher complexity and redundancy should be considered as possible solutions, to increase the power delivered to shore.

The offshore substation platform connects the transmission and the collection system, and reduces the power losses in the system. It is the largest construction in the OWF and many important components are installed, such as switchgears, transformers, converters, emergency diesel generators and j-tubes [23]. The MV power coming from the collection system is at this platform stepped up to a higher

voltage level to ensure lowest possible electrical losses in the transmission to shore. In an AC/DC OWF (MVAC collection system and HVDC transmission), the power is also converted from AC to DC at this platform, which is not necessary in an AC/AC OWF.

In the wind turbine, the most important component is the wind turbine generator (WTG). This generator can have various power ratings, in offshore wind ranging from a couple of MW to 7 MW [24]. It is important to remember that wind is a very unstable source of energy, and the annual average production level is commonly as low as 40 % of the installed capacity [14]. It is therefore important to have an optimal design of the wind turbine generator, making it possible to maximize the energy capture by controlling and limiting the mechanical power for different wind speeds. There are various generators used to convert wind energy to electricity today, with the doubly fed induction generator (DFIG) and the permanent magnet synchronous generator (PMSG) being most attractive. These are variable speed wind turbine generators, designed to achieve maximum aerodynamic efficiency over a wide range of wind speeds [6]. The two generators are continuously adapting the rotational speed to the wind speed, keeping the tip speed ratio constant. The generator torque is then kept nearly constant and the mechanical stress is reduced. Other advantages are the high level of controllability and the increased power capture.

In addition to the generator, the wind turbine also consist of other important components, such as the gearbox, shaft, yaw, pitch drive and control unit. These are all installed inside the nacelle and are working towards a more efficient utilization of the wind power, and a larger power production. Also installed in the turbine tower, but not inside the nacelle, is the step-up transformer. This transformer is connected to the WTG, stepping up the voltage from around 0.5-1 kV to the collection system voltage at 25-40 kV.

To optimize the output from an OWF, a protection system has to be installed to protect and isolate faulty components. Protection technology has to be installed at every wind turbine and coordinated over the whole wind farm, for a secure and reliable system operation [1]. Common components used in offshore wind are the circuit breaker (CB) and the disconnector switch (DS). A reconfiguration switch (RS) may also be installed and used to connect reserve connections when needed. All these components facilitate a more secure and reliable operation of the wind farm, protecting each component from high fault currents.

3.2 Sheringham Shoal

The Sheringham Shoal offshore wind farm is in this thesis used to investigate different inter array topologies, and the benefit of installing reserve connections. Sheringham Shoal is an operating wind farm, and the existing layout is therefore used as a base case in this master thesis. Different systems with reserve connections connected to the existing layout is compared with the Base Case, and an optimal topology is found with respect to the reliability and cost.

Sheringham Shoal is an offshore wind farm located on the east coast of England, with an installed capacity of 316.8 MW. It is operated by Scira Offshore Energy, which is owned by Statkraft (40 %), Statoil (40 %) and the UK Green Investment Bank (20 %). The wind farm consists of 88 turbines, each at 3.6 MW, and have an estimated production of 1100 GWh/year. The turbines are installed 17-23 kilometers from shore, and an illustration of the wind farm is shown in Figure 3.6.

The wind farm has two offshore export cables connected to each offshore substation, one at 23 km and one at 21 km. The cables are 145 kV XLPE cables and the transmission type is HVAC operating at 132 kV. The 88 turbines are connected in 12 radials from the offshore substation platforms, four with 8 turbines and eight with 7 turbines. An illustration of the IA cable system is shown in Figure 3.7. The IA cables are 36 kV XLPE cables operated at 33 kV, and the transmission type is MVAC.

The wind turbine generators are manufactured by Siemens and are rated 3.6 MW. The power output from the turbines vary however with the wind speeds, as shown in the power curve in Figure 3.8. The complete power curve data for

Figure 3.6: Sheringham Shoal, located on the east coast of England [3].

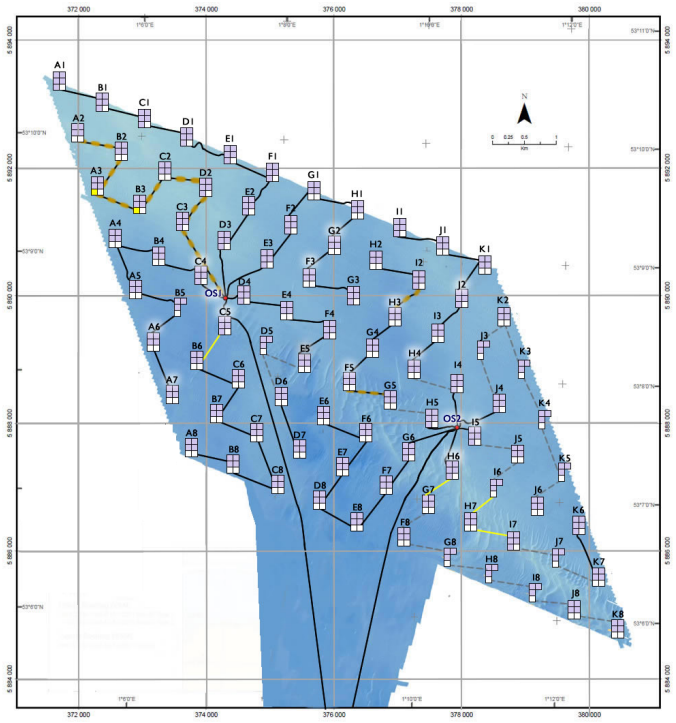

Figure 3.7: Illustration of the Sheringham Shoal inter-array layout [3].

this turbine model is shown in Appendix A. The cut-in speed for each turbine is 4 m/s, the cut-out speed is 25 m/s and the rated speed is 13.5 m/s. At the rated speed the power production is at its maximum, and the production is kept constant for higher wind speeds until the cut-off speed.

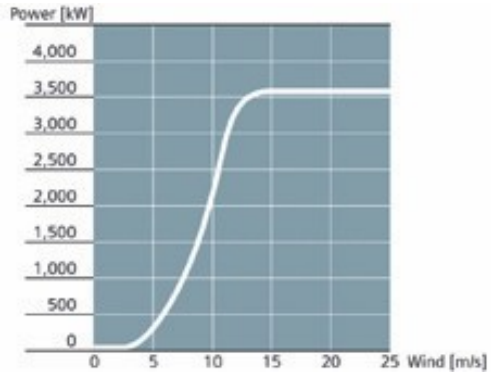

Figure 3.8: The power curve for the Siemens wind power turbine [3].

The construction work for the Sheringham Shoal wind farm started in 2009 and the first power generation was in 2011. Today the wind farm is fully operational,

and is supplying the National Grid in the UK annually with enough power for 220,000 homes [8]. The estimated total project cost was 1,287 million £ [3].

3.3 The Weibull Distribution

A probability curve has to be decided in order to find the probability of different wind speeds in the wind farm, due to the instability and variance of wind as an energy source. By using this probability in conjunction with the power curve for the wind turbine generators, illustrated in Figure 3.8, an estimated power output from the turbines may be found.

A distribution that gives a good fit to typical wind data, is the Weibull distribution. Its probability density function is shown in Equation 3.1 and the cumulative distribution function in Equation 3.2. The Weibull distribution takes in two parameters; the scale parameter, c, and the shape parameter, k. The scale parameter is measured in m/s and is proportional to the mean wind speed [25]. The shape parameter specifies the shape of the distribution and is chosen between 1 and 3. A small shape parameter value signifies variable winds, while a higher value implies more constant wind speeds. In Northern Europe, this parameter is approximately 2 for most wind farms [26].

$$f(v) = \frac{k}{c} \cdot (\frac{v}{c})^{k-1} \cdot exp(-(\frac{v}{c})^k) \tag{3.1}$$

$$F(v) = 1 - exp(-(\frac{v}{c})^k) \tag{3.2}$$

When finding the scale parameter used in this master thesis, Equation 3.3 from [27] is used. The mean wind speed, v_{mean}, for Sheringham Shoal is set to 9.16 m/s, found in [28]. Using k = 2 and the gamma function, the calculated scale parameter is found to be 10.3 m/s.

$$v_{mean} = c \cdot \Gamma(1 + \frac{1}{k}) \tag{3.3}$$

The probability density function and the cumulative distribution function for the Sheringham Shoal wind farm is calculated using the parameter values above, and the complete calculations are shown in Appendix B. Excel is used to plot these two functions, and the probability density function and the cumulative distribution function is shown in Figure 3.9 and 3.10 respectively.

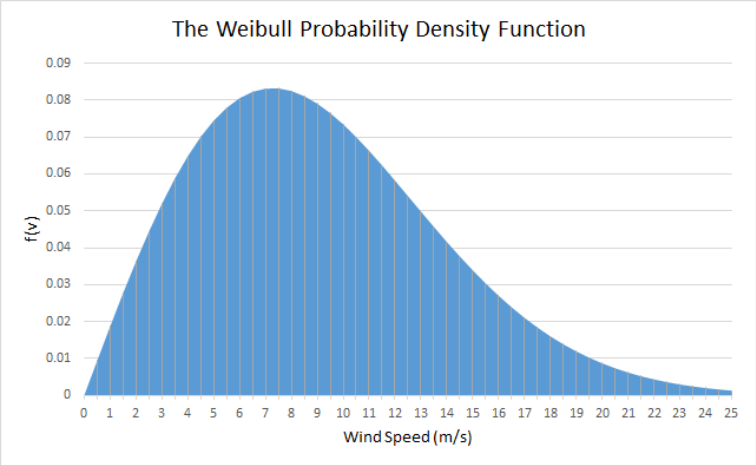

Figure 3.9: The Weibull probability density function.

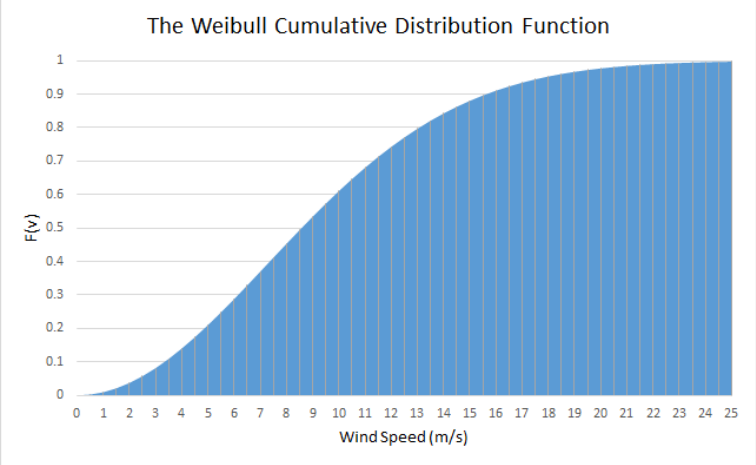

Figure 3.10: The Weibull cumulative distribution function.

From Figure 3.9 and the data in Appendix B, one can see that the most probable wind speed to occur is 7.5 m/s, and that the probability decreases for higher wind speeds. From the power curve in Figure 3.8, 7.5 m/s applies to a power generation of approximately 1 MW per generator. This is only 28 % of the rated power of the WTG at 3.6 MW.

The cumulative distribution function in Figure 3.10 may be used to investigate the probability of wind speeds below a certain limit. For example, the probability of wind speeds below 8.5 m/s is approximately 50 %, and approximately 80 % for wind speeds below 13 m/s.

Chapter 4

Power System Reliability

In this chapter, an introduction to power system reliability is given. The methodology used, Relrad, is explained and the different indices found in the reliability analysis in this master thesis are listed. A simple example of the methodology is also shown to present the steps taken in the reliability analysis. Two different load point considerations in offshore wind reliability analyses are also discussed using a simple example, and at last the failures included in this master thesis are presented.

Reliability is defined in [29] as *"the ability of an item to perform a required function under stated conditions for a stated period of time"*. In power systems, this applies to the system being able to deliver the expected power when needed. For the maximum power to be delivered to shore all the wind turbine generators have to be connected to the grid, and for each outage of these generators, the reliability decreases.

In [29], redundancy in a component is defined as *"the existence of more than one means of performing its function"*. This is an important factor, which may increase the reliability in a system significantly. In power systems, like the one included in this master thesis, increasing the redundancy corresponds to adding one or several reserve connections or cables to the system, making it better prepared for failures.

When discussing the reliability of a system, it becomes natural to include the cost of the system. In Figure 4.1, the relationship between the investment cost and the reliability in a system is shown. For a given increase in the investment, ΔC, the increment in reliability, ΔR, is reduced as the reliability is increased [4]. Therefore, when it comes to reliability it is more to gain in the beginning of a project than in the end, for the same amount of money invested.

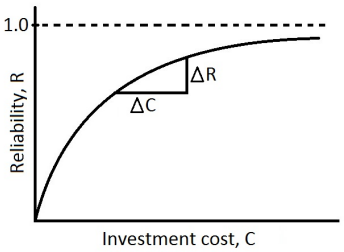

Figure 4.1: Incremental cost of reliability [4].

When doing power system planning on reserve connections, both the reliability and cost of the investment has to be considered, and an optimal layout has to be found taking into account different constraints and demands given.

4.1 Methodology

In power system reliability calculations, it is important to have a structured approach towards the goal of the analysis. It may then be easier to define the total system and the problems that may occur in the analysis conducted. The following steps, defined in [30], are recommended:

1. Understand how the system operates.
2. Identify the ways the system can fail.
3. Find the consequences of the failures.
4. Derive models to represent these consequences.
5. Select appropriate reliability evaluation techniques.

These steps are followed when doing the reliability analysis in this master thesis, with the goal of having a structured and clear approach.

4.1.1 Relrad

The reliability methodology used in this master thesis, is the Relrad method described in [12]. This methodology calculates the reliability at each individual load point, normally in radially operated MV distribution systems. Relrad is an analytical approach, and unlike some of the other well-known reliability methods, it is based on fault contribution from all components in the system. Instead of

looking at which components give an outage at the load point, this method looks at which load points will have an outage caused by the component [12]. When using the Relrad method some important assumptions have to be made, and the main assumptions are [12]:

- The network is operated radially.
- There are no transfer restrictions on reserve connections.
- All faults are isolated by the upstream circuit breakers, by the first or the second depending on the probability of malfunction of the circuit breaker.
- When the fault is located, the upstream disconnector will be opened and the circuit breaker closed.
- All failures are statistically independent.
- Multiple faults are not represented except for circuit breaker malfunction.
- All failures are repaired before next fault occurs.

These assumptions are made when conducting the reliability analysis in this master thesis. A more detailed explanation of the methodology, including flow charts and an example, is shown in Section 4.1.3.

4.1.2 Indices

The results from the reliability calculations are expressed through indices. These are expected values, and can be used to compare different system layouts. The indices are calculated using failure rates and repair times for different components, shown in Table 4.1. The indices used in this reliability analysis are shown in Table 4.2.

Symbol	Explanation
λ	Annual number of interruptions [failure/year]
MTTR	Mean Time To Repair [h]

Table 4.1: Inputs to the reliability analysis.

The failure duration and unavailability is a measure of how long the load point is disconnected, in both hours per failure and hours per year. The interrupted power and energy not supplied is a measure of how much power and energy is not supplied to the load point due to failures. The energy not delivered is a measure of how much power is not delivered by the load point, and is discussed more in Section

Indices	Explanation
r	Average failure duration [h/failure]
U	Unavailability [h/year]
P_{interr}	Annual interrupted power [MW/year]
ENS	Annual Energy Not Supplied [MWh/year]
END	Annual Energy Not Delivered [MWh/year]
ASAI	Annual System Availability Index [-]

Table 4.2: Indices found in the reliability calculations.

4.2. The annual system availability index says something about the portion of time the system is out.

It is important to say that these are expected values, and are very much depending on the parameters in Table 4.1. The dependency of these parameters will be discussed, as well as some other parameters, in the sensitivity analysis in Chapter 9.

4.1.3 Example of Methodology

A flow chart of the methodology is illustrated in Figure 4.2. It is taken from [30], with some small alterations. The main procedure is to go through all possible failures, and see how each failure affects the different load points. Total indices for the system are calculated at the end, using Equation 4.1, 4.2, 4.3, 4.4, 4.5 and 4.6.

$$\lambda_{system} = \sum_{i=1}^{N} \lambda_i \tag{4.1}$$

$$U_{system} = \sum_{i=1}^{N} U_i \tag{4.2}$$

$$r_{system} = \frac{U_{system}}{\lambda_{system}} \tag{4.3}$$

$$P_{interr} = P_{load} \cdot \lambda \tag{4.4}$$

$$ENS = P_{load} \cdot U \tag{4.5}$$

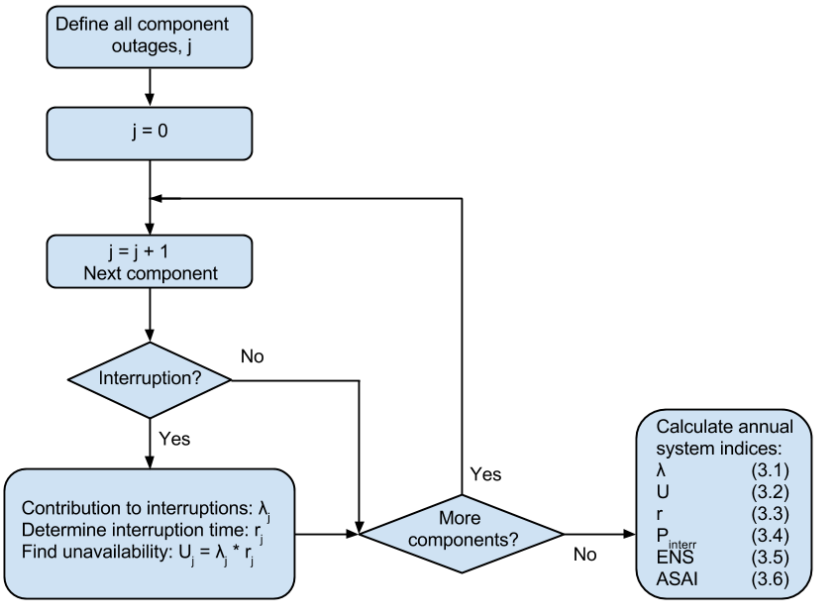

Figure 4.2: Flow chart of the Relrad methodology.

$$ASAI = \frac{\sum N_i \cdot 8760 - \sum U_i \cdot N_i}{\sum N_i \cdot 8769} \tag{4.6}$$

To show the steps used in the reliability calculations in this master thesis, a simple example is presented, illustrated in Figure 4.3. This is a small radial distribution system with three load points; A, B and C. The system consist of cables 1, 2, 3, a, b and c, in addition to one circuit breaker and several disconnector switches. There is also included a reconfiguration switch, operating only during faults, connecting the load points to an alternative power supply. In this example, only cable failures are included, but when introducing other failures the same procedure is followed.

The cable data is given in Table 4.3, and the expected power and number of customers for each load point is given in Table 4.4. A failure rate of 0.01 failures/year/km for the cables is used, which implies that the failure rate for each cable is dependent of its length. Also a MTTR of 5 and 3 hours is used for the main lines and the laterals respectively. The switching time for the disconnector switches and the reconfiguration is 0.5 hours.

Steps of the calculations:

1. Each failed component is investigated row-wise, as shown in Figure 4.2, looking at how the failure contributes to the load point outages. This means in-

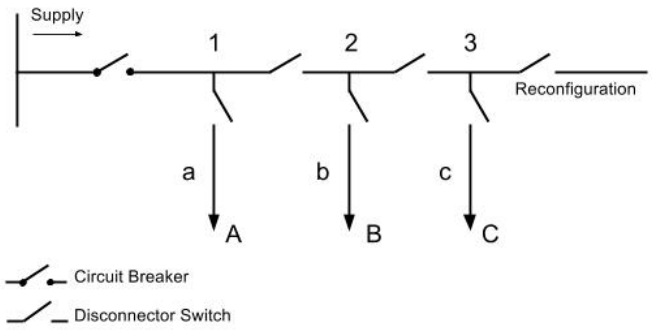

Figure 4.3: Example system used to show the Relrad methodology.

Line	Length [km]	Failure rate [failure/year]	MTTR [h]
1	3	0.03	5
2	2	0.02	5
3	1	0.01	5
a	1	0.01	3
b	2	0.01	3
c	3	0.01	3

Table 4.3: Cable data used in the Relrad example.

vestigating how long the load point is out (not connected to the supply) due to the given fault. It is important to understand the system and especially how the protection system works.

2. First the failure rates and the repair times are found using Table 4.3, and put into a new table, as done in Table 4.5. The failure duration, r, is found by looking at the failure in the system and how the different breakers are operating. A failure in Line 1 will cause the circuit breaker to open and clear the fault. There will be no current flowing in the system, and after 0.5 hours the disconnector switch between Line 1 and 2 will open and isolate the faulty area. Load point A is therefore out until Line 1 is repaired, which in this example is 5 hours. Load point B and C will be connected through reconfiguration after 0.5 hours.

3. The unavailability, U, is found by multiplying the failure rate and the failure duration for each load point.

This procedure is followed for all the remaining potential failing components, and the total results are shown in Table 4.5.

Load Point	Expected power [MW]	Number of customers, N
A	2	1000
B	3	1500
C	4	2000

Table 4.4: The power demand and number of customers for each load point used in the Relrad example.

	A			B			C		
Line	λ [fault/ year]	U [h/year]	r [h/fault]	λ [fault/ year]	U [h/year]	r [h/fault]	λ [fault/ year]	U [h/year]	r [h/fault]
1	0.030	0.150	5.00	0.030	0.015	0.50	0.030	0.015	0.50
2	0.020	0.010	0.50	0.020	0.100	5.00	0.020	0.010	0.50
3	0.010	0.005	0.50	0.010	0.005	0.50	0.010	0.050	5.00
a	0.010	0.030	3.00	0.010	0.005	0.50	0.010	0.005	0.50
b	0.010	0.005	0.50	0.010	0.030	3.00	0.010	0.005	0.50
c	0.010	0.005	0.50	0.010	0.005	0.50	0.010	0.030	3.00
Sum/ average	0.090	0.205	2.28	0.090	0.205	2.28	0.090	0.205	2.28
P_{interr} [MW/ year]	0.180			0.270			0.360		
ENS [MWh/ year]		0.410			0.615			0.820	

Table 4.5: Calculations done in the Relrad example.

The total failure rate, unavailability and repair time for each load point is found by using Equation 4.1, 4.2 and 4.3. The interrupted power and energy not supplied at each load point is calculated using 4.4 and 4.5.

Total P_{interr}	0.810 MW/year
Total ENS	1.85 MWh/year

Table 4.6: Total results from the Relrad example.

The total results for this system is then found by summing the P_{interr} and ENS for the three load points A, B and C, and are shown in Table 4.6. The ASAI is found by using Equation 4.6 with the number of customers found in Table 4.4 (the

N_i is the number of customers at load point i). The total interrupted power for this small system is 0.810 MW/year and the total energy not supplied to the load points is 1.85 MWh/year. The ASAI for this small example system is 0.999977.

4.2 Load Point Considerations

In reliability studies, the load points are the focus of the analysis. It is where the reliability indices are calculated and where the results from the analysis are expressed. In regular distribution systems, these load points are often known and given as an exact value. In offshore wind studies however, it is not given where these load points are and how big each load point is, because the load is located somewhere onshore. The load points should therefore be decided and defined inside the analyzing scope. In this section, two different load point considerations are introduced and compared: the negative load and the lumped load consideration. Two simple example systems are used to show the methodology and results for each case, and one of the considerations is chosen to be used in this master thesis. The simplified example systems are shown in Figure 4.4, and illustrates a radial system and a radial system with a reserve connection, also called a radial loop system.

The five wind turbines in the radial are rated at 2 MW, and are assumed to produce rated power at all times. The failures included in this comparison are only the cable failures, occurring in the cables L1 to L5. Breakers are assumed ideal (opening and closing when requested), and reconfiguration is only possible in the radial loop system during a fault. In steady state, the radial loop system is equal to the simple radial system. The input data used is shown in Table 4.7.

	Cable	DS and RS
λ [failures/year/km]	0.0094	-
MTTR [hours]	1440	-
Switching Time [h]	-	1

Table 4.7: Input data for the example calculations using different load point considerations.

In this example, the cables L1 to L5 are assumed to have the same length equal to 1 kilometer. This leads to failure rates equal to the number in the table: 0.0094 failures per year for the cables L1-L5. The reserve connection is assumed ideal. The breakers are installed to clear the fault and isolate the faulty area, operating

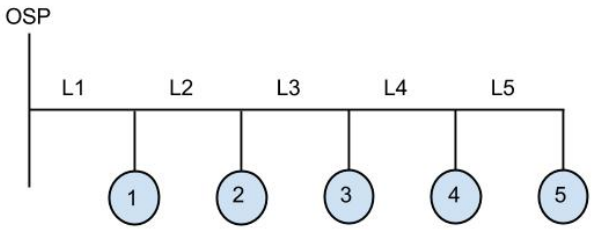

(a) The simple radial system.

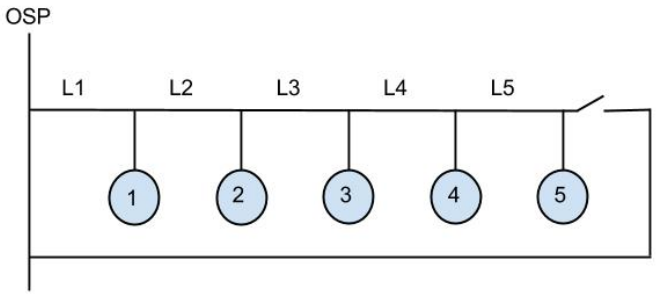

(b) The simple radial loop system.

Figure 4.4: The two systems used in the comparison of different load point considerations.

in the same way as in the small example in Section 4.1.3, with the CB clearing the failure and the DSs isolating after 1 hour.

4.2.1 Negative Load

When looking at the load points as negative loads, the total reliability results are found by summing the results for all the load points, as done in the earlier example. A wind turbine may be considered a negative load by looking at the turbines as load consuming negative power, as done in [10]. The advantage of using this perspective is that it enables the use of power system analyzing tools, such as DIgSILENT PowerFactory. A disadvantage of using this perspective in offshore wind calculations is the large amount of load points existing in the system. If one wind turbine is one negative load point, the amount of load points will be ranging from around 50 to over a hundred load points. This would require a significant amount of calculations before the total result is found. The methodology used is the same as shown in the example, but now having negative load instead of

positive. The energy not supplied (to the load point), ENS, is changed to energy not delivered (from the wind turbine), END, due to this small modification. The calculations for one load point/turbine in both the radial and the radial loop system are shown in Table 4.8 and 4.9 respectively. This is done for all turbines in the system, and the total results are shown in Table 4.10. The calculations for all turbines are shown in Appendix C.

WTG1			
	λ [failures/ year]	Unavailability [hours/year]	Repair time [hours/failure]
L1	0.00940	13.5	1440
L2	0.00940	0.00940	1
L3	0.00940	0.00940	1
L4	0.00940	0.00940	1
L5	0.00940	0.00940	1
Sum/Average	0.0470	13.6	289
Energy not delivered from WTG1 [MWh/year]			27.1

Table 4.8: Energy not delivered from WTG1 in the example radial system using negative load consideration.

WTG1			
	λ [failures/ year]	Unavailability [hours/year]	Repair time [hours/failure]
L1	0.00940	0.00940	1
L2	0.00940	0.00940	1
L3	0.00940	0.00940	1
L4	0.00940	0.00940	1
L5	0.00940	0.00940	1
Sum/Average	0.0470	0.0470	1
Energy not delivered from WTG1 [MWh/year]			0.0940

Table 4.9: Energy not delivered from WTG1 in the example radial loop system using negative load consideration.

	END [MWh/year]
WTG 1	27.15
WTG 2	54.20
WTG 3	81.25
WTG 4	108.3
WTG 5	135.4
Total END radial system	406.3

	END [MWh/year]
WTG 1	0.0940
WTG 2	0.0940
WTG 3	0.0940
WTG 4	0.0940
WTG 5	0.0940
Total END radial loop system	0.470

Table 4.10: Total energy not delivered from the example radial and radial loop system using negative load consideration.

4.2.2 Lumped Load

When looking at the total load as a lumped load, all the loads onshore receiving power from this wind farm are gathered to one big load. In this example, the lumped load is chosen to be equal the total capacity of the wind farm, as done in [5]. The lumped load is considered at the OSP, at the connection between the transmission system and the collection system. When calculating the reliability the Relrad methodology is used, but now the fraction of lost capacity associated with each fault has to be calculated. In Figure 4.5, the flow chart of the procedure is illustrated, and the results from the calculations are shown in Table 4.11 and 4.12 for the radial and the radial loop system respectively.

The failure rates, MTTRs and switching times are found in Table 4.7. When using lumped load the fraction of the lost production over a period of time has to be found, taking into account the switching times for the disconnectors and the reconfiguration switch. For example, if there is a fault on L1 in the radial system, the whole system will be out until the cable is repaired, which is 1440 hours. If there is a fault on L2 however, 100 % of the system is out for one hour, but then L1 may be connected due to isolation of the failure at L2. The disconnector switches will then open, the circuit breaker will close and L1 will be connected. After 1 hour only 80 % of the system is out until the cable is repaired. The same procedure is done with the remaining cables. The relation between the lost production and repair time is represented with a "dash" in the table. The unavailability is calculated by multiplying the repair time with the failure rate. At last the energy not supplied (ENS) to the lumped load point is found by multiplying the lost production with the corresponding unavailability and summing all these up at the end.

As one can see both load point considerations give somewhat the same results,

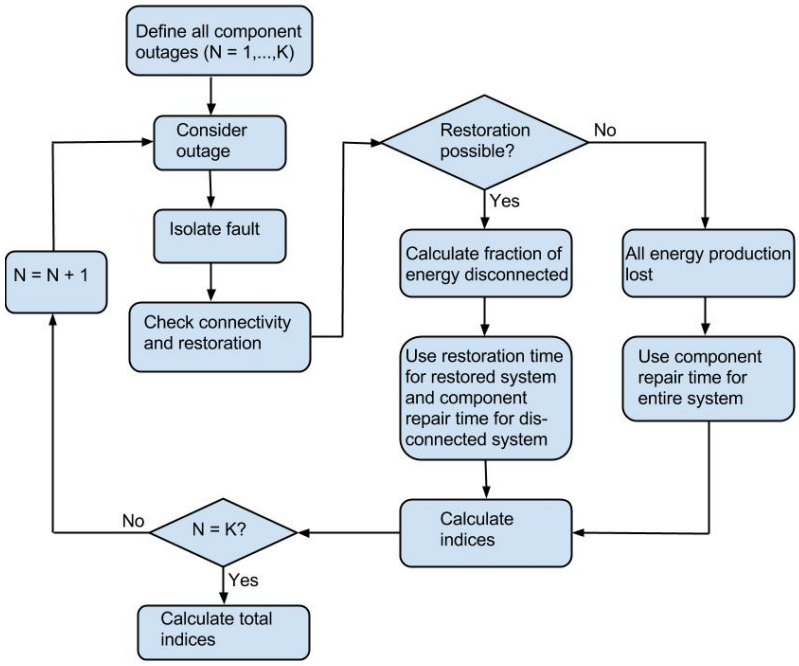

Figure 4.5: Flow chart used in the lumped load calculations [5].

	λ [failures/ year]	Unavailability [hours/year]	Repair time [hours/failure]	Fraction of lost production [%]	Lost pro-duction [MW]	ENS [MWh/year]
L1	0.00940	13.6	1440	100	10	135.6
L2	0.00940	0.0094/13.6	1/1440	100/80	10/8	108.6
L3	0.00940	0.0094/13.6	1/1440	100/60	10/6	81.47
L4	0.00940	0.0094/13.6	1/1440	100/40	10/4	54.35
L5	0.00940	0.0094/13.6	1/1440	100/20	10/2	27.22
Total energy not supplied [MWh/year]						407.0

Table 4.11: Total energy not supplied in the example radial system using lumped load consideration.

and it is therefore fair to say that one may choose which to use, and still get the same results. In this master thesis, the negative load consideration is chosen due to the simplicity and the easy implementation of the model in Microsoft Excel.

	λ [failures/ year]	Unavailability [hours/year]	Repair time [hours/failure]	Fraction of lost production [%]	Lost pro- duction [MW]	ENS [MWh/year]
L1	0.00940	0.00940	1	100	10	0.0940
L2	0.00940	0.00940	1	100	10	0.0940
L3	0.00940	0.00940	1	100	10	0.0940
L4	0.00940	0.00940	1	100	10	0.0940
L5	0.00940	0.00940	1	100	10	0.0940
Total energy not supplied [MWh/year]						0.470

Table 4.12: Total energy not supplied in the example radial loop system using lumped load consideration.

4.3 Failures Included In This Master Thesis

A failure is defined in [31] as *"the termination of the ability of an item to perform its required function"*. These functions may be continuously required, like carrying current or providing isolation, or it may be functions required as a response to a condition, for example opening of a breaker [31]. A failure may be caused by various reasons, like construction and installation work, maintenance, production or use.

Different failure modes are introduced in [32], and are shown in Table 4.13. Failure modes make it easier to categorize failures in a reliability analysis.

Failure	**Description**
Independent failure of component	Sudden occurance of short-circuits on component during normal operation.
Common-Mode-Failure	Failure of several elements due to a common cause.
Failure of protection system	Loss of selectivity due to failing protection devices.
Protection overfunction	Unwanted operation of protection system in response to network problems.
Failure of several components	Due to multiple ground fault.
Overlapping of determined shutdown of one element with failure of a second element	Maintenance.

Table 4.13: Different failure modes used to categorize failures in a system.

In this master thesis, only two of the failure modes are included, the first and the third mode. The different failures included in the reliability analysis are listed and described in Table 4.14. A distinction is made between independent and dependent failures in the cable. An independent cable failure is when there is a failure in the cable and the nearest CB opens and clears the fault. If however a dependent failure occur, the nearest breaker fails to open during a cable failure, and the second breaker in the system is assumed to open. In such situations, several components are disconnected by the CB, and the number of outages will increase compared to an independent cable failure.

The reserve connections analyzed are assumed ideal and may not fail. The failure rates for the IA and export cables, CBs and DSs are discussed in Chapter 5, and are used in the reliability analysis.

Failure	Failed component	Description	Failure mode
Independent IA cable failure	IA cable	A failure occur due to short-circuiting in the IA cable. The nearest breaker clears the fault.	1
Dependent IA cable/CB failure	IA cable	A failure occur due to short circuiting in the IA cable. The nearest breaker do not clear the fault. The next breaker(s) in the system clears the fault.	3
Independent export cable failure	Export cable	A failure occur due to short-circuiting in the export cable. The nearest breaker clears the fault.	1
Dependent export cable/CB failure	Export cable	A failure occur due to short circuiting in the export cable. The nearest breaker do not clear the fault. The next breaker(s) in the system clears the fault.	3
CB failure	CB	A failure occur due to short circuiting in the CB. The nearest breaker (not itself) clears the fault.	1
DS failure	DS	A failure occur due to short circuiting in the DS. The nearest breaker (not itself) clears the fault	1

Table 4.14: The failures included in the reliability analysis.

Chapter 5

System Components

In this chapter, the main system components are introduced and discussed. The components presented are used in the Sheringham Shoal offshore wind farm, and important component data from this wind farm is shown. In addition to reliability data, the failure and cost data used in the calculations is shown.

5.1 Submarine Cables

A submarine cable is a large, submerged transmission cable for carrying electrical power. Such cables require special manufacturing and laying techniques, and are constantly being improved by the cable providers. In the Sheringham Shoal offshore wind farm, both export cables and IA cables are submarine cables, carrying power all the way from the turbines to shore. Some of the cable and cost data given in this section is typical values given by Statkraft, and is assumed to be approximate, but not exact, data for the Sheringham Shoal wind farm.

5.1.1 Export Cables

The Sheringham Shoal offshore wind farm has two export cables transferring the power to shore from two offshore substation platforms. These are HVAC Nexans XLPE cables operating at 132 kV. The first cable is referred to as Export Cable 1, and is transferring power from the left half of the windfarm, referred to as Area 1 in this master thesis. The second cable, Export Cable 2, is transferring the rest of the power from the right half of the wind farm, Area 2. This is illustrated in Figure 5.1. Export Cable 1 has a length of 23 km, while Export Cable 2 is 21 km.

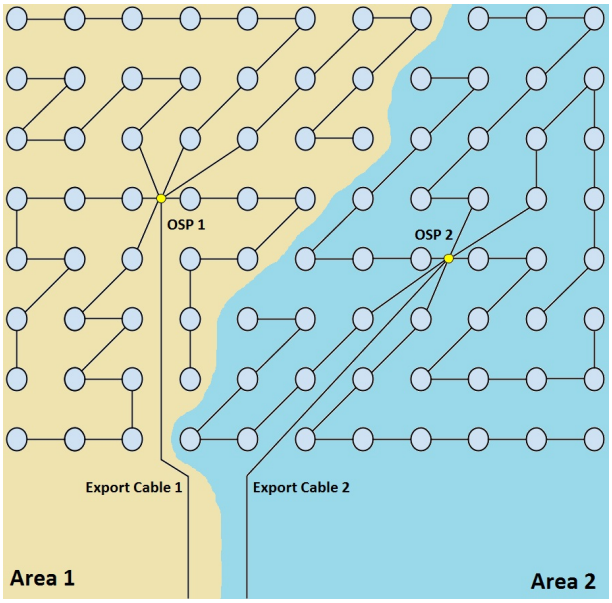

Figure 5.1: The export cables transferring power from two different areas of the wind farm.

From Figure 3.5 in Chapter 3, one can see that these distances and the voltage level used is far within the HVAC limits. The conductor sizes of both export cables are 630 mm^2, and are set to have a power capacity of 183 MVA, as shown in Appendix D. The data given in the appendix is originally data for a single core XLPE insulated HV cable, and not a three core HV cable which is installed in the Sheringham Shoal wind farm. After conversations with my supervisor at Statkraft, it is assumed that the difference in capacity between the single core and the three core cable is not significant, and that the single core value may be used for this purpose.

Export cable data	
Nominal cross sectional area [mm^2]	630
AC resistance at 90 °[ohm]	0.0480
Capacitance [μF/km]	0.200
Line Reactance [ohm/km]	0.140
Capacity [MVA]	183

Table 5.1: Export cable data used in the power flow calculations.

The detailed cable data used in the power flow analysis is shown in Table 5.1, where the AC resistance, capacitance and line reactance is given by Statkraft. Different cable failure data is found in [5], [9], [10], [14], [21] and [33], and based

Export cable failure data	
Failure rate [1/year/km]	0.00940
MTTR [h]	720

Table 5.2: Export cable failure data used in the reliability calculations.

on these studies the failure data for the export cables is given in Table 5.2.

5.1.2 Inter Array Cables

The inter array cables used in the Sheringham Shoal offshore wind farm are 33 kV MVAC cables, also produced by Nexans. The cables are XLPE insulated and use copper conductors to transfer current. The XLPE insulated cables have many advantages, such as low maintenance, lighter weight and easier transportation and laying [34]. The cable data used in the power flow calculations for both the 185 mm^2 cross section and the 400 mm^2 cross section cable is shown in Table 5.3, and again is the AC resistance, capacitance and line reactance given by Statkraft.

IA cable data		
Nominal cross sectional area [mm^2]	185	400
AC resistance at 90 °[ohm]	0.128	0.079
Capacitance [μF/km]	0.210	0.280
Line reactance [ohm/km]	0.120	0.110
Capacity [MVA]	28.0	41.0

Table 5.3: IA cable data used in the power flow calculations.

The IA cables are connected in either 7- or 8-turbine radials. The lengths of these cables are varying from 0.42 km to 1.5 km, depending on the distance between the turbines. An overview of the different cable lengths is shown in Appendix E. There are 82 km with IA cables in total. The cross section of the IA cable is either 400 mm^2 or 185 mm^2 depending on the distance from the OSP, as illustrated in Figure 5.2. In this figure the 8-turbine radial is shown, with eight wind turbine generators (WTG1-WTG8) and eight IA cables (L1-L8). The five IA cables located furthest away from the OSP are rated 185 mm^2 while the remaining IA cables located closer to the OSP are rated 400 mm^2. This applies for both types of radials, both with 7 and 8 turbines. The cables have a transfer capacity of 28 MVA and 41 MVA, for the 185 mm^2 and the 400 mm^2 cables respectively, as shown in Appendix D. The closest turbines are rated higher because of the increased need of power transfer capacity, since the nearest cables have to transfer power from all the WTGs located

further out. In steady state without any reserve connection, the cables further out only have to transfer power from a few turbines, which lower the need for high capacity.

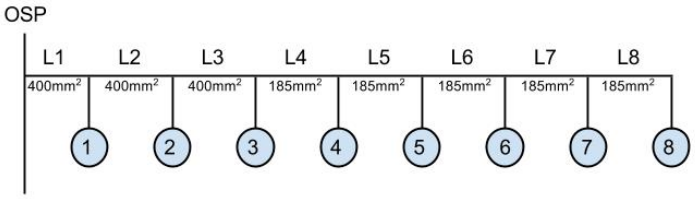

Figure 5.2: The 8-turbine radial in the Sheringham Shoal offshore windfarm, illustrated with the cable cross sections.

IA cable failure data	
Failure rate [1/year/km]	0.0094
MTTR [h]	1440

Table 5.4: IA cable failure data used in the reliability calculations.

The failure data for the IA cables is set to the values given in Table 5.4, after again investigating failure data from [5], [9], [10], [14], [21] and [33].

5.2 Protection System

The protection system consists of circuit breakers and disconnector switches, working together for a safer electrical system. The circuit breakers are responsible of clearing the fault, while the disconnector switches will isolate the faulty area after some time. The disconnector switches will operate only when there is no current flowing through it, and will therefore open after a given time. In this thesis, the switching time is set to 1 hour for the disconnector switches. During steady state (no fault in the system), all CBs and DSs will be closed.

To ensure a safe operation of the wind farm the breakers are arranged to clear and isolate the fault as fast as possible, having the economical aspect in mind. There are different protection zones in an electrical system, where one circuit breaker is responsible for protecting its zone. As illustrated in Figure 5.3 the different protection zones in a wind farm are: Wind generator protection zone, Feeder protection zone, Busbar protection zone and HV transformer protection zone. A

more detailed illustration of the feeder protection zone in Sheringham Shoal is shown in Figure 5.4. This figure shows nine circuit breakers (CB1-CB9), nine disconnector switches (DS1-DS9) and eight IA cables (L1-L8) connected to one radial. This is an 8-turbine radial, and is representative for the one used in the calculations in this master thesis.

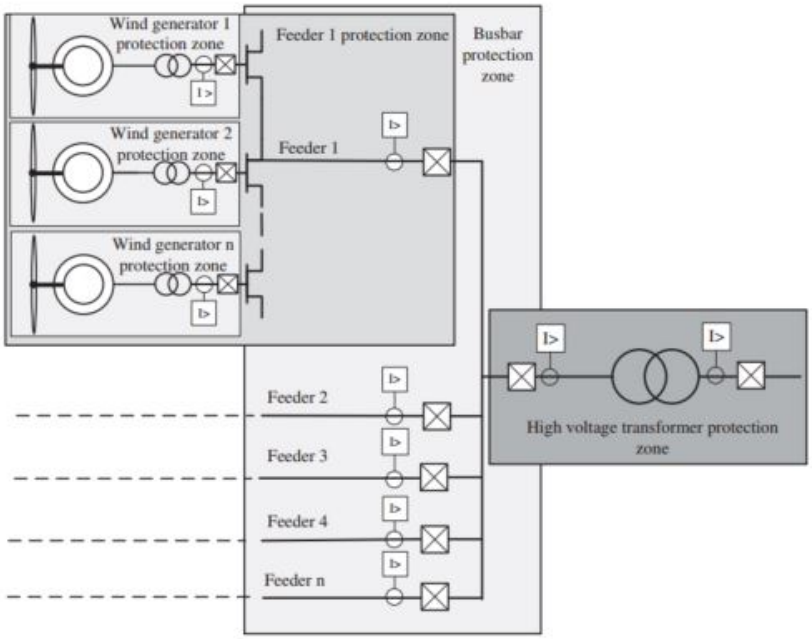

Figure 5.3: The protection zones in an offshore wind farm [1].

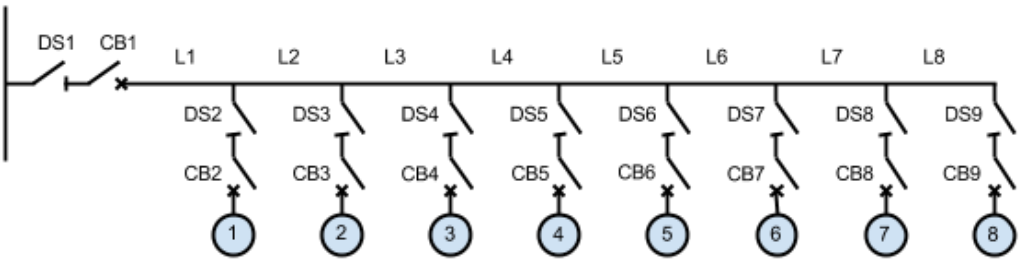

Figure 5.4: The feeder protection zone in the Sheringham Shoal offshore wind farm.

In this section, the operation of the protection system is also explained. As mentioned above the circuit breakers are the ones clearing the fault, and will operate immediately after a fault is detected. After one hour, disconnector switches will

open and isolate the area, making it accessible for repair and maintenance. In Figure 5.5 a fault in cable L3 is illustrated. The circuit breaker closest to the OSP, CB1, will open and clear the fault current, and after some time no current will flow in the system. A disconnector switch, DS1, will open after 1 hour and isolate the area, and the circuit breaker may close again. The DS will be open until the faulty cable is disconnected from the rest of the system, and may only then close again. WTG1 and WTG2 will have an outage time equal to this disconnecting time, and if no reserve connection is available WTG3-WTG8 will be out until L3 is repaired. If there is a reserve connection, as the one in the example in Chapter 4, the disconnected WTGs may be connected again with a reconfiguration switch after L3 is taken out of the system.

In a breaker configuration like the one used in the master thesis, the system is dependent of the removal of the faulty cable before the rest of the system is reconnected. In Sheringham Shoal, this is done by workers travelling out and manually disconnecting the faulty cable. This action is very weather dependent and it may take a long time before the workers are able to go out to the faulty cable. The time for disconnecting the cable manually is set to 24 hours, but is investigated more in the sensitivity analysis.

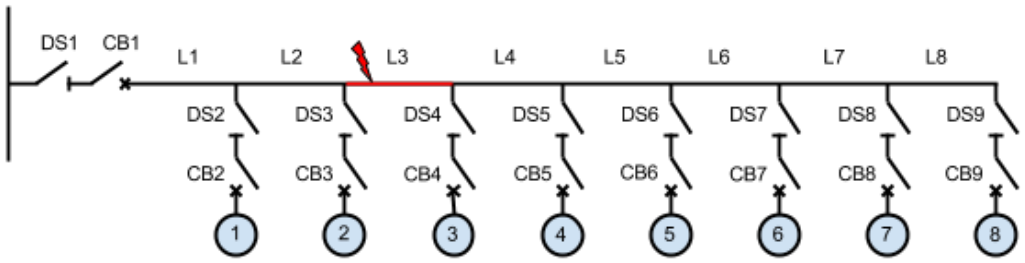

Figure 5.5: An illustration of a failure on L3.

In the reliability analysis conducted, a breaker failure (not a dependent failure) is treated the same way as a failed cable. In Figure 5.4, if there is a failure in CB2, CB1 will open to clear the fault, and after some time DS2 will open and isolate the faulty area. The rest of the turbines may then be connected, but WTG1 will have an outage time equal to the repair time for the CB. It is also assumed, as for the cables, that a manual disconnection may be done when it is needed. For example if there is a failure in one of the OSP breakers, a manual disconnection may be beneficial (manual disconnection is for example beneficial in the failure of MVCB3 in Figure 5.6).

The placement of these breakers and switches are critical when designing a safe

electrical system, reducing the consequences of a failure to a minimum. If any of these breakers fail, either by itself or as a consequence of another fault (dependent fault, explained in Chapter 4), the rest of the system may be seriously damaged. In this master thesis, failure data from Table 5.5 is used. Again values from the different reliability studies [5], [9], [10], [14], [21] and [33] are considered.

	HV Circuit Breaker	MV Circuit Breaker	HV Disconnector Switch	MV Disconnector Switch
Failure rate [1/year/km]	0.032	0.024	0.012	0.0024
MTTR [h]	720	720	720	720
Switching time [h]	-	-	1	1
Probability of operating when requested	0.97623	0.97623	-	-
Probability of not operating when requested	0.02377	0.02377	-	-

Table 5.5: Protection system failure data used in the reliability calculations.

5.3 Wind Turbines

The wind turbine model used in Sheringham Shoal is the Siemens SWT-3.6-107 wind turbine. It has a rated power of 3.6 MW, and uses a 4 pole asynchronous machine to convert energy from wind to electricity. The turbine voltage level is 690 V, and a transformer is installed in the turbine tower to step up this voltage to the IA voltage. In this master thesis, failures in the wind turbines are not included. The reliability results for these components will be the same for all the different layouts analyzed, since the amount of wind turbines and their location in the wind farm is already set. A failure in the wind turbine would be cleared immediately by the circuit breaker connected to it, as shown in Figure 5.4, and would not affect the rest of the system significantly. It is therefore decided to focus on the components that have various contributions in the different layouts, such as cables and breakers.

One aspect that is included and discussed in this master thesis, is the power production from the turbine. As the production is not constant at a maximum value, the reliability and power flow is investigated at a different production level. This is included in the calculations in Chapter 10.

5.4 Transformers

In the Sheringham Shoal wind farm there are two different types of transformers used, one low voltage (LV) transformer and one high voltage (HV) transformer. The LV transformer is connected to the turbine, and is stepping the voltage up from the turbine voltage at 690 V to the IA voltage at 33 kV. The HV transformer is installed at the offshore substation platform, and is transforming the IA voltage to the export voltage at 132 kV. Failures in the transformers are not included in this master thesis, using the same argument as for the wind turbines. When comparing different layouts, the reliability results from the transformers will be the same, and the focus is therefore on other components.

5.5 Offshore Substation Platform

There are two offshore substation platforms installed to transfer power to shore through two export cables, introduced above. Both transformers and breakers are installed at this big construction, but only failures in the breakers are included in the master thesis. The breaker configuration for one offshore platform is shown in Figure 5.6.

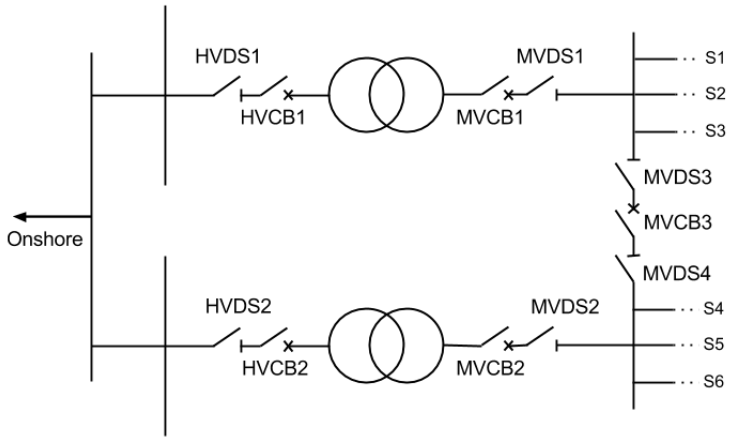

Figure 5.6: The breaker configuration at one OSP.

Both CBs and DSs illustrated in this figure are assumed to may fail, and is included as part of the reliability analysis.

Chapter 6

Park Layout

In this chapter, the existing layout of the Sheringham Shoal offshore wind farm is introduced in detail. Two different types of reserve connections, the End connection and the Split connection, are presented and advantages and disadvantages are discussed. The different layouts with their reserve connections are shown, and the location and length of the connections are presented.

6.1 The Existing Layout

The existing layout is in this master thesis referred to as the Base Case. It consists of 88 turbines connected in 12 radials, as shown in Figure 6.1. The turbines are labeled after their column (A-K) and row (1-8). No reserve connections are installed, and a lot of power may be lost if a fault occur. A failure early in one radial results in an outage of the entire string, and if the export cables have an outage, the entire wind farm is affected and several turbines may be isolated from the system over a long period of time.

Advantages with the radial system already installed at Sheringham Shoal are the high level of simplicity and easy controllability. As more reserve connections are installed the system gets more complex and it may be more difficult to control the power flow and the protection system. Also the investment cost increases as the reserve connections are installed.

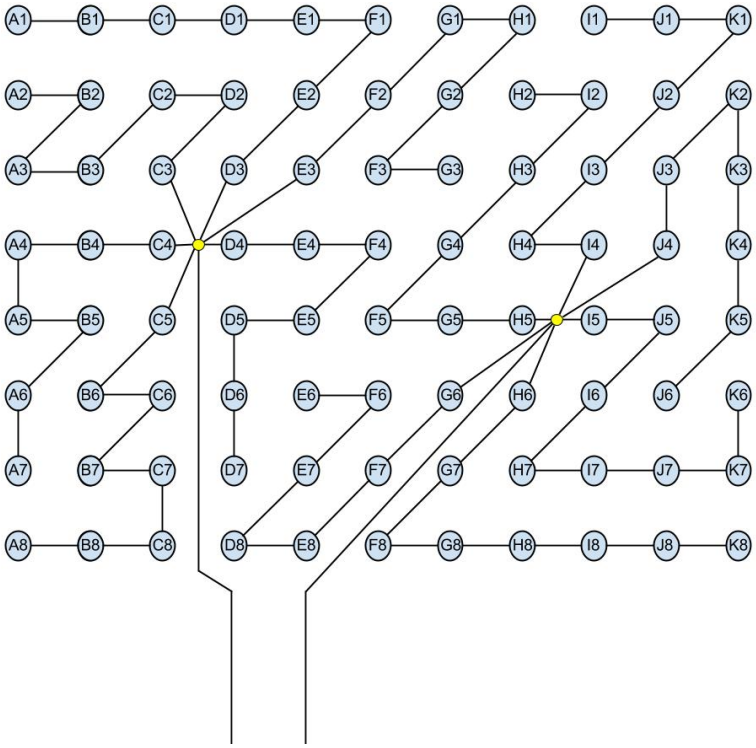

Figure 6.1: Illustration of the existing radial IA system in Sheringham Shoal.

6.2 The Reserve Connection Layouts

When investigating the reliability in alternative offshore systems, five different layouts with reserve connections have been chosen. The additional connections are installed to increase the system reliability, making it possible for the turbines isolated by a failure to be connected through an alternative path. Disadvantages with these connections are the higher level of complexity and the increased costs. The reserve connections are assumed ideal, and in steady state, the reserve connection layouts are equal to the existing layout.

The layouts with reserve connections are labeled Layout 1-5 and are presented in this section. They all consist of the same turbines and cables as the Base Case, but with additional reserve connections. The connections have been chosen with the existing layout map from Figure 3.7 in mind, trying to minimize the reserve cable lengths. The rating and cross section of the additional cables in Layout 1-4 is chosen to be equal to the rating and cross section for the end cables (located furthest from the OSP) in each radial. In Layout 5, a direct reserve connection between the two OSPs is installed, and this is chosen to have larger cross section

and rating than in the other layouts. The remaining connections in Layout 5 have the same rating and cross section as the end cables of each radial.

There are two reserve connections used in this master thesis; the End connection and the Split connection. The End connection is illustrated in Figure 6.2. The two radials are connected in the ends, making the additional cable an alternative path for the power to flow during a failure. If there is a fault anywhere in one of the radials, the isolated power may be transferred through the reserve connection after a few breaker operations. This is the most common reserve connection used today. A disadvantage with this connection is the need for higher capacity in the radial cables, due to the additional amount of power being transferred in the outermost cables during a fault.

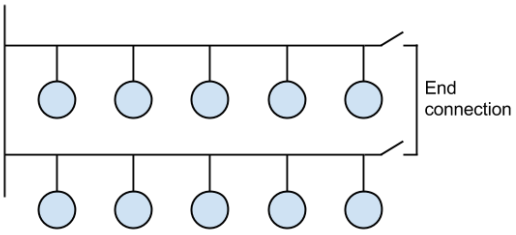

Figure 6.2: Illustration of the End connection.

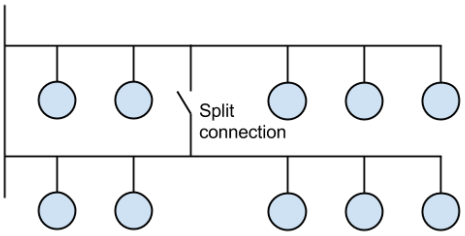

Figure 6.3: Illustration of the Split connection.

A Split connection between two radials is illustrated in Figure 6.3. The alternative path is now located in the middle of the radial, rather than at the end. In this master thesis a Split connection may also refer to a connection where one of the radial ends is connected in the middle of another radial.

If there is a failure in a Split connection occurring close to the end of the radial (for example in the cable located furthest from the OSP), the reserve connection may not connect the isolated turbine(s). If however a failure is occurring close to the OSP, this connection will work as an alternative path for the isolated power. The need for higher capacity in the outer cables is not as high as in the End connection,

but now also the reliability is expected to decrease. The connection between the reserve connection and the existing bus may also be more complex than in the End connection.

The approximate length of each reserve connection is decided by studying Figure 3.7. These are only approximate lengths decided by the writer.

6.2.1 Layout 1

The first layout have six reserve connections, and are illustrated in red in Figure 6.4. The reserve connections are located between pairs of radials, either as End or Split connections, depending on the existing layout and its turbine locations. The reserve connections and their cable lengths are listed in Table 6.1.

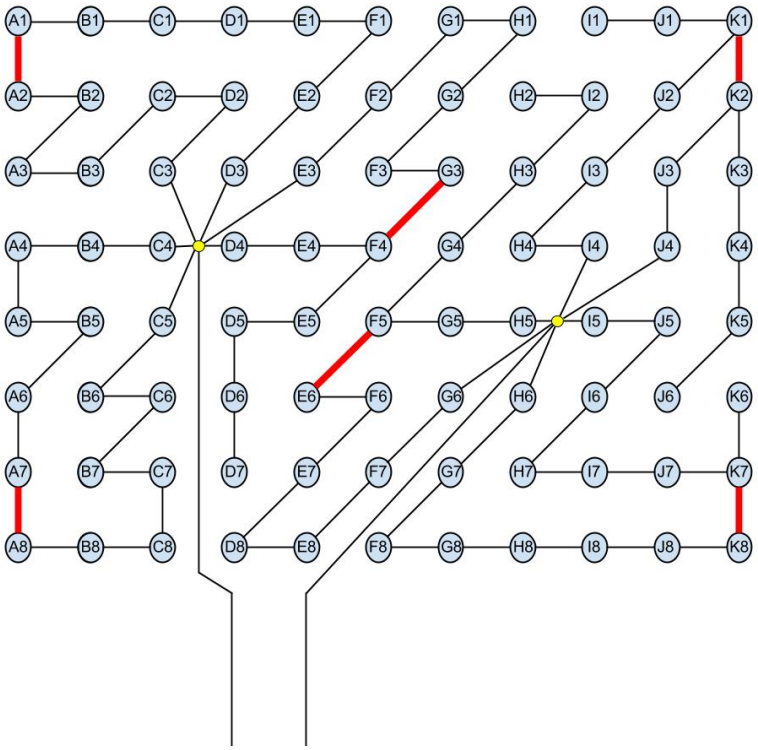

Figure 6.4: Illustration of Layout 1 with six reserve connections.

Connection	Type of connection	Length [km]
A7-A8	End	0.90
A1-A2	End	0.90
F4-G3	Split	0.80
E6-F5	Split	0.80
K1-K2	Split	0.90
K7-K8	Split	0.90

Table 6.1: The reserve connections in Layout 1.

6.2.2 Layout 2

In the second layout, four reserve connections are installed, shown in Figure 6.5. As before, pairs of radials are connected, but now only End connections are made. There are four radials not connected to a reserve connection, which will have a negative impact on the reliability in the system. The reserve connections in this layout are listed in Table 6.2.

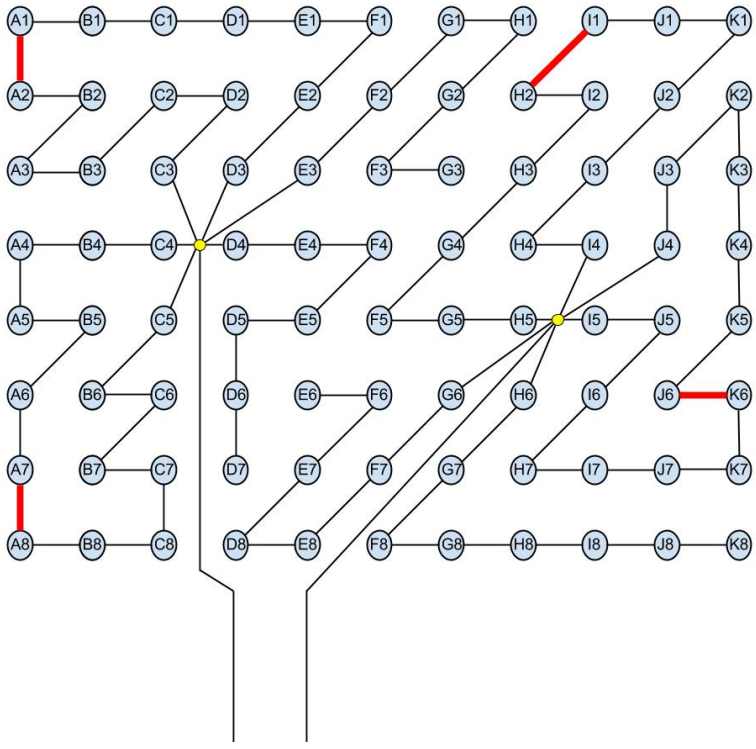

Figure 6.5: Illustration of Layout 2 with four reserve connections.

Connection	Type of connection	Length [km]
A7-A8	End	0.90
A1-A2	End	0.90
H2-I1	End	0.85
J6-K6	End	0.85

Table 6.2: The reserve connections in Layout 2.

6.2.3 Layout 3

In the third layout, six reserve connections are installed, as in Layout 1, but now with only Split connections. All radials are now connected to a reserve connection. The connections are illustrated in Figure 6.6, and listed in Table 6.3.

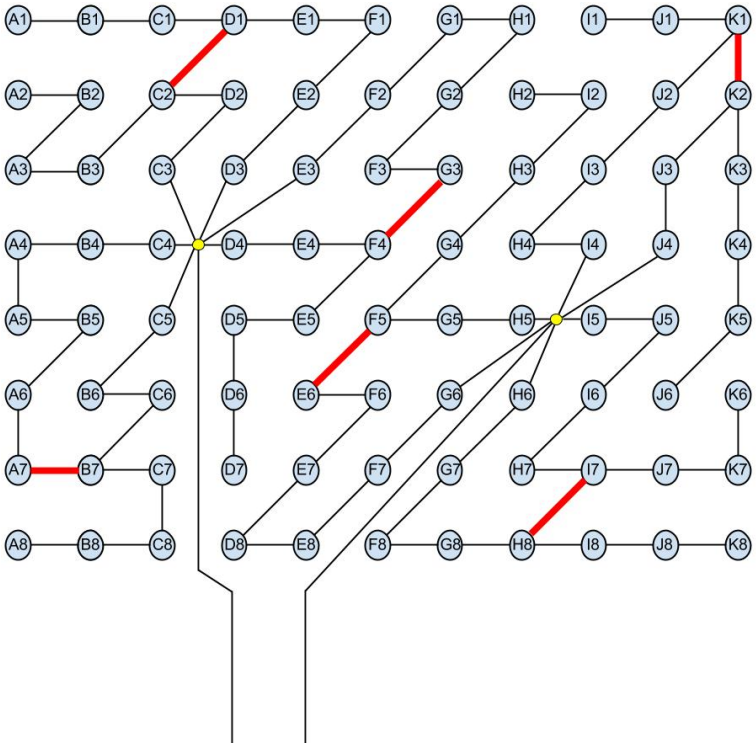

Figure 6.6: Illustration of Layout 3 with six reserve connections.

6.2.4 Layout 4

In Layout 4, there are six reserve connections, shown in Figure 6.7 and Table 6.4. This layout stands out from the previous layouts because it has two reserve

Connection	Type of connection	Length [km]
A7-B7	Split	0.90
C2-D1	Split	0.85
F4-G3	Split	0.80
E6-F5	Split	0.80
H8-I7	Split	0.80
K1-K2	Split	0.90

Table 6.3: The reserve connections in Layout 3.

connections (D7-E6 and G3-H2) going between the two different areas. If there is a failure in one of the export cables, the connection between the areas may be very beneficial, with the system being able to transfer power from one area to another. An issue with these reserve connections is the capacity of the cables and the large power flows. This is investigated in the power flow calculations in Chapter 10.

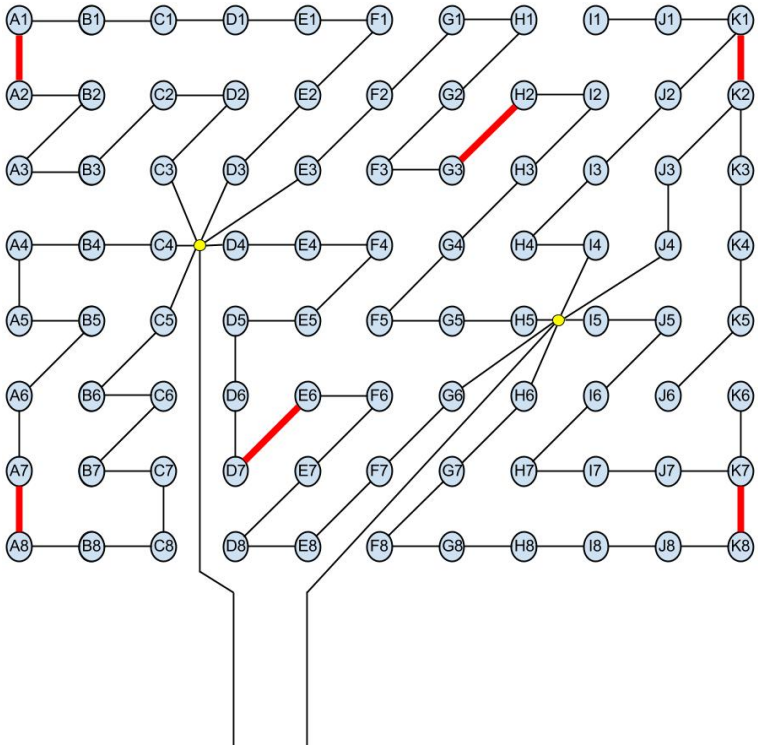

Figure 6.7: Illustration of Layout 4 with six reserve connections.

Connection	Type of connection	Length [km]
A7-A8	End	0.90
A1-A2	End	0.90
D7-E6	End	0.80
G3-H2	End	0.80
K1-K2	Split	0.90
K7-K8	Split	0.90

Table 6.4: The reserve connections in Layout 4.

6.2.5 Layout 5

In the fifth and last layout, five reserve connections are installed, including one direct connection between the two OSPs, as illustrated in Figure 6.8. The connection between the OSPs is chosen to have a higher rating and a larger cross section than the other reserve connections, investigating both a 33kV cable with 400 mm^2 cross section and a 132 kV cable with a 630 mm^2 cross section. The reserve connections and their lengths are listed in Table 6.5.

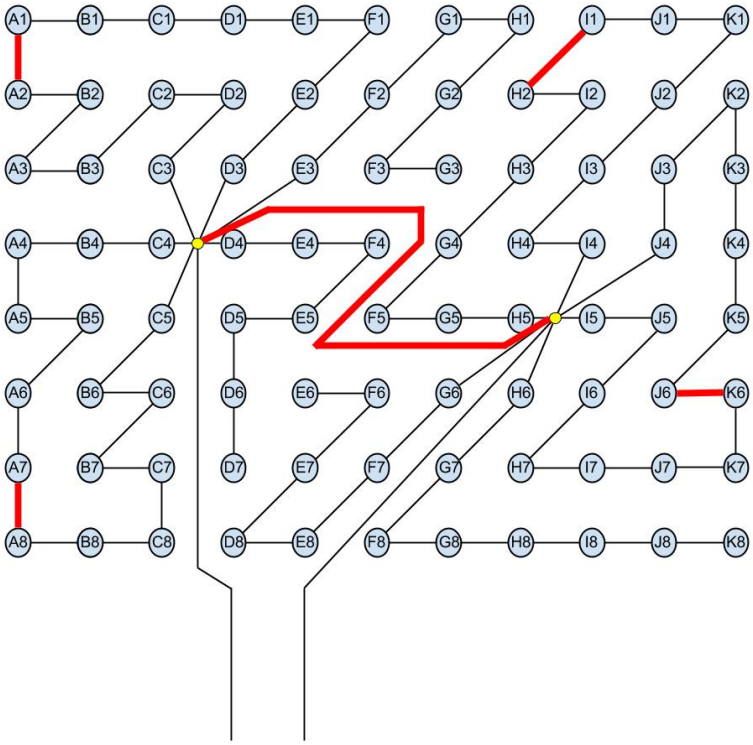

Figure 6.8: Illustration of Layout 5 with five reserve connections.

Connection	Type of connection	Length [km]
A7-A8	End	0.90
A1-A2	End	0.90
H2-I1	End	0.85
J6-K6	End	0.85
OSP1-OSP2	-	16

Table 6.5: The reserve connections in Layout 5.

Chapter 7

Power Flow Analysis

When conducting an analysis on reserve connections, an important aspect is to investigate if the installed connections manage to carry all the power they are intended to. By doing a power flow analysis one is able to calculate how much power is expected to go through the cable if there is a fault in other parts of the system. If the power flow exceeds the capacity of the cable, actions have to be taken to keep this from happening during operation. Actions to prevent overload of cables may be installation of higher capacity cables or control systems for the wind power production. In this chapter is the program used to calculate the power flow in the different layouts, Matpower, presented. The classification of buses and the example input and ouput data is also shown. At the end the general steps in the load flow analysis is listed to give an overview of the calculations done in Chapter 10.

7.1 Matpower

In this master thesis, Matpower is used to do power flow calculations on the inter array system. Matpower is a package of Matlab-files and is developed for solving power flow problems [13]. Each layout investigated in this master thesis is represented in Matpower by its 88 turbines, the existing distribution cables and the additional reserve connections. Only the IA system is included in the calculations and not the transmission system. Both the input and output data is explained in this section, together with examples in Matpower.

In Matpower, the user may choose among different power flow methods, like the Gauss-Seidel method, Newton's method and Fast Decoupled Power Flow Method.

The default option, Newton's method, is chosen to do the load flow calculations in this master thesis.

As in an ordinary load flow analysis, the different buses in the system are classified using the principles in [13], and the connection between them (branches) are decided. The buses are classified either as a reference/slack bus, PV bus or PQ bus. The first generator bus is set to a slack bus, while the other generator buses are set to PV buses, as shown in Figure 7.1. Each OSP is set to a PQ bus, with approximate power demand equal to half of the capacity of the wind farm (summing up to the total capacity of the wind farm).

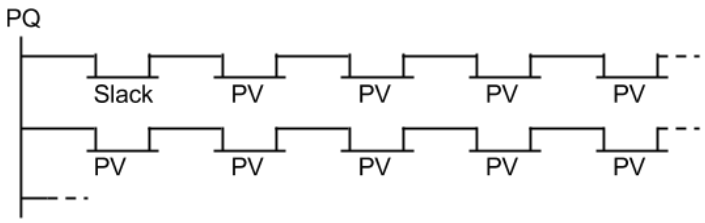

Figure 7.1: The classification of buses in Matpower.

In Matpower, both OSPs are included in the same script, but are not connected by branches. This is done to prevent the program from running several times for the same system investigated. It is also easier to see the system as a whole when the user only has one implementation to focus on.

Some of the Matpower bus input data is shown in Figure 7.2. In the two columns to the left, the bus number (1-90) and the bus type (1=PQ, 2=PV and 3=slack) is shown. Other important columns are the power demand (Pd and Qd) and the voltage limits (Vmax and Vmin).

```
%% bus data
%   bus_i   type    Pd  Qd  Gs  Bs  area    Vm  Va  baseKV  zone    Vmax    Vmin
mpc.bus = [
    1   1   155 0   0   0   1   1   0   33  1   1.1 0.9;
    2   3   0   0   0   0   1   1   0   33  1   1.1 0.9;
    3   2   0   0   0   0   1   1   0   33  1   1.1 0.9;
    4   2   0   0   0   0   1   1   0   33  1   1.1 0.9;
    5   2   0   0   0   0   1   1   0   33  1   1.1 0.9;
    6   2   0   0   0   0   1   1   0   33  1   1.1 0.9;
```

Figure 7.2: The bus input data in Matpower.

A section of the generator input data is shown in Figure 7.3. The column all the way to the left is the number of the bus where the generator is connected. The

power generation (Pg and Qg) is in the next two columns. The small "p" in this section refers to the power generation in the WTG, and is varied depending on the production level in the system. Initially, this p is equal to 3.6 MW.

```
%% generator data
%   bus Pg  Qg  Qmax    Qmin    Vg  mBase   status  Pmax    Pmin    Pc1 Pc2 Qc1min  Qc1max  Qc
mpc.gen = [
    2   p   0   999 -999    1   p   1   p   0   0   0   0   0   0   0   0   0   0   0;
    3   p   0   999 -999    1   p   1   p   0   0   0   0   0   0   0   0   0   0   0;
    4   p   0   999 -999    1   p   1   p   0   0   0   0   0   0   0   0   0   0   0;
    5   p   0   999 -999    1   p   1   p   0   0   0   0   0   0   0   0   0   0   0;
    6   p   0   999 -999    1   p   1   p   0   0   0   0   0   0   0   0   0   0   0;
```

Figure 7.3: The generator input data in Matpower.

The branch input data for the first radial is shown in Figure 7.4. This is an important section, and shows the connection between the buses (from bus and to bus). The cable data is inserted in this part, which is the AC resistance (r), reactance (x) and line charging susceptance (b) in p.u. for each cable. In steady state the cable status in column 11 is set to 0 for the reserve connections and 1 for the existing radial connections. To simulate a fault in a cable this status is set to zero.

```
%% branch data
%   fbus    tbus    r   x   b   rateA   rateB   rateC   ratio   angle   status  angmin  angmax
mpc.branch = [
    2   1   0.0001853   0.0002581   0.00000021  41 41   41  0   0   1   -360    360;
    3   2   0.0002122   0.0002955   0.00000024  41 41   41  0   0   1   -360    360;
    4   3   0.0002345   0.0003266   0.00000026  41 41   41  0   0   1   -360    360;
    5   4   0.0003439   0.0003224   0.00000018  28 28   28  0   0   1   -360    360;
    6   5   0.0003800   0.0003562   0.00000020  28 28   28  0   0   1   -360    360;
    7   6   0.0004463   0.0004184   0.00000023  28 28   28  0   0   1   -360    360;
    8   7   0.0003800   0.0003562   0.00000020  28 28   28  0   0   1   -360    360;
    9   8   0.0003800   0.0003562   0.00000020  28 28   28  0   0   1   -360    360;
```

Figure 7.4: The branch input data in Matpower.

The output from the Matpower program is an overview of the bus voltage, generation and load, as shown in Figure 7.5. The branch power flow and losses are also included, illustrated in Figure 7.6, and are used in this master thesis to compare with the cable capacities.

Conventional load flow methods, as the Newton Raphson method used in this master thesis, are not always guaranteed to converge for distribution systems. A distribution system with high R/X ratio can create ill-conditioning in the Jacobian, and may lead to non-convergence. However, lack of convergence does not necessarily mean the absence of a feasible solution. In such situations alternative algorithmic approaches [35] [36] should be investigated for solving the load flow

Bus #	Voltage Mag(pu)	Voltage Ang(deg)	Generation P (MW)	Generation Q (MVAr)	Load P (MW)	Load Q (MVAr)
1	0.999	-0.118	-	-	156.50	0.00
2	1.000	0.000*	3.29	17.32	-	-
3	1.000	0.178	3.60	-2.48	-	-
4	1.000	0.347	3.60	3.75	-	-
5	1.000	0.543	3.60	-3.73	-	-
6	1.000	0.717	3.60	-3.76	-	-

Figure 7.5: The bus output data from Matpower.

Brnch #	From Bus	To Bus	From Bus Injection P (MW)	From Bus Injection Q (MVAr)	To Bus Injection P (MW)	To Bus Injection Q (MVAr)	Loss (I^2 * Z) P (MW)	Loss (I^2 * Z) Q (MVAr)
1	2	1	28.24	-0.65	-28.19	0.70	0.041	0.06
2	3	2	25.00	-17.89	-24.94	17.97	0.056	0.08
3	4	3	21.44	-15.35	-21.40	15.41	0.045	0.06
4	5	4	17.91	-19.04	-17.84	19.10	0.065	0.06
5	6	5	14.35	-15.27	-14.31	15.31	0.046	0.04
6	7	6	10.79	-11.47	-10.75	11.50	0.031	0.03

Figure 7.6: The branch output data from Matpower.

equations. In this master thesis, the R/X ratio for the system was not high enough to create convergence issues, and the standard Matpower load package could be used.

Due to the availability of the program and simple user interface the Matpower package was chosen to investigate basic power flow problems in the system.

7.2 Steps in Power Flow Analysis

When doing the power flow simulations the function "runpf" in Matpower is used. This function takes the different cases (Layout 1, Layout 2 etc.) as input, and generates the output as shown in the previous section. This function does power flow simulations without considering the MVA limits, which have to be investigated manually by the user.

The following steps are used when investigating the power flows in each layout:

1. Failures are simulated setting the cable status to 0. The applicable reserve connection status is set to 1.

2. Start by looking at the "worst case" failures in each radial to find the weak

cables in the system. The worst case is usually a failure in one of the cables located closest to the OSP.

3. If the power flows in the cables are exceeding the cable capacity given, make a note of the cables with exceeding power and the real power flow.
4. Lower the power production level in the wind turbine generators, and find the maximum power generation possible without exceeding the cable capacities during the worst case failure.
5. Compare the different layouts using various power production levels.

The power flow calculations from Matpower are used when determining the optimal reserve connections in the Sheringham Shoal offshore wind farm, and when discussing various actions that should be taken to prevent overloading of the IA cables in the system.

Chapter 8

Economic Analysis

In this chapter, the economic analysis used in the master thesis is introduced. An economic analysis is often conducted to see if the potential investments are economically reasonable or not. An economic analysis may be carried out in different ways, investigating different economical aspects of the system. In an electrical system, these may be the investment cost, operational and maintenance cost, cost of energy losses and energy not delivered, and of course the income generated in the system. A common thread in different economic analyses is the comparison of money going out vs money coming in.

The economic analysis in this master thesis is conducted by comparing the additional investment costs (going out) with the potential income (coming in) over the next 20 years.

8.1 The Additional Investment Cost

When calculating the investment cost for each layout, only the additional cost of the reserve connections are included. The cost of the existing turbines and cables are not included, since these are the same for all layouts. Also the maintenance and operational costs are excluded, as they are assumed to be equal in each case. The costs that are included is the cost of the components (the material), also called the supply cost, and the installation cost (cost of installing the component).

The additional cables are the only components that are included in the cost calculations. Potential CBs, DSs and RSs are not included since the cost of the breaker installations on already existing buses was hard to determine.

The length of each cable is determined in Chapter 6, and is used to calculate the cable supply cost and the installation cost using the values in Table 8.1. These are typical values given by Statkraft, in addition to using data from [37]. In Table 8.1 the cost of the 33 kV cable with 185 mm^2 cross section is shown, in addition to both the 33 kV cable with 400 mm^2 cross section and the 132 kV cable with 630 mm^2 cross section, used in Layout 5.

	Cost [£/m]
33 kV cable supply, 185 mm^2	160
33 kV cable supply, 400 mm^2	200
33 kV cable installation	400
132 kV cable supply, 630 mm^2	300
132 kV cable installation	400

Table 8.1: Cost of additional cables in the reserve connections.

Another aspect investigated in the sensitivity analysis is the installation of more disconnector switches in the system. The price of these switches was hard to find, and several cost alternatives are investigated in Chapter 10.

8.2 The Potential Income

The income from each system is found by calculating the potential income one may get from the saved energy in the various reserve connection layouts. The END in each layout, calculated in the reliability analysis, is compared with the END in the Base Case, investigating how much the END has decreased by installing reserve connections. A 40 % value is used, which is the annual expected production for an offshore wind farm [14], and the income is calculated as explained below. The data used in the calculations is shown in Table 8.2.

Lifetime	20 years	
Energy price *	27.00 €/MWh	21.31 £/MWh

*Per 20.05.2016

Table 8.2: Data used in the potential income calculations.

In [16], the expected lifetime of the Sheringham Shoal wind farm is set to 25 years. Since the wind farm was built in 2012, and some years have to be assumed used for building the potential reserve connections, the remaining period of the wind

farm is set to 20 years. The British energy price is found in [38], a continuously updated overview of the energy price.

The following steps are used to calculate the potential income:

1. The expected END in both the Base Case and the chosen layout is found by taking 40 % of the full production END, calculated in the reliability analysis.
2. The additional energy delivered per year in the chosen layout, is calculated by looking at the difference between the expected END in the Base Case and the reserve connection layout.
3. The additional energy per year is multiplied with the number of years in the period, and the total additional energy is found over the whole period.
4. The potential income is found by multiplying the additional energy with the value of the energy, the energy price.

The potential income calculated is then compared with the investment cost calculated in the previous section, and one can easily see if the investment is economically reasonable or not. This is done for all layouts.

Chapter 9

Sensitivity Analysis

A sensitivity analysis measures the model output variance against the variance in the model inputs [39]. It can be used to understand the dependency of each model input, and various methods exist to investigate the relation between the inputs and the output. In this chapter, the different parameters investigated are presented and the variance of the inputs is decided.

In the master thesis five different input parameters are investigated:

1. The cable failure rate.
2. The cable MTTR.
3. The manual disconnecting time.
4. Installation of more disconnector switches.
5. The energy price.

A simple sensitivity analysis is made, varying the different input parameters and looking at the model output variance. The first four parameters in the list above are used in the reliability model, and analyzed using cost considerations. The remaining parameter is used only in the cost model.

The parameters chosen are inputs that are not consistent and may vary, both now and in the future. Several parameters may correlate, for example the failure rate and the MTTR during summer, but still only one parameter is varied at a time.

9.1 The Cable Failure Rate

In Chapter 5, the cable failure rate is set to 0.094 failures/year/km for both IA cables and export cables. When looking at different studies, various failure rates are applied, and there is no consistent failure rate used. This may be because wind power generation, and especially offshore wind, has not existed for a long period of time, and good data on this subject may therefore be hard to find.

Failure rate [1/year/km]					
IA and export cables	0.0008	0.0051	0.0094	0.0137	0.0180

Table 9.1: The failure rates used in the sensitivity analysis.

The cable failure rate is dependent on the cable itself and its strength to resist faults, the length of the cable and the weather. In [21] a worst case failure rate and a best case failure rate is introduced, and these are included in this sensitivity analysis. Failure rates from other reliability analyses like [5], [9], [10], [14] and [33] are also investigated. All failure rates included in the sensitivity analysis are listed in Table 9.1.

9.2 The Cable MTTR

The MTTR is originally set to 1440 and 720 hours/failure for the IA and export cables respectively. The MTTR is very dependent on the weather conditions, since maintenance on a cable may be challenging in bad weather. The same reliability analyses as mentioned above are used to find an appropriate range of MTTRs to investigate, shown in Table 9.2. The export cable MTTR is set to half of the IA cable MTTR, as shown in the table.

MTTR [h]			
IA Cable	720	1440	2160
Export Cable	360	720	1080

Table 9.2: The IA and export cable MTTRs used in the sensitivity analysis.

9.3 The Manual Disconnecting Time

The manual disconnecting time is, as introduced in Chapter 5, the time it takes for workers to travel out to the cable/breaker and manually disconnect it from the rest of the system. This time is set to 24 hours in Chapter 5, but may vary depending on the weather conditions. The disconnecting time decides how long some turbines may be isolated because of failures, and when they can be connected again to the rest of the system. The different disconnecting times investigated are shown in Table 9.3.

Manual disconnecting time [h]						
Cables and breakers	12	24	36	48	60	72

Table 9.3: The manual disconnecting times used in the sensitivity analysis.

9.4 Installation of Disconnector Switches

To reduce the expected outage time for each turbine, an option is to install automatic disconnector switches in conjunction with the cables. If there is a fault on a cable, it may be disconnected from the system faster by using a DS instead of manual disconnection. The isolated turbines may then be connected sooner through the reserve connection. The number of DSs installed in the system is shown in Table 9.4. This number is equal for all layouts, since the breakers only are installed on the existing radials. From a reliability perspective this is the same as setting the manual disconnecting time equal to the switching time for the DSs, ie. 1 hour in this master thesis.

Installed DSs	164

Table 9.4: The number of installed disconnector switches.

The number of breakers installed is determined by the number of cables in the system. In a 8-turbine radial, 15 DSs are installed (two for each cable, minus the one already installed at L1), and in a 7-turbine radial, 13 DSs are installed. Since there are four 8-turbine radials and eight 7-turbine radials the number of DSs is calculated to be 164, as shown in the table. No DSs are installed in the reserve connections.

Since it was hard to determine the expenses of installing DSs on already existing cables and switchgears, the cost of the DSs is also investigated. The cost is varied

from 1,000 £ to 10,000 £ for each breaker, and the different investment costs are calculated and compared to the income.

9.5 The Energy Price

The energy price is a floating parameter and is exposed to daily variations. In Chapter 8, this input is set to 27 €/MWh and was found 20.05.2016. It is hard to predict how this price will vary in the future, but various articles are envisioning an increase in the energy price due to a higher electricity demand and an increase in oil and gas prices [40], [41].

Energy price [€/MWh]	15	25	35	45	55	65

Table 9.5: The energy prices investigated in the sensitivity analysis.

The energy prices investigated are shown in Table 9.5. Both a decrease and an increase of the price is looked in to. The potential additional income is calculated for each case and compared with the investment cost.

Chapter 10

Calculations

In this chapter, three analyses are conducted, in addition to the sensitivity analysis, to find the optimal reserve connections in the system: A reliability analysis, a power flow analysis and an economic analysis. Each analysis may give different results for the reserve connections, and by comparing these results in the end an optimal layout should be possible to find. The comparison and discussion of the results are shown in Chapter 11.

10.1 The Reliability Analysis

In the reliability calculations, two indices are found for each layout, the END and the ASAI. The P_{interr} is also found, but is the same for all layouts since the failure rate is constant for all components. The reserve connections are assumed ideal, and are therefore not contributing to the P_{interr}. The indices are introduced in Chapter 4, and are used to compare the reliability for each case investigated. The END contribution from each type of component is also shown in this section, making it easy to see the weak points in the system and what components one should look more in to. The P_{interr} is calculated to be 226.9 MW/year for all the layouts, including the radial system.

For calculations of the ASAI, Equation 4.6 is utilized. When using this equation in a wind farm system instead of a regular distribution system, the number of customers, N_i, has to be decided. As done in [10], this number is set to one for each load point/turbine and the unavailability for each load point is found from the reliability calculations. The formula used may then be simplified to Equation 10.1, where T is the total number of turbines and U is the total unavailability for

the system.

$$ASAI = \frac{T * 8760 - U}{T * 8760} = \frac{8760 - \frac{U}{T}}{8760}, \tag{10.1}$$

24	Independent Cable failure									
25										
26		S1-WTG1			S1-WTG2			S1-WTG3		
27		Failure rate	Unavailability	Repair time	Failure rate	Unavailabilit	Repair time	Failure rate	Unavailabilit	Repair time
28	Ex1	0.211060926	151.9638667	720	0.21106093	151.963867	720	0.21106093	151.963867	720
29										
30	S1-L1	0.006514295	9.380584136	1440	0.00651429	9.38058414	1440	0.00651429	9.38058414	1440
31	S1-L2	0.007457801	0.178987227	24	0.0074578	10.7392336	1440	0.0074578	10.7392336	1440
32	S1-L3	0.008240709	0.197777008	24	0.00824071	0.19777701	24	0.00824071	11.8666205	1440
33	S1-L4	0.0074577	0.178984804	24	0.0074577	0.1789848	24	0.0074577	0.1789848	24
34	S1-L5	0.008240608	0.197774586	24	0.00824061	0.19777459	24	0.00824061	0.19777459	24
35	S1-L6	0.009678731	0.232289544	24	0.00967873	0.23228954	24	0.00967873	0.23228954	24
36	S1-L7	0.008240709	0.197777008	24	0.00824071	0.19777701	24	0.00824071	0.19777701	24
37	S1-L8	0.008240709	0.197777008	24	0.00824071	0.19777701	24	0.00824071	0.19777701	24
38										
39	S2-L1									
40	S2-L2									
41	S2-L3									
42	S2-L4									

Figure 10.1: The setup of the Relrad methodology in Excel.

To do the reliability calculations, the Relrad methodology is implemented in Microsoft Excel, as shown in Figure 10.1. All turbines in the system are modeled in the same Excel sheet, along with all failed components contributing to outages in the system. Figure 10.1 shows the setup for the independent cable failure calculations, but the same principle is followed for the dependent cable failures, the CB failures and the DS failures.

To distinguish between the independent and dependent failure rate in the cables, Equation 10.2 and 10.3 are used. Two events may happen if there is a failure in a cable: the nearest breaker operates or the nearest breaker do not operate. Equation 10.2 represent the failure rate for the cable where the nearest breaker is operating, and refers to the independent failure discussed in Chapter 4. The failure rate for the cable, λ_{cable}, is multiplied with the probability of the nearest breaker operating, P(functioning CB), to find the failure rate for this event. Equation 10.3 represent the failure rate for the cable when the nearest breaker fails to operate and the second breaker has to open. This is a dependent failure, and may cause several component outages. The failure rate for this second event is found by multiplying the failure rate for the cable, λ_{cable}, with the probability of the nearest breaker not operating, P(not functioning CB).

$$\lambda_{independentcablefailure} = \lambda_{cable} * P(functioningCB) \tag{10.2}$$

$$\lambda_{dependentcablefailure} = \lambda_{cable} * P(notfunctioningCB) \tag{10.3}$$

In addition to the independent and dependent cable failures, both CB and DS failures are included in the calculations. All breakers present in the system are assumed to may fail, both in the radials and in the OSPs. The breaker configurations in the radials and OSPs are illustrated in Figure 5.4 and 5.6 respectively.

The Radial System

The radial system (i.e. the existing system) has no reserve connections, only radial strings connected to the two OSPs. The energy not delivered from this system is shown in Table 10.1, listing the END due to each type of failed component, in addition to the total END for the system.

Failing component	END [GWh/year]	Percentage of total END [%]
Export Cable	46.05	60.91
IA Cable	15.31	20.25
Dependent Cable/CB	1.553	2.054
CB	11.22	14.84
DS	1.466	1.939
Total END Radial system	75.60	

Table 10.1: The energy not delivered from the radial system.

The portion of the total END for each contributing component is shown in both Table 10.1 and in Figure 10.2a. One can clearly see that a lot of the END comes from failures in the export cables, but also from failures in the IA cables and the CBs. The ASAI is calculated to be 0.97276, using Equation 10.1.

Layout 1

Layout 1 has six reserve connections, connected in both End and Split connections. The energy not delivered from this system is shown in Table 10.2, and one can see that the END is less than in the radial system, which is to be expected.

When looking at the contribution to the END from all the components in both Table 10.2 and Figure 10.2b it is again clear that the biggest failure contribution

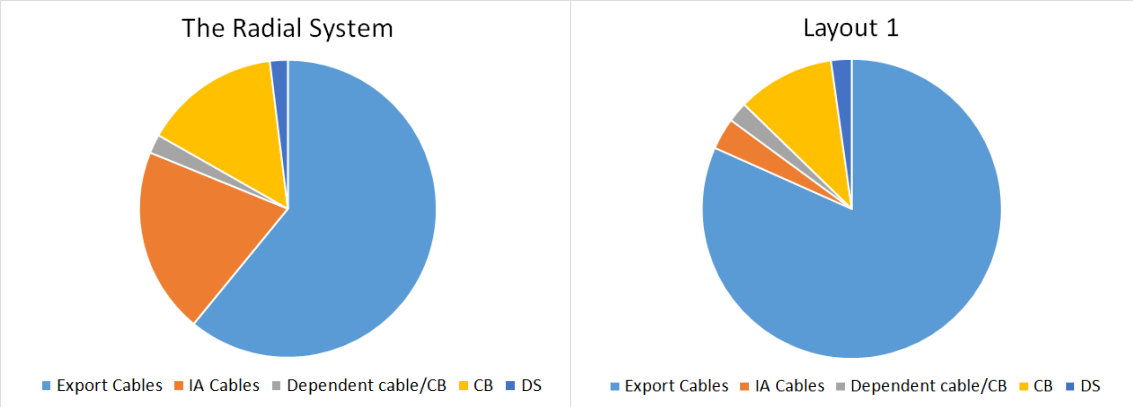

(a) The Radial System. (b) Layout 1.

Figure 10.2: The calculated END in the radial system and in Layout 1.

Failing component	END [GWh/year]	Percentage of total END [%]
Export Cable	46.05	81.68
IA Cable	1.919	3.404
Dependent Cable/CB	1.230	2.182
CB	5.931	10.52
DS	1.254	2.224
Total END Layout 1	56.38	

Table 10.2: The energy not delivered from Layout 1.

is from the export cables. Now the IA cables are contributing less to the END because of the reserve connections. The ASAI calculated from this system is 0.97968.

Layout 2

Layout 2 has four reserve connections, only End connections. In this layout, four radials are not connected to a reserve connection, which has a negative impact on the END from the IA cables. The results from the END calculations for this system is shown in Table 10.3. In this layout the total END is lower than in the radial system, but higher than in Layout 1.

From Table 10.3 and Figure 10.3a one can see that failures in the export cables

Failing component	END [GWh/year]	Percentage of total END [%]
Export Cable	46.05	74.96
IA Cable	5.276	8.589
Dependent Cable/CB	1.309	2.131
CB	7.675	12.49
DS	1.126	1.833
Total END Layout 2	61.43	

Table 10.3: The energy not delivered from Layout 2.

are responsible for 75 % of the END. The IA cables and the CBs also contribute to a large part of the END. The ASAI is calculated to be 0.97786.

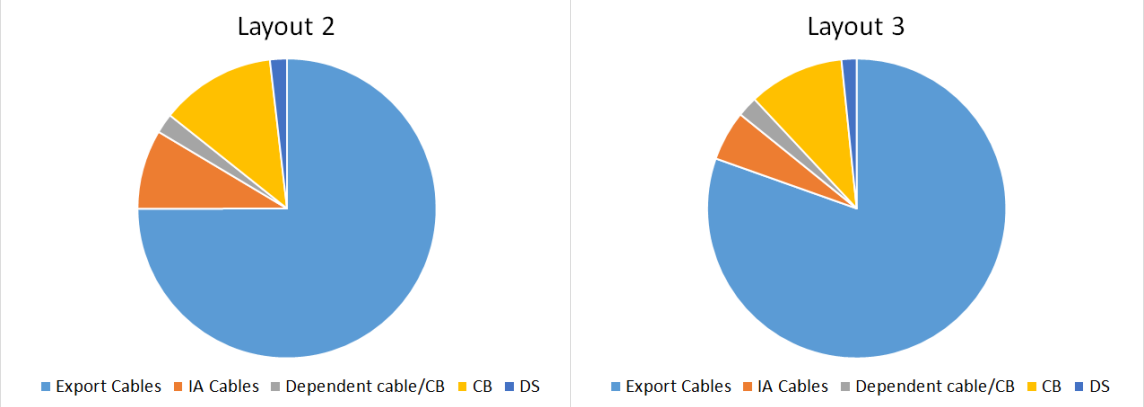

(a) Layout 2. (b) Layout 3.

Figure 10.3: The calculated END in Layout 2 and 3.

Layout 3

Layout 3 has six reserve connections, but now only Split connections are installed. In this layout, the END is still lower than in the radial system, but higher than in Layout 1, which has the same number of reserve connections. The advantages of the Split connections are explained in detail in Chapter 6, but the main benefit is that the power flow in each cable is reduced compared with the End connection, and there are fewer overloaded cables. This is discussed and investigated more in Section 10.2.

Failing component	END [GWh/year]	Percentage of total END [%]
Export Cable	46.05	80.41
IA Cable	3.088	5.392
Dependent Cable/CB	1.265	2.209
CB	5.931	10.36
DS	0.9373	1.637
Total END Layout 3	57.27	

Table 10.4: The energy not delivered from Layout 3.

The portion of the total END for each component is shown in Table 10.4 and Figure 10.3b. As in previous layouts the export cable failures are the main contributors to the total END, with the CBs and the IA cables also contributing. The ASAI is calculated to be 0.97936.

Layout 4

In Layout 4, there are six reserve connections, but now the two OSPs are indirectly connected through two of the End connections. By doing this, the END is reduced significantly, as shown in Table 10.5. Now a lot of power go through the reserve connections between the two OSPs, if a failure occur in one of the export cables. This is investigated further in the power flow analysis in Section 10.2

Failing component	END [GWh/year]	Percentage of total END [%]
Export Cable	1.605	16.49
IA Cable	1.108	11.38
Dependent Cable/CB	0.1236	1.270
CB	5.931	60.93
DS	0.9663	9.927
Total END Layout 4	9.734	

Table 10.5: The energy not delivered from Layout 4.

The END contribution from each failed component is shown in Table 10.5 and Figure 10.4a. Now the significant END contribution has shifted over to the CBs from the export cables. The CBs and DSs are contributing almost the same as

before, but now the remaining components have reduced their contribution to the END. The ASAI has increased and is now calculated to be 0.99649.

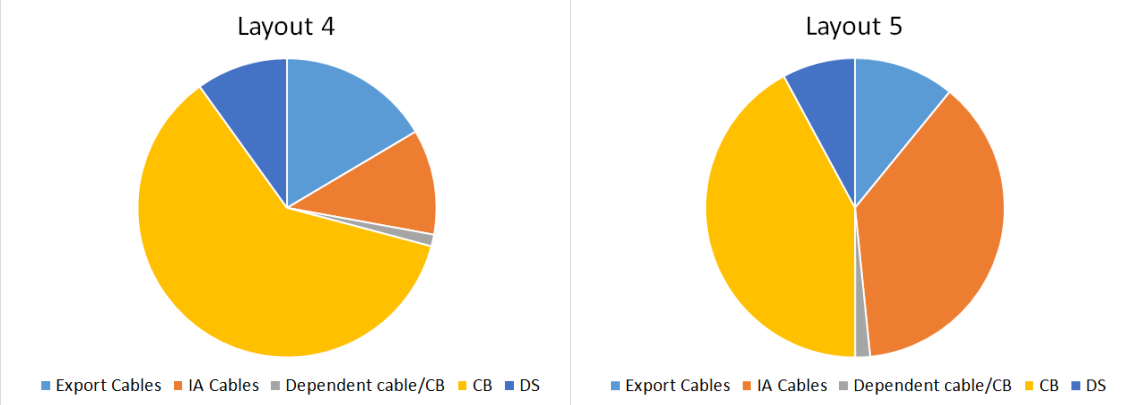

(a) Layout 4. (b) Layout 5.

Figure 10.4: The calculated END in Layout 4 and 5.

Layout 5

Layout 5 has five reserve connections, including one direct connection between the OSPs. This reserve connection has a larger cross section and a higher rating than the reserve connections in Layout 4, which has to be taken into account when doing the power flow analysis. In this layout, four of the radials are not connected to a reserve connection, which has a negative impact on the END from the IA cables, as shown in Table 10.6.

Failing component	END [GWh/year]	Percentage of total END [%]
Export Cable	1.535	10.90
IA Cable	5.276	37.47
Dependent Cable/CB	0.2251	1.599
CB	5.931	42.12
DS	1.112	7.898
Total END Layout 5	14.08	

Table 10.6: The energy not delivered from Layout 5.

From Table 10.6 and Figure 10.4b one can see that the CBs and the IA cables are contributing the most to the END.

10.2 Power Flow Analysis

The power flow analysis is conducted following the steps in Chapter 7. The different production levels investigated are 100 %, 70 % and 60 % production. Faulty cables are simulated in each layout, and the overloaded cables are found. An overloaded cable is in this analysis defined as a cable with power flow exceeding the capacity of the cable. In each layout, the simulated faulty connection, the following reserve connection and type of connection is shown in a table. Only some of the failures in each layout are shown in this section, the rest are shown in Appendix F. In the table, also the overloaded cables related to the faulty cable are listed, along with the capacity of the cable (S_{cap}) and the real power flow ($P_{ex.cable}$) calculated by Matpower. The power delivered to the two OSPs (P_{load}) and the losses in the system (P_{loss}) are also shown. The capacity limits used are the ones introduced in Chapter 5: 41 MVA for the 400 mm^2 cross section cables and 28 MVA for the 185 mm^2 cross section cables. In Layout 5, the 630 mm^2 cross section cable has a 183 MVA capacity.

The reactive power is also calculated by Matpower, but is not included in this power flow analysis. This because the values found by the program not can be assumed to be accurate, since limited reactive power data is given by the user. An example is that all the reactive power production in one radial is set to be on only one of the turbines, which not necessarily is the case. This negligence of reactive power production is handled when investigating the real power flow and the capacities, by assuming that a small amount of the capacity in the cable should be available for the reactive power. An example that may explain better is if the capacity is 28 MVA and the real power is 27 MW, then we may assume the cable is overloaded because of the additional reactive power in the cable.

In the results shown, only the cables with exceeding powers are included. The overloaded cables are shown using both a table and an illustration of the overloaded cables. When comparing the power flow and the cable capacity, a small margin is included due to the reactive power neglected.

The Radial System

In the radial system, no reserve connections are added to the 90 bus system in Matpower. Of the 90 buses, there are two PQ buses, one slack bus and 87 PV buses. When running this system in Matpower, none of the cables are exceeding their capacity limits, as expected. The largest power flow in the 41 MVA cables is 28.5 MW (8-turbine radial), and the maximum power flow in the 28 MVA cables

is 17.9 MW.

Layout 1

In Layout 1, power flow in six reserve connections is investigated. Six lines located close to the OSP is set to faulty lines (status = 0) and six reserve connections are set to operational lines (status = 1).

The power flow in two of the reserve connections in Layout 1 is shown in Table 10.7. The first connection is an End connection, the second is a Split connection. If a worst case failure occur in one of the radials during full production and an End connection is used, the opposing radial is clearly overloaded, as shown in the table. This is also shown in red in Figure 10.5. In the Split connection however, only the cables located closest to the OSP are overloaded, due to the placement of the connection. This is shown in both Table 10.7 and Figure 10.6.

Faulty connection	Reserve connection	Type of reserve connection	P_{load} [MW]	P_{loss} [MW]	Cables with exceeding power	S_{cap} [MVA]	$P_{ex.cable}$ [MW]
OSP1 - D3	A1 - A2	End	310.5	5.33	OSP1 - C3	41.0	51.6
					C3 - D2	41.0	48.2
					D2 - C2	28.0	45.1
					C2 - B3	28.0	41.8
					B3 - A3	28.0	38.6
					A3 - B2	28.0	35.2
					B2 - A2	28.0	31.8
					A1 - A2 (res.)	28.0	28.2
OSP1 - E3	G3 - F4	Split	312.5	3.82	OSP1 - D4	41.0	49.3
					D4 - E4	41.0	45.9
					E4 - F4	28.0	42.7

Table 10.7: The power flow results for two reserve connections in Layout 1, using a 100 % production level.

If failures in Layout 1 occur when the system is at a 60 % production level, the number of overloaded cables is reduced, as shown in Table 10.8. The power flow in the previously overloaded cables, $P_{ex.cable}$, is now reduced to below the capacity limit, S_{cap}. Some of the IA cables however, are still on a critical level where the real power is below the capacity limit, but leaving limited "space" for the reactive

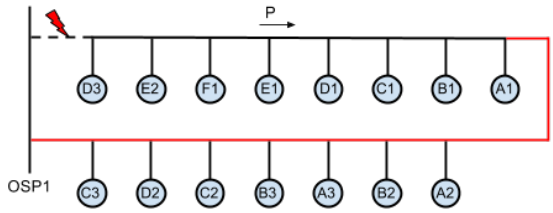

Figure 10.5: The overloaded cables in an End connection, Layout 1.

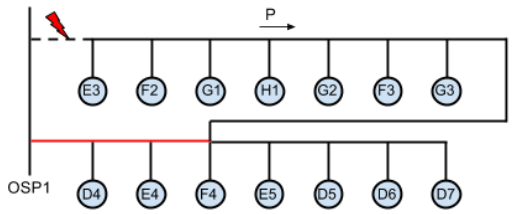

Figure 10.6: The overloaded cables in a Split connection, Layout 1.

power. This production level is therefore chosen as the maximum production level, where the system is able to withstand all failures without overloading any cables.

Faulty connection	Reserve connection	Type of reserve connection	P_{load} [MW]	P_{loss} [MW]	Cables with exceeding power	S_{cap} [MVA]	$P_{ex.cable}$ [MW]
OSP1 - D3	A1 - A2	End	186.5	3.20	OSP1 - C3	41.0	31.0
					C3 - D2	41.0	28.9
					D2 - C2	28.0	27.0
					C2 - B3	28.0	25.1
					B3 - A3	28.0	23.1
					A3 - B2	28.0	21.1
					B2 - A2	28.0	19.1
					A1 - A2 (res.)	28.0	16.9
OSP1 - E3	G3 - F4	Split	187.5	2.29	OSP1 - D4	41.0	29.6
					D4 - E4	41.0	27.6
					E4 - F4	28.0	25.6

Table 10.8: The power flow results for two reserve connections in Layout 1, using a 60 % production level.

Layout 2

In Layout 2, only four reserve connections are installed, all End connections. Two of the connections are also used in Layout 1, but now two new connections are introduced. One of these connections is shown in Table 10.9 during a critical failure at full production. As in Layout 1, this End connection is overloading the opposing radial, making the power flow exceed the capacity of the cable, as shown in Figure 10.7.

Faulty connection	Reserve connection	Type of reserve connection	P_{load} [MW]	P_{loss} [MW]	Cables with exceeding power	S_{cap} [MVA]	$P_{ex.cable}$ [MW]
OSP2 - I5	J6 - K6	End	311.0	5.42	OSP2 - J4	41.0	51.4
					J4 - J3	41.0	48.0
					J3 - K2	28.0	44.8
					K2 - K3	28.0	41.7
					K3 - K4	28.0	38.5
					K4 - K5	28.0	35.2
					K5 - J6	28.0	31.8
					K6 - K7 (res.)	28.0	28.2

Table 10.9: The power flow results for one reserve connection in Layout 2, using a 100 % production level.

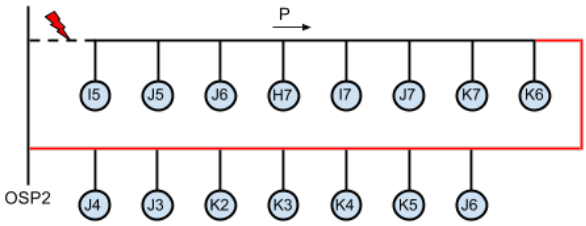

Figure 10.7: The overloaded cables in an End connection, Layout 2.

If the production level however is reduced to 60 %, as done in Layout 1, the power flow in the cables is also being reduced, as shown in Table 10.10. The power flow is now just within the capacity limits and the cables may be operated safely.

Faulty connection	Reserve connection	Type of reserve connection	P_{load} [MW]	P_{loss} [MW]	Cables with exceeding power	S_{cap} [MVA]	$P_{ex.cable}$ [MW]
OSP2 - I5	J6 - K6	End	186.5	40.08	OSP2 - J4	41.0	30.8
					J4 - J3	41.0	28.8
					J3 - K2	28.0	26.9
					K2 - K3	28.0	25.0
					K3 - K4	28.0	23.1
					K4 - K5	28.0	21.1
					K5 - J6	28.0	19.1
					J6 - K6 (res.)	28.0	16.9

Table 10.10: The power flow results for one reserve connection in Layout 2, using a 60 % production level.

Layout 3

In Layout 3, six Split connections are installed, two of them listed in Table 10.11 during a critical failure and full production. From the table it is clear to see that the location of the reserve connection is important when it comes to cable overload. The first reserve connection is located further out in the radial, and therefore several cables are exceeding their capacity, as shown in Figure 10.8. In the second connection the additional cable is located closer to the OSP, which leads to fewer overloaded IA cables, shown in Figure 10.9.

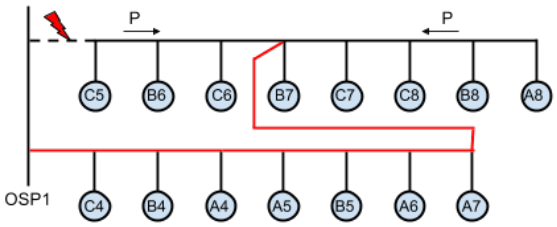

Figure 10.8: The overloaded cables in a Split connection, Layout 3.

Again the power flow and production level is reduced to 60 % in Matpower. From Table 10.12 one may see the that the power flow has decreased below the capacity limits for the IA cables, for both 400 and 185 mm^2 cross section.

Faulty connection	Reserve connection	Type of reserve connection	P_{load} [MW]	P_{loss} [MW]	Cables with exceeding power	S_{cap} [MVA]	$P_{ex.cable}$ [MW]
OSP1 - C5	A7 - B7	Split	311.0	4.99	OSP1 - C4	41.0	51.3
					C4 - B4	41.0	47.9
					B4 - A4	28.0	44.8
					A4 - A5	28.0	41.6
					A5 - B5	28.0	38.3
					B5 - A6	28.0	35.0
					A6 - A7	28.0	31.6
					A7 - B7 (res.)	28.0	28.2
OSP2 - I4	K1 - K2	Split	312.5	3.78	OSP2 - J4	41.0	49.2
					J4 - J3	41.0	45.9
					J3 - K2	28.0	42.7

Table 10.11: The power flow results for two reserve connections in Layout 3, using a 100 % production level.

Faulty connection	Reserve connection	Type of reserve connection	P_{load} (MW)	P_{loss} (MW)	Cables with exceeding power	S_{cap} (MVA)	$P_{ex.cable}$ (MW)
OSP1 - C5	A7 - B7	Split	186.5	2.97	OSP1 - C4	41.0	30.6
					C4 - B4	41.0	28.5
					B4 - A4	28.0	26.6
					A4 - A5	28.0	24.8
					A5 - B5	28.0	22.8
					B5 - A6	28.0	20.8
					A6 - A7	28.0	18.8
					A7 - B7 (res.)	28.0	16.7
OSP2 - I4	K1 - K2	Split	187.5	2.26	OSP2 - J4	41.0	29.5
					J4 - J3	41.0	27.4
					J3 - K2	28.0	25.5
					K1 - K2 (res.)	28.0	14.8

Table 10.12: The power flow results for two reserve connections in Layout 3, using a 60 % production level.

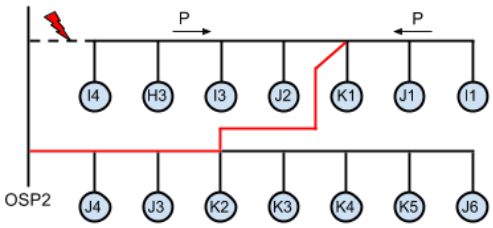

Figure 10.9: The overloaded cables in a Split connection, Layout 3.

Layout 4

Layout 4 has four of the same reserve connections as Layout 1, but with two additional connections between Area 1 and 2. Two of the regular connections (not between the areas) are shown in Table 10.13 with a 100 % production level. As before several cables are overloaded, as shown in Figure 10.10 and 10.11.

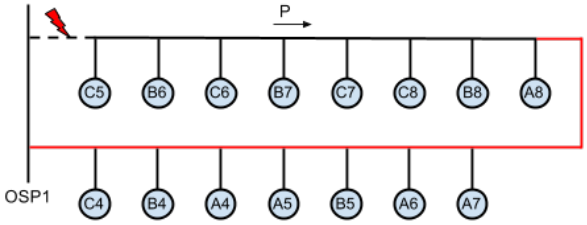

Figure 10.10: The overloaded cables in an End connection, Layout 4.

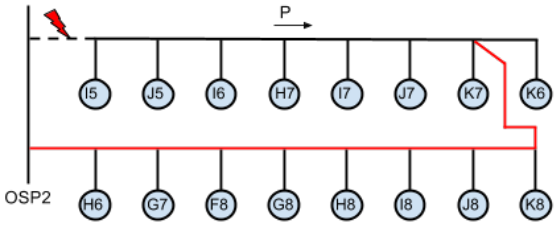

Figure 10.11: The overloaded cables in an End connection, Layout 4.

The same reserve connections, but now with a 60 % production level, is shown in Table 10.14. As previous layouts, the power flow is within the cable capacity limits.

Faulty connection	Reserve connection	Type of reserve connection	P_{load} [MW]	P_{loss} [MW]	Cables with exceeding power	S_{cap} [MVA]	$P_{ex.cable}$ [MW]
OSP1 - C5	A7 - A8	End	310.5	5.18	OSP1 - C4	41.0	50.8
					C4 - B4	41.0	47.4
					B4 - A4	28.0	44.2
					A4 - A5	28.0	41.1
					A5 - B5	28.0	37.8
					B5 - A6	28.0	34.4
					A6 - A7	28.0	31.1
					A7 - A8 (res.)	28.0	27.7
OSP2 - I5	K7 - K8	Split	311.0	5.36	OSP2 - H6	41.0	55.0
					H6 - G7	41.0	51.7
					G7 - F8	41.0	48.3
					F8 - G8	28.0	45.1
					G8 - H8	28.0	41.9
					H8 - I8	28.0	38.7
					I8 - J8	28.0	35.3
					J8 - K8	28.0	32.0
					K7 - K8 (res.)	28.0	28.5

Table 10.13: The power flow results for two reserve connections in Layout 4, using a 100 % production level.

When looking at Layout 4 and its reserve connections, it is clear that the most vulnerable cables in the system are the cables between the two areas, connection D7-E6 and G3-H2. If there is a fault in one of the export cables, these two connections are supposed to transfer all the power from one area to the other area, which is at least 150 MW at full production (75 MW per connection). When the capacity of both the additional cables and many of the cables in the radial are only 28 MVA, the cables are going to be overloaded.

Due to failed convergence in the Matpower program, an approximate estimate is done in Table 10.15, to calculate the critical power flows in the system. The estimate is based on the power flow being higher closer to the OSP, than further out in the radial. The connection investigated is shown in Figure 10.12, where L3 is set to be a "critical cable", since this is the most overloaded cable in the radial. In the table, the approximate power flow in L3 is calculated, summing the power from the reserve connections and the power from already connected turbines in the radial (F4, E5, D5, D6 and D7). Different production levels are investigated.

Faulty connection	Reserve connection	Type of reserve connection	P_{load} [MW]	P_{loss} [MW]	Cables with exceeding power	S_{cap} [MVA]	$P_{ex.cable}$ [MW]
OSP1 - C5	A7 - A8	End	186.5	3.13	OSP1 - C4	41.0	30.6
					C4 - B4	41.0	28.5
					B4 - A4	28.0	26.6
					A4 - A5	28.0	24.8
					A5 - B5	28.0	22.8
					B5 - A6	28.0	20.8
					A6 - A7	28.0	18.8
					A7 - A8 (res.)	28.0	16.7
OSP2 - I5	K7 - K8	Split	186.5	3.21	OSP2 - H6	41.0	33.0
					H6 - G7	41.0	31.0
					G7 - F8	41.0	29.0
					F8 - G8	28.0	27.1
					G8 - H8	28.0	25.2
					H8 - I8	28.0	23.2
					I8 - J8	28.0	21.2
					J8 - K8	28.0	19.2
					K7 - K8 (res.)	28.0	17.1

Table 10.14: The power flow results for two reserve connections in Layout 4, using a 60 % production level.

The figure shows the D7-E6 reserve connection, but applies for both connections between the areas in Layout 4. As shown in the table a production level around 30 % will reduce the power flow below the capacity limits for L3.

Production level [%]	Power flow in reserve connection [MW]	Power flow from connected turbines [MW]	Total power flow in critical cable, L3 [MW]
100	75.0	18.0	93.0
60	45.0	10.8	55.8
40	30.0	7.20	37.2
30	22.5	5.40	27.9
25	18.8	4.50	23.3

Table 10.15: The estimated power flow in the critical reserve connection and cable L3 in Layout 4.

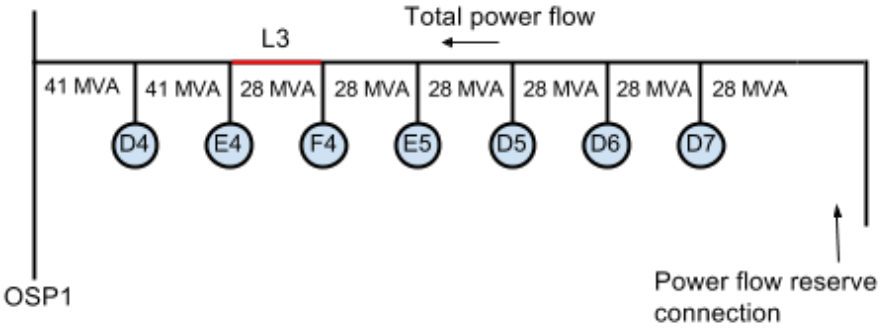

Figure 10.12: The power flow in the critical reserve connection and cable L3 in Layout 4.

Layout 5

Layout 5 has the exact same reserve connections as Layout 2, but with one additional cable between the two OSPs. One of the End connections is shown in Table 10.16, and again several cables are overloaded, as illustrated in Figure 10.13.

Faulty connection	Reserve connection	Type of reserve connection	P_{load} [MW]	P_{loss} [MW]	Cables with exceeding power	S_{cap} [MVA]	$P_{ex.cable}$ [MW]
OSP2 - I4	H2 - I1	End	311.5	4.67	OSP2 - H5	41.0	48.2
					H5 - G5	41.0	44.8
					G5 - F5	28.0	41.6
					F5 - G4	28.0	38.3
					G4 - H3	28.0	34.9
					H3 - I2	28.0	31.5
					I2 - H2	28.0	28.1

Table 10.16: The power flow results for one reserve connection in Layout 5, using a 100 % production level.

The same reserve connection with production level equal to 60 % is shown in Table 10.17. Again the power flow in the previous overloaded cables has been reduced to below the capacity limits and may be operated safely.

The direct reserve connection between the two OSPs is investigated using both a 33 kV cable and a 132 kV cable. The 33 kV cable has a capacity of 41 MVA while the 132 kV has the same capacity as the export cables, 183 MVA. An estimate is

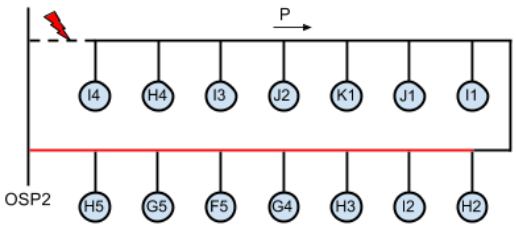

Figure 10.13: The overloaded cables in an End connection, Layout 5.

Faulty connection	Reserve connection	Type of reserve connection	P_{load} [MW]	P_{loss} [MW]	Cables with exceeding power	S_{cap} [MVA]	$P_{ex.cable}$ [MW]
OSP2 - I4	H2 - I1	End	187.0	2.80	OSP2 - H5 H5 - G5 G5 - F5 F5 - G4 G4 - H3 H3 - I2 I2 - H2	41.0 41.0 28.0 28.0 28.0 28.0 28.0	28.9 26.9 25.0 23.0 21.0 18.9 16.9

Table 10.17: The power flow results for one reserve connection in Layout 5, using a 60 % production level.

done as in Layout 4, finding the approximate power flow in the reserve connection and the critical cable, for different production levels. Since the reserve connection is installed directly to the OSP, the critical cable is now one of the export cables, instead of L3. The power flow estimates for the direct reserve connection are shown in Table 10.18, and one can see that a 60 % production level is the maximum acceptable level. In the case where a 132 kV cable is installed, the export cable is limiting the power transfer, and not the reserve connection. The 132 kV connection is able to transfer the 90 MW estimated in the table, and the system may be operated at a 60 % production level without overloading the export cable.

When using the 33 kV cable, only 41 MVA may be transferred between the areas, and a 60 % production level may therefore not be used due to the limitations in the reserve connection. An acceptable power flow in the reserve connection can therefore be accomplished by lowering the production level to around 25 %, as calculated in Table 10.18. Neither the reserve connection or the export cable is now overloaded, but the total power delivered to the PCC is significantly reduced.

Production level [%]	Power flow in reserve connection [MW]	Power flow from connected OSP [MW]	Total power flow in critical cable [MW]
100	150	150	300
60	90.0	90.0	180
40	60.0	60.0	120
30	45.0	45.0	90.0
25	37.5	37.5	75.0

Table 10.18: The estimated power flow in the critical reserve connection and export cable in Layout 5.

Manageable Failures by the End Connection

After doing the power flow calculations in Matpower, it is clear that the End connections are the most critical connections in the system, apart from the connections between the two areas. Matpower is therefore used to see how much power that may be handled by the End connection, without overloading any cables.

Matpower shows that a radial connected to an End connection may be able to handle power from two turbines in the opposing radial. For example in the A7-A8 reserve connection, if there is a failure in the cable between B8 and C8, the reserve connection and the opposing radial is able to transfer the power without overloading the cables. If there is a failure in C7-C8 however, the cables are overloaded with a small amount of power during full production. This applies for both 7-turbine and 8-turbine radials. This is used further in the discussion in Chapter 11.

10.3 Economic Analysis

In the economic analysis, both the additional investment cost for the reserve connections and the potential income is calculated. The cost and income data from Chapter 8 is used, and the results for all layouts are shown in one table. The results are discussed in Chapter 11.

10.3.1 The Additional Investment Cost

The radial system is set to have costs equal to zero, since only the additional costs are included in this analysis, and not the initial cost of the offshore wind farm. The maintenance and operational costs are not included either, since they are assumed equal for all layouts.

The total lengths of the cables installed in each layout is found in Chapter 6, and shown in Table 10.19. Using these, in addition to the cost data given in Table 8.1, the total cost for each layout is calculated and shown in Table 10.20. Both the supply and installation cost is shown in the table. Layout 5 is shown with both alternatives for the installed cable, either a 33 kV or 132 kV reserve connection.

	Layout 1	Layout 2	Layout 3	Layout 4	Layout 5, Alt.1	Layout 5, Alt.2
185 mm^2 IA cables [km]	5.20	3.50	5.05	5.20	3.50	3.50
400 mm^2 IA cables [km]	-	-	-	-	16.0	-
630 mm^2 export cables [km]	-	-	-	-	-	16.0

Table 10.19: The total lengths of the installed cables in each layout.

As shown in the table the largest part of the investment is due to the installation, and not the supply. Layout 1-4 are around the same level of investment cost, while Layout 5 is significant more expensive due to the long cable installed.

10.3.2 The Potential Income

The potential income is calculated using data given in Table 8.2. The results are shown in Table 10.21 for all layouts.

	Cost per meter [£/m]	Layout 1 [M£]	Layout 2 [M£]	Layout 3 [M£]	Layout 4 [M£]	Layout 5, Alt. 1 [M£]	Layout 5, Alt. 2 [M£]
Supply cost, 185 mm^2	160.0	0.8320	0.5600	0.8080	0.8320	0.5600	0.5600
Supply cost, 400 mm^2	200.0	0	0	0	0	3.200	0
Supply cost, 630 mm^2	300.0	0	0	0	0	0	4.800
Installation cost	400.0	2.080	1.400	2.020	2.080	7.800	7.800
Total costs		2.912	1.960	2.828	2.912	11.56	13.16

Table 10.20: The total additional cost calculated for each layout.

	Energy not delivered at rated power [GWh/year]	Energy not delivered at 40 % production level [GWh/year]	Additional energy that can be delivered per year [GWh/year]	Additional energy that can be delivered over the whole period [GWh]	Potential income over the period [M£]
Radial	75.60	30.24			
Layout 1	56.38	22.55	7.686	153.7	3.276
Layout 2	61.44	24.57	5.665	113.3	2.415
Layout 3	57.27	22.91	7.331	146.6	3.125
Layout 4	9.734	3.894	26.34	526.9	11.23
Layout 5	14.09	5.632	24.61	492.1	10.49

Table 10.21: The total potential income calculated for each layout.

The potential income from Layout 4 and 5 is clearly higher than from the other layouts, due to the reduced END in these systems. Layout 1-3 all have a potential income above 2.4 million £, while Layout 4 and 5 both have an income above 10 million £. These incomes however, have to be compared with the investment cost to get a good overview of the economy in the different systems. The profit from each alternative layout is calculated and discussed in Chapter 11.

10.4 Sensitivity Analysis

The result from the sensitivity analysis is divided in five sections, one for each input parameter varied. The sensitivity analysis is done for each layout, to see if the output results are varying.

The Cable Failure Rate

The cable failure rate is varied in the range 0.0008-0.0180 failures/year/km for all layouts. The END is calculated using the different failure rates, and is shown in Table 10.22. As shown in Figure 10.14, the END is proportional to the failure rate. The varying income is calculated as done in the economic analysis, and compared to the cost in Figure 10.16. The total income calculations are shown in Appendix G.

Failure rate [1/year/km]	END Radial [GWh/year]	END Layout 1 [GWh/year]	END Layout 2 [GWh/year]	END Layout 3 [GWh/year]	END Layout 4 [GWh/year]	END Layout 5 [GWh/year]
0.0008	18.04	11.37	13.28	11.16	7.138	7.641
0.0051	46.82	33.88	37.36	34.21	8.436	10.86
0.0094	75.60	56.38	61.43	57.27	9.734	14.08
0.0137	10.44	78.89	85.51	80.33	11.03	17.30
0.0180	133.1	101.4	109.6	103.4	12.33	20.52

Table 10.22: The calculated END for all layouts with varying failure rate.

In the radial system and in Layout 1-3, the END is varying a lot with the failure rate. The END is varying from around 10 GWh/year in the best case, to over a 100 GWh/year in the worst case. The END in Layout 4 and 5 is not varying as much as in the other layouts.

An investment is profitable as long as the income is higher than the costs. As shown in Figure 10.16, the cost in each layout is constant for all failure rates, while the income however, is varying. For the chosen failure rate in Chapter 5, Layout 1-4 is profitable, while Layout 5 is not. As the failure rate is decreased, each layout becomes unprofitable. Layout 4 is a special case, where the income is significantly higher than the cost for almost all failure rates. To make Layout 5 economically reasonable, the failure rate has to increase.

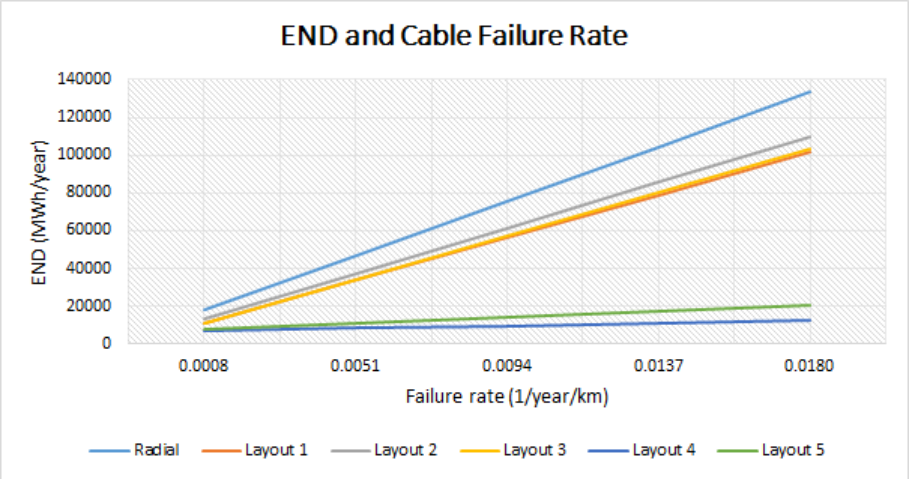

Figure 10.14: The calculated END for all layouts with varying failure rate.

The Cable MTTR

The MTTR is varied for both the IA cables and the export cables. As discussed in Chapter 9, three different MTTRs are used for the IA cables and export cables; 720, 1440 and 2160 hours for the IA cables and 360, 720 and 1080 hours for the export cables. The END is calculated using these three scenarios, and is shown in Table 10.23. The END is also proportional to the MTTR, as shown in Figure 10.15. Again the END in Layout 1-3 is varying a lot with the input parameter, but not as much in Layout 4 and 5. The output variance is not as high as with the failure rate.

MTTR IA/ export cables [h]	END Radial [GWh/ year]	END Layout 1 [GWh/ year]	END Layout 2 [GWh/ year]	END Layout 3 [GWh/ year]	END Layout 4 [GWh/ year]	END Layout 5 [GWh/ year]
720/360	44.27	32.03	35.34	32.11	9.391	11.57
1440/720	75.60	56.38	61.43	57.27	9.734	14.08
2160/1080	106.9	80.73	87.53	82.43	10.08	16.59

Table 10.23: The calculated END for all layouts with varying cable MTTR.

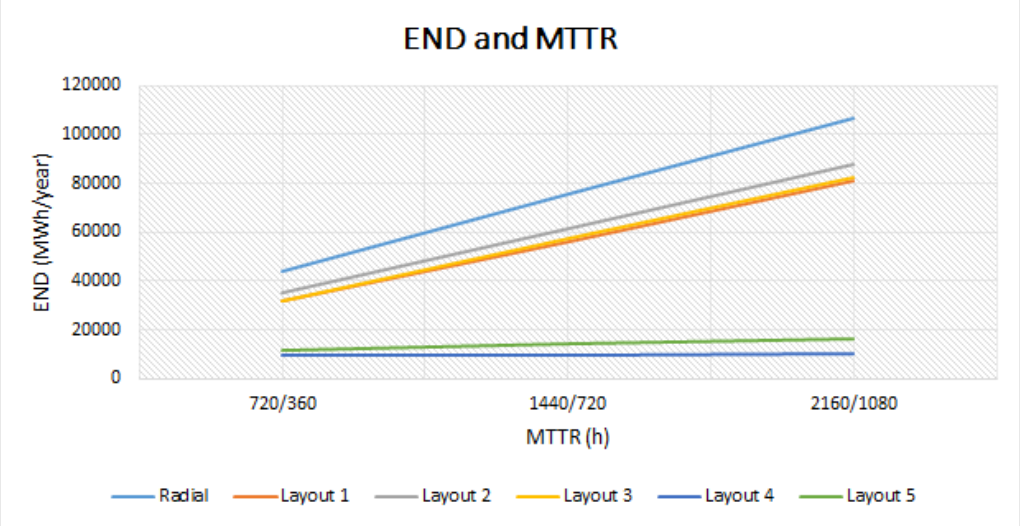

Figure 10.15: The calculated END for all layouts with varying cable MTTR.

The same cost vs income analysis is done for the MTTR, as done for the failure rate. The results are shown in Figure 10.17 and in Appendix G.

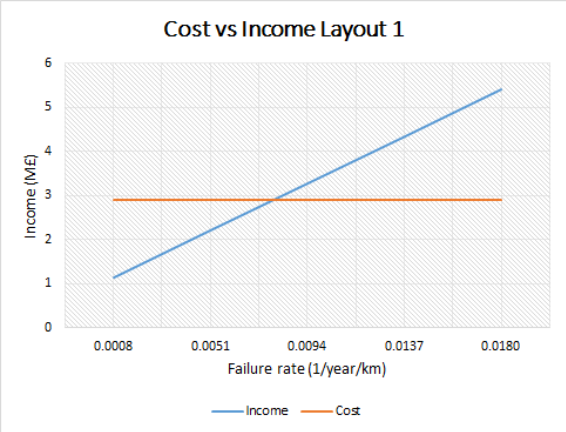

(a) Layout 1.

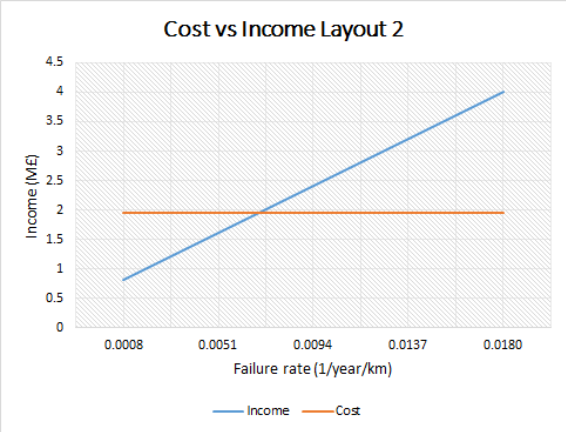

(b) Layout 2.

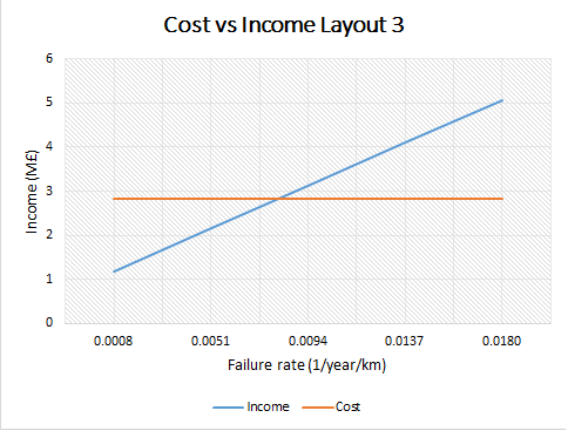

(c) Layout 3.

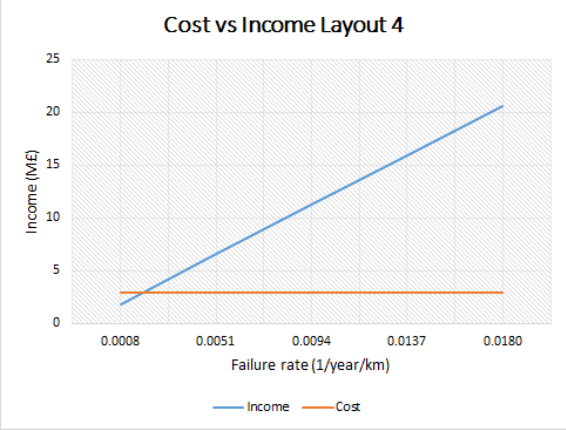

(d) Layout 4.

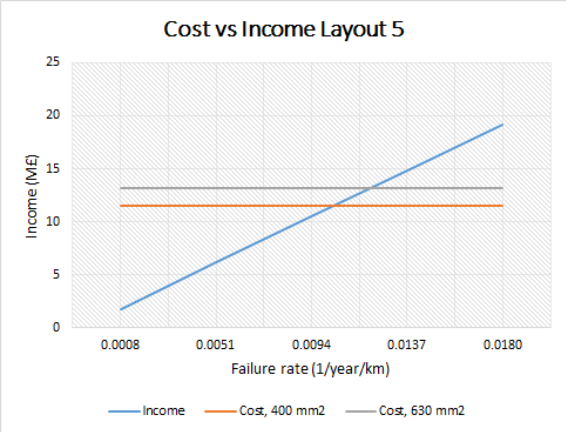

(e) Layout 5.

Figure 10.16: The cost and income with varying failure rate.

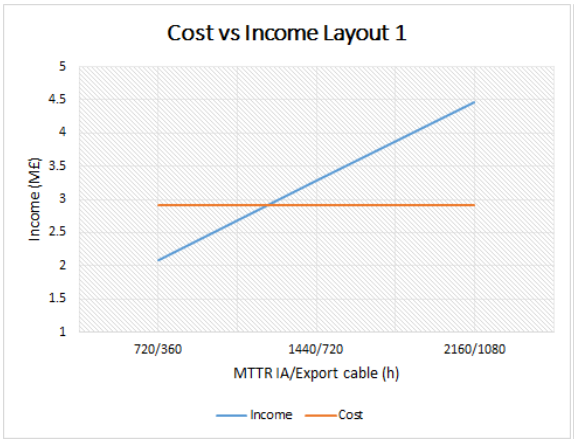

(a) Layout 1.

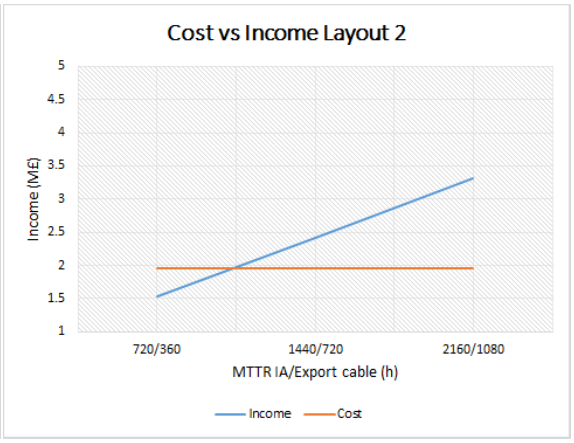

(b) Layout 2.

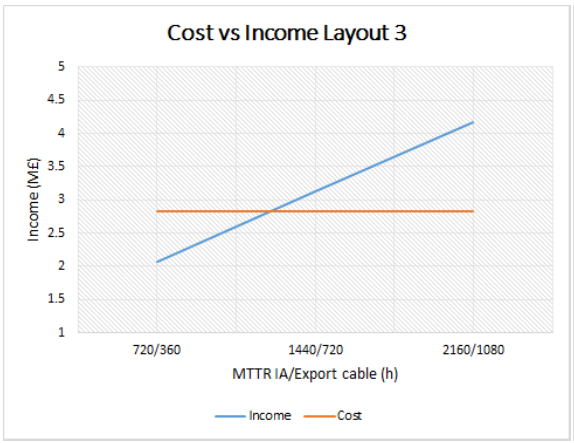

(c) Layout 3.

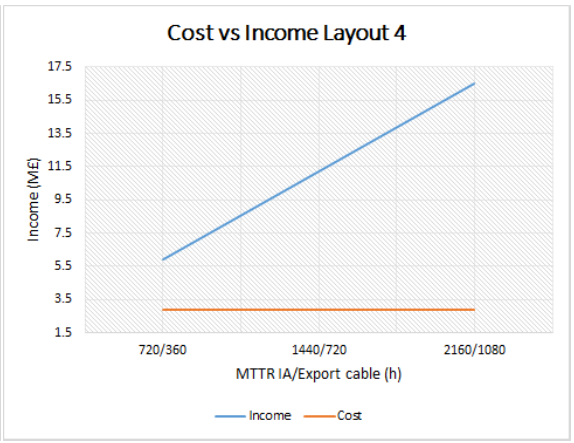

(d) Layout 4.

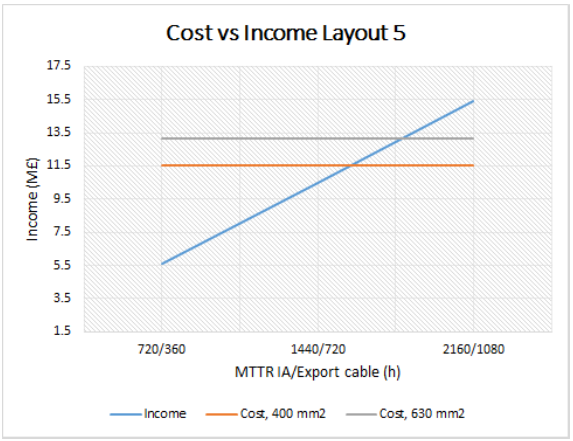

(e) Layout 5.

Figure 10.17: The cost and income with varying MTTR.

As with the failure rate, Layout 1-4 is profitable with the MTTR chosen in Chapter 5. If the MTTR however is decreased in Layout 1-3, the income drops below the cost, and the reserve connections becomes unprofitable. Layout 4 is economically reasonable for all MTTRs investigated, while Layout 5 needs a higher MTTR to become profitable.

The Manual Disconnecting Time

The manual disconnecting time is varied between 12 and 72 hours. The END is calculated for each disconnecting time, and is shown in Table 10.24 and Figure 10.18. From the figure, one may see that the calculated END is not varying much with the manual disconnecting time compared with the other parameters investigated, only around 2-5 GWh/year. When varying the disconnecting time, the END variance in Layout 4 and 5 is higher than in the other layouts, unlike the previous input parameters investigated.

Manual disconn-ecting time [h]	END Radial [GWh/ year]	END Layout 1 [GWh/ year]	END Layout 2 [GWh/ year]	END Layout 3 [GWh/ year]	END Layout 4 [GWh/ year]	END Layout 5 [GWh/ year]
12	75.19	55.60	60.86	56.86	8.266	12.70
24	75.60	56.38	61.43	57.27	9.734	14.08
36	76.00	57.17	62.01	57.68	11.20	15.46
48	76.41	57.95	62.58	58.09	12.67	16.84
60	76.82	58.73	63.15	58.51	14.14	18.22
72	77.23	59.52	63.72	58.92	15.61	19.60

Table 10.24: The calculated END for all layouts with varying manual disconnecting time.

The income from the reduced END in each layout is calculated and compared with the cost of the reserve cables, as done in the economic analysis in Section 10.3. The results are shown in Figure 10.19, and the complete calculations are shown in Appendix G. The figure shows that for Layout 1-4, the income is above the cost for all disconnecting times investigated. The income in Layout 5 is below the cost for all disconnecting times.

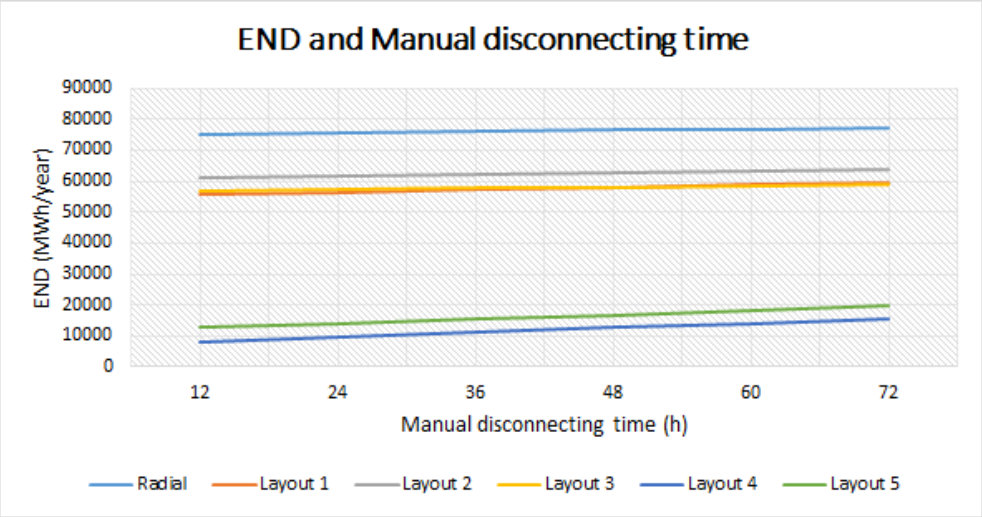

Figure 10.18: The calculated END for all layouts with varying manual disconnecting time.

Installation of More Disconnector Switches

To reduce the outage times for each turbine, an option is to install several disconnector switches to isolate the cables if a failure occur. The number of breakers installed is set to 164 in Chapter 9, and the price of each breaker is varied between 1,000-10,000 £.

	END Radial [GWh/ year]	END Layout 1 [GWh/ year]	END Layout 2 [GWh/ year]	END Layout 3 [GWh/ year]	END Layout 4 [GWh/ year]	END Layout 5 [GWh/ year]
With manual disconnection	75.60	56.38	61.43	57.27	9.734	14.08
With installed DSs	74.81	54.88	60.34	56.48	6.920	11.44

Table 10.25: The calculated END with and without additional DSs installed.

Installation of DSs reduces the END from each system, as shown in Table 10.25. The additional cost is calculated for each DS price, as shown in Figure 10.20, and compared to the income generated by installing DSs. The total cost calculations are shown in Appendix G.

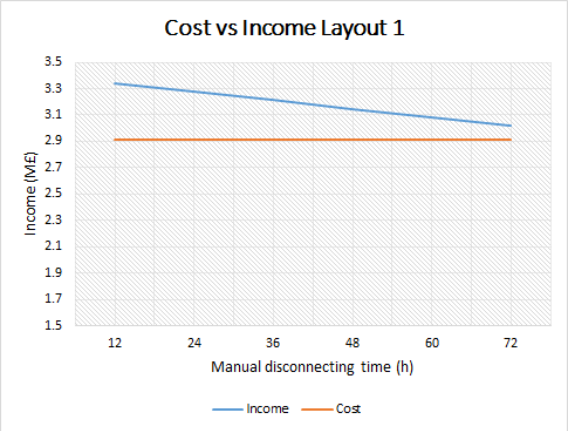

(a) Layout 1.

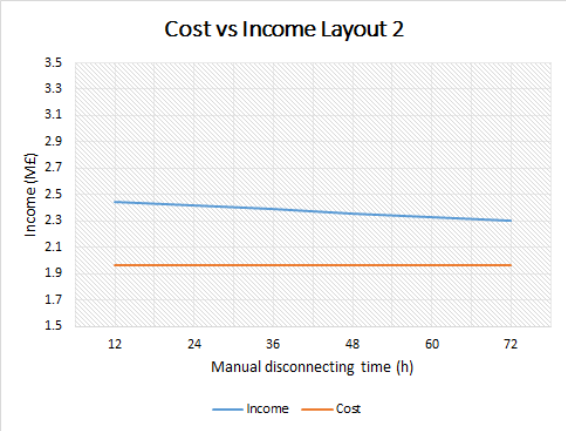

(b) Layout 2.

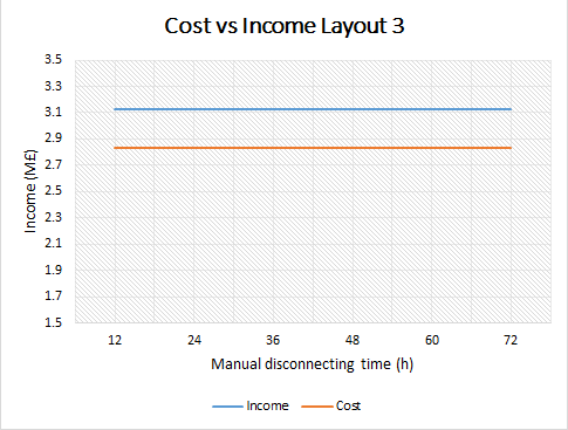

(c) Layout 3.

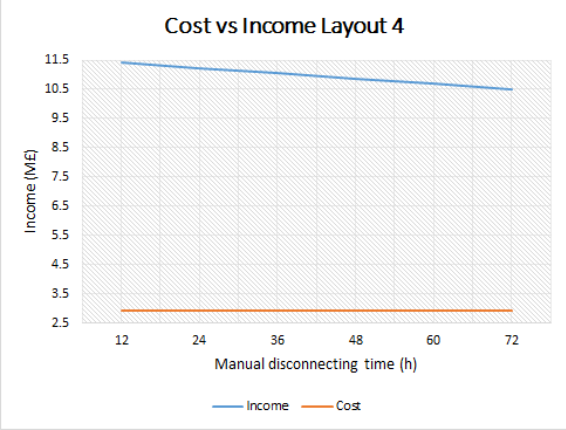

(d) Layout 4.

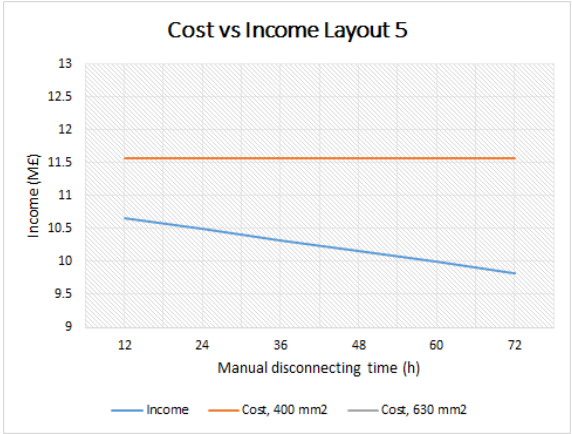

(e) Layout 5.

Figure 10.19: The cost and income with varying manual disconnecting time.

From the figure, one can see that the cost of the breakers are higher than the income in the radial system and Layout 1-3, as long as the DSs are more expensive than around 4,000 £. In Layout 4 and 5, the price of the DSs has to be lower than 7,500 £ for the installment to be profitable. In [10], the price of a 66kV DS is found to be over 40,000 £, and one may therefore assume that the 33 kV DS breakers will cost at least more than 10,000 £. The installation of the DSs may therefore be assumed non-profitable.

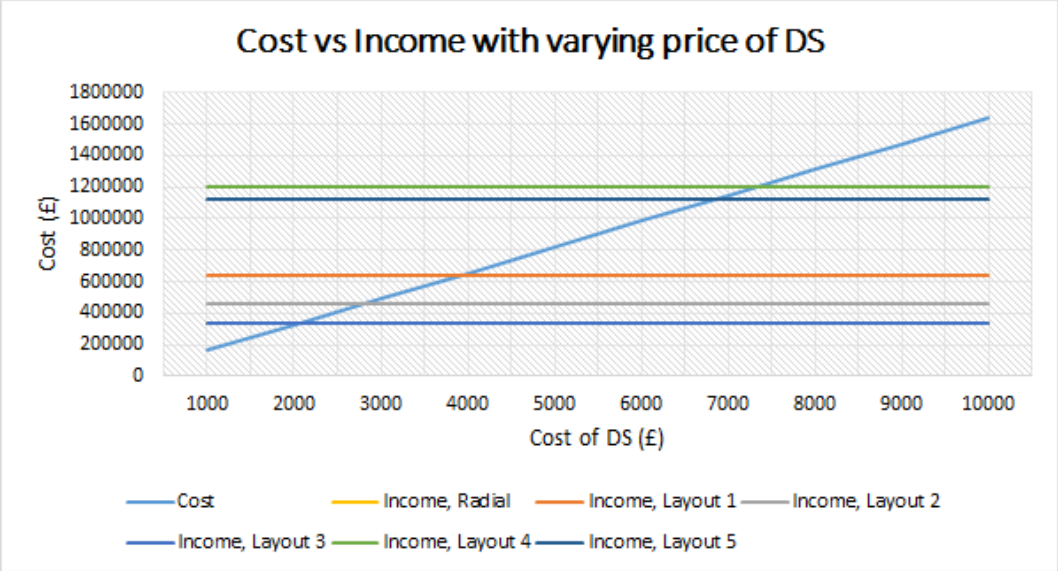

Figure 10.20: The calculated cost for the installed DSs with varying price of DS.

The Energy Price

The energy price is varied from 15 to 65 €/MWh, and the potential income is therefore also changed. The results are shown in Table 10.26 and Figure 10.21.

The varying potential income for each layout is compared with the cost calculated in Section 10.3, and shown in Figure 10.22. The energy price is most likely to increase in the future, and if the energy price increases above 34 €/MWh all layouts becomes profitable, even Layout 5.

Power price [€/MWh]	Income Layout 1 [M£]	Income Layout 2 [M£]	Income Layout 3 [M£]	Income Layout 4 [M£]	Income Layout 5 [M£]
15	1.820	1.341	1.736	6.239	5.827
25	3.033	2.236	2.893	10.40	9.712
35	4.247	3.130	4.051	14.56	13.60
45	5.460	4.024	5.208	18.72	17.48
55	6.674	4.919	6.365	22.88	21.37
65	7.887	5.813	7.523	27.04	25.25

Table 10.26: The calculated potential income for all layouts with varying energy price.

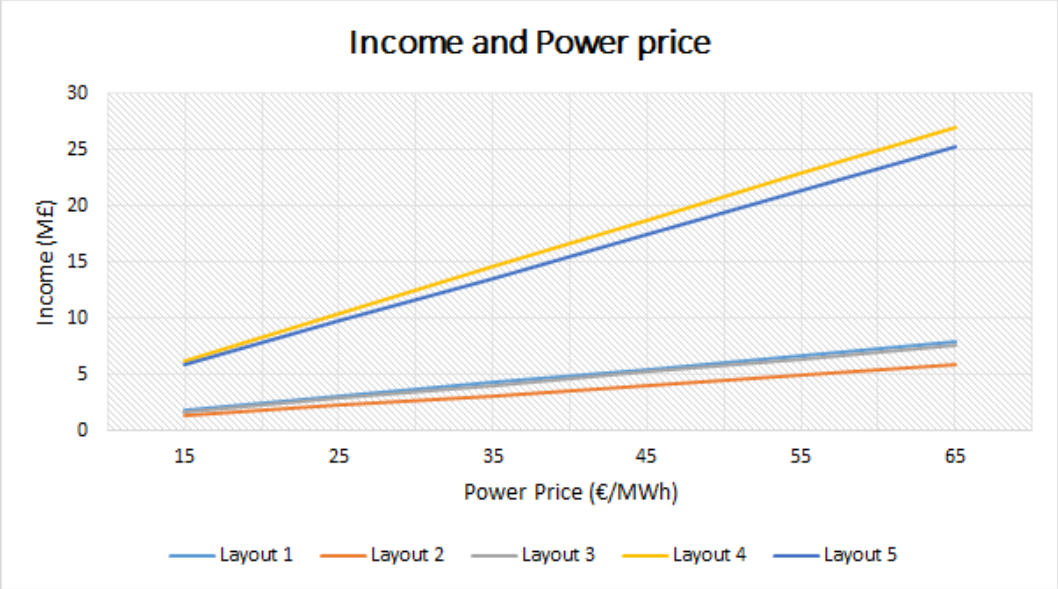

Figure 10.21: The calculated potential income for all layouts with varying energy price.

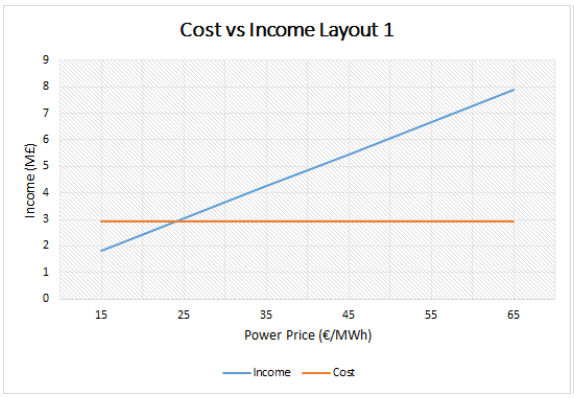

(a) Layout 1.

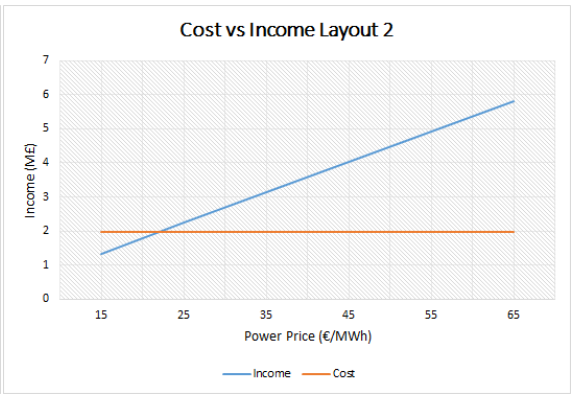

(b) Layout 2.

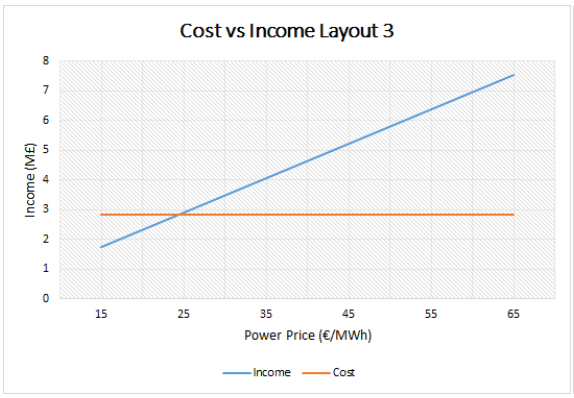

(c) Layout 3.

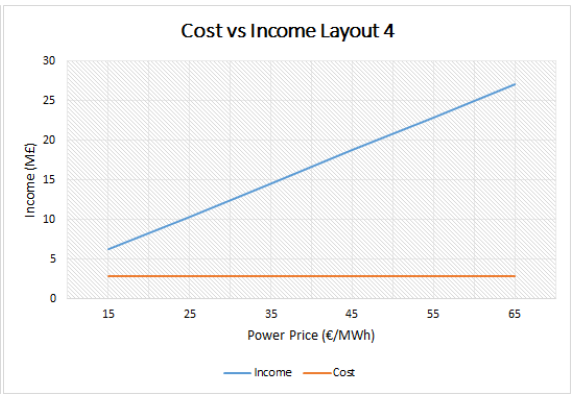

(d) Layout 4.

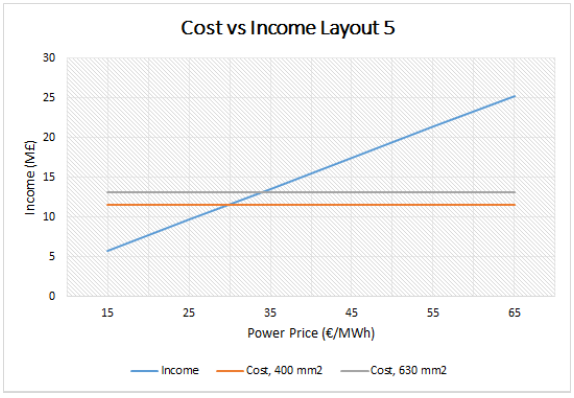

(e) Layout 5.

Figure 10.22: The cost and income with varying energy price.

Chapter 11

Discussion

A comparison is done between the calculated END in the radial system and the END in the different layouts (using the initial input parameters), and is shown in Figure 11.1. The contribution from the different failed components is also illustrated, along with the total END for each system. The calculated ASAI for the different layouts are shown in Table 11.1.

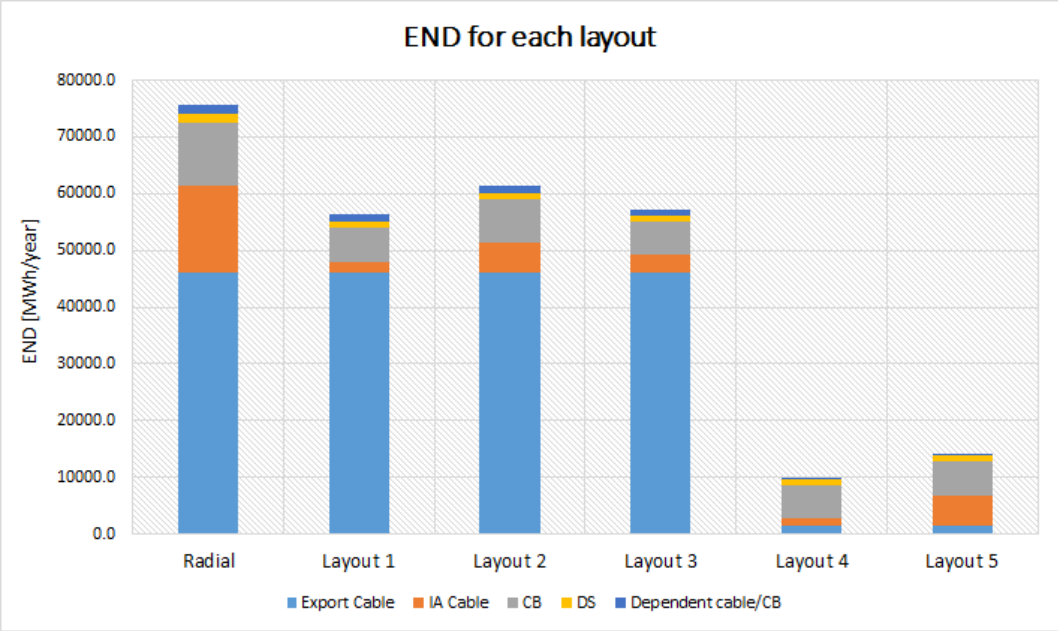

Figure 11.1: The calculated END in the different layouts.

A summary of the results from the economic analysis is shown in Figure 11.2, where the cost of both alternatives in Layout 5 is shown with a constant income.

The profit (the income minus the cost) for each layout is shown in Table 11.2.

	Radial	Layout 1	Layout 2	Layout 3	Layout 4	Layout 5
ASAI	0.97276	0.97968	0.97786	0.97936	0.99649	0.99493

Table 11.1: The calculated ASAI for the different layouts.

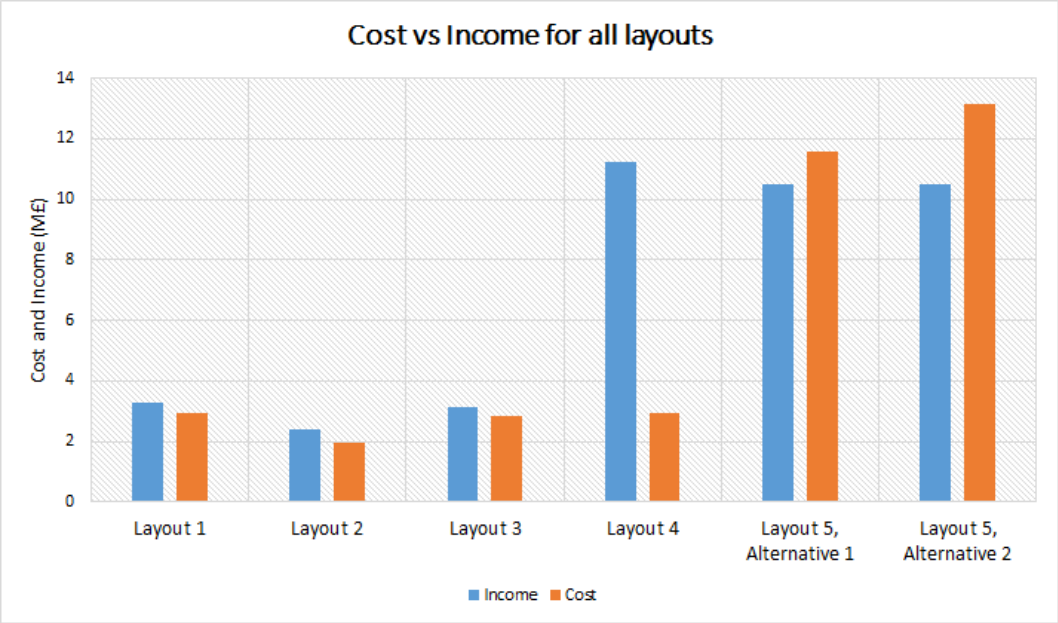

Figure 11.2: The calculated cost and income in the different layouts.

	Layout 1	Layout 2	Layout 3	Layout 4	Layout 5, Alt. 1	Layout 5, Alt. 2
Profit [£]	364,174	454,602	296,773	8,318,046	- 1,070,833	- 2,670,833

Table 11.2: The profit for each layout using energy price equal to 27 €/MWh.

The radial system has clearly higher END than the reserve connection layouts, shown in Figure 11.1. It has the advantage of being simple and easy to control, but is less reliable than the alternative layouts. No additional costs have to be invested in this system, but a lot of money may be lost if failures occur, especially in the export cables or other components near the OSP.

Layout 1 is a system with reduced energy not delivered, due to its six End connections. From the results of the economic analysis, shown in Figure 11.2 and

Table 11.2, this also is proven to be a profitable layout comparing the costs and income of the system. If looking only on the reliability and economy, this is clearly a beneficial layout when it comes to delivered energy to the PCC onshore. When doing the power flow analysis however, this system had many overloaded cables during full production, due to the End connections used. Only with a power production below 60 % could this system be operated safely with a worst possible fault. Using the power curve and Weibull distribution introduced in Chapter 3, the probability of a production level below 60 % (wind speeds equal to 10 m/s) is around 60 %. If we also include the probability of a manageable failure during full production, discussed at the end in Section 10.2, the probability of a manageable fault regardless of wind speed, will increase. To make this system resistible for all faults and wind speeds, two actions may be done: install higher rated cables or install a control system in each wind turbine, to limit the power production in the affected wind turbine generators. Installation of new IA cables may be very expensive, and is more an alternative in wind farms not yet been built. The control systems however, may be an alternative solution due to the components already installed in the nacelle. Since the power production already is being limited when the wind speed is at rated wind speeds, maybe there exist (or could be developed) a control system that limit the power production when a 60 % production level is reached, at wind speeds equal to 10 m/s. It is important to clarify, that only the two radials affected by the failure have to reduce their production level, not the entire system! Another alternative is to shut down some of the turbines in the faulty radial, to reduce the power flow in the reserve connection. As discussed in Section 10.2, the operational radial may handle two turbines from the faulty radial during full production, and to stop any production beyond this level may be a good solution to prevent overloading of cables.

Layout 2 has a higher END and lower ASAI than Layout 1, which means that this system is less reliable. This layout has less reserve connections, which reduces the cost of the system, and from Table 11.2, one may see that the profit is higher for this system than Layout 1. Layout 2 has four End connections, and will have the same power flow problems as in the End connections in Layout 1: for worst case failures, the system is only safe below a 60 % production level. The probability of this production level is the same as before, equal to 60 %. To make this system resistible to all failures and wind speeds, the same actions may be taken as in Layout 1, installation of higher rated cables or control systems, or limit the power production by stopping some of the turbines in the faulty radial.

Layout 3 has a higher reliability than Layout 2, but lower than Layout 1, as expressed in both the END and the ASAI. The cost for this system is around the same as Layout 1 (100,000 £ less), but the income is lower, which lead to a

lower profit, as shown in Table 11.2. Also this system is safely operated for all wind speeds only below a 60 % production level. To make this system safe for all wind speeds the installation of higher rated cables is a better alternative in this system, than in the previous layouts. As shown in the power flow analysis, fewer cables were overloaded, and the amount of higher rated cables needed, is therefore also reduced. When using Split connections, only the cables located from the connection point in the middle of the radial and in to the OSP, needs to be "upgraded" to higher rated cables. Still, this could be very expensive, and would increase the investment cost of the system significantly. Control of the power production in the affected radials is also an alternative action to limit the power flow, as in the previous systems.

Layout 4 has much lower END because of the reserve connections between Area 1 and 2, in addition to having connections between the IA cables. Both the END from the export cables and the IA cables is significantly reduced, and looking only on the reliability analysis, this seems to be a good solution. From the economy analysis, this is also the layout with the highest profit because of the large income. From the power flow analysis however, this is a bad solution. The cables between the areas are highly overloaded, and the production level has to be under 30 %, for this system to operate safely with a worst case failure. The probability of power production below this level (wind speeds equal to 7.5 m/s) is around 40 %. For this layout then to be safely operated during a worst case failure (failure in export cable at full production), control of the power production in the entire OSP connected to the faulty cable may be needed. This could be done either by lowering the production level for all the turbines connected to the OSP below 30 %, or by stopping many turbines entirely until the failure is repaired. Under full production many cables are overloaded due to the large amount of power being transferred, and it would be costly to invest in new cables with much higher capacities.

Layout 5 is the only layout with negative profit, for both cable alternatives between the OSPs. The END is significantly lower than the radial system and Layout 1-3, which means that a lot of power may be saved by installing the reserve connections in this system. However, the cost of the direct connection between the two OSPs is too expensive, for both the 33kV and the 132 kV cable, due to the length of the cable installed (16km). The results from the power flow analysis shows that the 132 kV cable may be handled safely at a 60 % production level during a worst case failure, while the 33 kV cable is down in 25 % production. For this system to be safe during full production, control of the production level would be the best alternative. Installation of higher rated export cables would increase the cost of the system significantly, and it is hard to imagine this system then being profitable.

The sensitivity analysis shows that the results are very much depending on the

failure rate, the cable repair times and the energy price. The END is not varying a lot with the manual disconnecting time and the installment of the DSs. As the failure rate increases, all layout's potential income also increase, and the systems become more profitable, even Layout 5. When increasing the repair times in the IA and export cables, again all layouts experience an increase in the income and profit. For lower MTTRs all layouts, except Layout 4, becomes unprofitable. As discussed in Chapter 9, the energy price is an important parameter that may change a lot in the future. All layouts vary with the energy price, especially Layout 4 and 5. As the energy price increases, the incomes are increasing too, and all layouts become profitable. Layout 1-3 are profitable as long as the energy price is above 24 €/MWh. Layout 4 is profitable for all energy prices investigated, and Layout 5 becomes profitable when the price is above 34 €/MWh. For a energy price above 40 €/MWh for example, the profits calculated are shown in Table 11.3. All layouts have now become significantly more profitable, only by increasing the energy price. Especially Layout 5, which before had a negative profit, has now become significantly more profitable. This due to the big output variance related to the change in energy price.

	Layout 1	Layout 2	Layout 3	Layout 4	Layout 5, Alt. 1	Layout 5, Alt. 2
Profit [£]	1,941,591.2	1,617,188.1	1,801,293.7	13,725,105	3,979,507.2	2,379,507.2

Table 11.3: The profit for each layout using energy price equal to 40 €/MWh.

The main results from the different analyses are:

1. Reliability analysis: The biggest reduction of END is when a connection between the two OSPs is installed. The impacts from failures in the export cables are then minimized, and would significantly increase the reliability in the system. If no such connection is possible, the End connection introduced in this master thesis is recommended due to the reduced energy not delivered from the IA system. The Split connection is not as reliable as the End connection, but still an alternative.

2. Power flow analysis: If one is to install a connection between the OSPs a higher rated cable should be installed directly between the OSPs, not indirectly between the IA cables. Of the two IA cable connections presented in this thesis, the End connection is the one with the most overloaded cables, while the Split connection has overloaded cables from the connection point and in to the OSP.

3. Economic analysis: A direct connection between the OSPs is very expensive

due to the length of the cable. The connections between the IA cables are cheaper and may therefore be more profitable.

4. Sensitivity analysis: Of the parameters investigated, the END is varying the most with the failure rate, the MTTR and the energy price. The layouts introduced become better alternatives when using "worst case" failure data, such as high failure rates and long MTTRs. Also an increase in the energy price would lead to the layouts becoming more attractive, especially Layout 4 and 5, where a lot of energy can be saved by installing the reserve connections.

To make a suggestion on an optimal layout, the results from all three analyses should be included and considered. A feasible solution with high reliability and minimal costs is desirable, and Layout 2 is therefore chosen as an alternative layout to the radial system already operational today.

Chapter 12

Conclusion

From the work done in this master thesis, it is concluded that it is beneficial to install reserve connections in the Sheringham Shoal offshore wind farm. After doing a reliability analysis, a power flow analysis and an economic analysis, Layout 2 is considered the best opportunity for the existing layout, due to higher profits and potential manageable power flows. This would require installation of four reserve connections, all End connections, and a control system to prevent the reserve connections from overloading the radials. This control system only has to be installed in the radials connected to a reserve connection, and would have to limit the power production when a 60 % production level is reached. Layout 2 is considered the best alternative because of the increased energy delivered to shore compared to the radial system, the high profits and the limited future costs.

As the demand of electricity is constantly increasing the need for reliable systems becomes critical. When new offshore wind farms are being built, more reliable systems than Layout 2 may therefore also be beneficial, even if the profits calculated in this thesis were lower. From a general perspective, Layout 1 could be considered a good alternative, because of the increased energy delivered to shore. This layout would require higher rating in the IA cables than in the Sheringham Shoal wind farm, which would cause higher supply costs. When building a new wind farm however, these costs are a part of the initial investment cost anyway, and would not lead to a significant increase in the expenses (only 40 £/m difference in the two IA cable types used in Sheringham Shoal).

Also Layout 5, installed with a 132 kV cable between the OSPs, would be an alternative system in the future, if the energy prices are to increase. As shown in this master thesis, the expected energy delivered to shore is highly increased if there exist a connection between the two offshore platforms. Layout 5 would, as

the previous layouts, require a control system or higher rating in the export cables to be entirely safe for all failures and wind speeds.

The three layouts suggested above would lead to higher redundancy in the system and an increase in the reliability, and should therefore not be excluded from future investment alternatives.

Chapter 13

Further Work

In this chapter, the further work is presented. It consists of ideas and tasks that are not a part of the master thesis, but should be investigated when analyzing the benefits of reserve connections.

In this master thesis is the Relrad methodology, with its limitations and simplifications, utilized. It is assumed that only one failure may occur at a time, and that there are no transfer restrictions on the reserve connections. These assumptions should be investigated more in a future analysis. After seeing the amount of overloaded cables in the power flow analysis, one should go back to the reliability analysis and modify the methodology. The energy not delivered should be calculated using the transfer restrictions in the reserve connections and existing IA cables, to get accurate reliability indices. The optimal rating of the IA cables and the reserve connections should also be studied, as they have a big influence on the transfer restrictions and reliability.

It may also be interesting to not only look at the Sheringham Shoal offshore wind farm, but expand the analyzing scope to a more general perspective.

Bibliography

[1] O. Anaya-Lara, D. Campos-Gaona, E. L. Moreno-Goytia, and G. P. Adam. *Offshore Wind Energy Generation: Control, Protection, and Integration to Electrical Systems*. Wiley Blackwell, 2014.

[2] X. Kong and H. Jia. Techno-economic analysis of svc-hvdc transmission system for offshore wind. In *Asia-Pacific Power and Energy Engineering Conference, APPEEC*, 2011.

[3] LORC Knowledge. Sheringham shoal offshore wind farm. Retrieved from: http://www.lorc.dk/offshore-wind-farms-map/sheringham-shoal.

[4] R. Billinton and R. N. Allan. *Reliability Evaluation of Power Systems, second edition*. Plenum Press, New York, 1996.

[5] H. J. Bahirat, B. A. Mork, and H. K. Hoidalen. Comparison of wind farm topologies for offshore applications. In *IEEE Power and Energy Society General Meeting*, 2012.

[6] F. Blaabjerg, F. Iov, Z. Chen, and K. Ma. Power electronics and controls for wind turbine systems. In *2010 IEEE International Energy Conference and Exhibition, EnergyCon 2010*, pages 333–344, 2010.

[7] Renewable UK. Offshore wind energy. Retrieved from: http://www.renewableuk.com/en/renewable-energy/wind-energy/offshore-wind/.

[8] Statkraft. Sheringham shoal wind farm. Retrieved from: http://www.statkraft.com/energy-sources/Power-plants/UK/Sheringham-Shoal/.

[9] Siri Veila. Impacts of interconnecting the wind farm projects within the dogger bank zone, December 2013.

[10] Kari Vingdal. Optimal redundans i dogger bank referansevindpark, June 2015.

[11] H. J. Bahirat, G. H. Kjolle, B. A. Mork, and H. K. Hoidalen. Reliability assessment of dc wind farms. In *IEEE Power and Energy Society General Meeting*, 2012.

[12] G. Kjølle and K. Sand. Relrad - an analytical approach for distribution system reliability assessment. *IEEE Transactions on Power Delivery*, 7(2):809–814, 1992.

[13] R. D. Zimmerman and C. E. Murillo-Sànchez. *MATPOWER 5.1 User's Manual*, March 2015.

[14] B. Frankén. Reliability study, analysis of electrical systems within offshore wind parks. Technical report, Energimyndigheten, Vindforsk and ELFORSK, November 2007. Elforsk report 07:65. Retrieved from: http://www.neplan.ch/wp-content/uploads/2015/01/V-118-R-07-65-Reliability-Windpark.pdf.

[15] M. Nandigam and S. K. Dhali. Optimal design of an offshore wind farm layout. In *SPEEDAM 2008 - International Symposium on Power Electronics, Electrical Drives, Automation and Motion*, 2008.

[16] 4Coffshore. Sheringham shoal offshore wind farm. Retrieved from: http://www.4coffshore.com/windfarms/sheringham-shoal-united-kingdom-uk27.html.

[17] European Wind Energy Association. Wind energy scenarios for 2030, August 2015. Retrieved from: http://www.ewea.org/fileadmin/files/library/publications/reports/EWEA-Wind-energy-scenarios-2030.pdf.

[18] Global Wind Energy Council. Global offshore. Retrieved from: http://www.gwec.net/global-figures/global-offshore/.

[19] G. F. Reed, H. A. Al Hassan, M. J. Korytowski, P. T. Lewis, and B. M. Grainger. Comparison of hvac and hvdc solutions for offshore wind farms with a procedure for system economic evaluation. In *2013 IEEE Energytech, Energytech 2013*, 2013.

[20] J. Green, A. Bowen, L. J. Fingersh, and Y. H. Wan. Electrical collection and transmission systems for offshore wind power. In *Offshore Technology Conference, Proceedings*, volume 4, pages 2215–2221, 2007.

[21] A. Ferguson, P. de Villiers, B. Fitzgerald, and J. Matthiesen. Benefits of moving the inter-array voltage from 33 kv to 66 kv ac for large offshore wind farms, 2012. Carbon Trust, London, United Kingdom. Retrieved

from: http://wiki-cleantech.com/wind-energy/benefits-in-moving-the-inter-array-voltage-from-33-kv-to-66-kv-ac-for-large-offshore-wind-farms.

[22] F. Deng and Z. Chen. Operation and control of a dc-grid offshore wind farm under dc transmission system faults. *IEEE Transactions on Power Delivery*, 28(3):1356–1363, 2013.

[23] W. S. Moon, J. C. Kim, A. Jo, and J. N. Won. Grid optimization for offshore wind farm layout and substation location. In *IEEE Transportation Electrification Conference and Expo, ITEC Asia-Pacific 2014 - Conference Proceedings*, 2014.

[24] H. Tiegna, Y. Amara, G. Barakat, and B. Dakyo. Overview of high power wind turbine generators. In *2012 International Conference on Renewable Energy Research and Applications, ICRERA 2012*, 2012.

[25] The Swiss Windpower Data Website. Weibull distribution. Retrieved from: http://wind-data.ch/tools/weibull.php?lng=en.

[26] REUK.co.uk The Renewable Energy Website. Wind speed distribution weibull. Retrieved from: http://www.reuk.co.uk/Wind-Speed-Distribution-Weibull.htm.

[27] K. Ulgen and A. Hepbasli. Determination of weibull parameters for wind energy analysis of izmir, turkey. *International Journal of Energy Research*, 26(6):495–506, 2002.

[28] 4Coffshore. Global offshore wind speed rankings. Retrieved from: http://www.4coffshore.com/windfarms/windspeeds.aspx.

[29] J. J. Naresky. Reliability definitions. *IEEE Transactions on Reliability*, R-19(4):198–200, 1970.

[30] *Lecture notes in the course ET8207 Power System Reliability*, 2015.

[31] D. W. Forrest, P. F. Albrecht, R. N. Allan, M. P. Bhavaraju, R. Billinton, G. L. Landgren, M. F. McCoy, and N. D. Reppen. Proposed terms for reporting and anlyzing outages of electrical transmission and distribution facilities. *IEEE Transactions on Power Apparatus and Systems*, PAS-104(2):337–348, 1985.

[32] A. Underbrink, J. Hanson, A. Osterholt, and W. Zimmermann. Probabilistic reliability calculations for the grid connection of an offshore wind farm. In *2006 9th International Conference on Probabilistic Methods Applied to Power Systems, PMAPS*, 2006.

[33] I. Athamna, M. Zdrallek, E. Wiebe, and F. Koch. Sensitivity analysis of offshore wind farm topology based on reliability calculation. In *2014 International Conference on Probabilistic Methods Applied to Power Systems, PMAPS 2014 - Conference Proceedings*, 2014.

[34] Nexans. Submarine power cables. Retrieved from: http://www.nexans.no/Germany/2013/SubmPowCables_FINAL_10jun13_engl.pdf.

[35] M. H. Haque. Efficient load flow method for distribution systems with radial or mesh configuration. *IEE Proceedings: Generation, Transmission and Distribution*, 143(1):33–38, 1996.

[36] M. E. Baran and F. F. Wu. Optimal sizing of capacitors placed on a radial distribution system. *IEEE Transactions on Power Delivery*, 4(1):735–743, 1989.

[37] National Grid. 2015 electricity ten year statement, appendix e technology, 2015. Retrieved from: http://www2.nationalgrid.com/UK/Industry-information/Future-of-Energy/Electricity-Ten-Year-Statement/.

[38] APX. Power spot exchange. Retrieved from: https://www.apxgroup.com/.

[39] R. Martin, I. Lazakis, S. Barbouchi, and L. Johanning. Sensitivity analysis of offshore wind farm operation and maintenance cost and availability. *Renewable Energy*, 85:1226–1236, 2016.

[40] Worldwatch Institute Vision for a Sustainable World. Energy agency predicts high prices in future. Retrieved from: http://www.worldwatch.org/node/5936.

[41] UK Power The energy price comparison services. Energy price forecast. Retrieved from: https://www.ukpower.co.uk/home_energy/future-gas-electricity-price-forecast.

Appendix A

The Power Curve Data

Wind Speeds [m/s]	Power generation [kW]	Wind Speeds [m/s]	Power generation [kW]
25	3600	12	3488
24	3600	11	3082
23	3600	10	2432
22	3600	9	1778
21	3600	8	1243
20	3600	7	824
19	3600	6	507
18	3600	5	276
17	3600	4	131
16	3600	3	0
15	3600	2	0
14	3600	1	0
13	3591	0	0

Table A.1: The power curve data for the wind turbine generators in The Sheringham Shoal Offshore Wind Farm.

Appendix B

The Weibull Distribution Data

Wind Speeds, v [m/s]	f(v)	F(v)
0.0	0	0
0.5	0.009404	0.002354
1.0	0.01868	0.009382
1.5	0.02768	0.02099
2.0	0.03631	0.03700
2.5	0.04443	0.05721
3.0	0.05196	0.08133
3.5	0.05879	0.1091
4.0	0.06485	0.1400
4.5	0.07009	0.1738
5.0	0.07447	0.2099
5.5	0.07796	0.2481
6.0	0.08056	0.2878
6.5	0.08228	0.3285
7.0	0.08315	0.3699
7.5	0.08321	0.4115
8.0	0.08250	0.4530
8.5	0.08110	0.4939
9.0	0.07907	0.5340
9.5	0.07649	0.5729
10.0	0.07345	0.6104
10.5	0.07002	0.6463
11.0	0.06629	0.6804
11.5	0.06233	0.7125
12.0	0.05822	0.7427
12.5	0.05403	0.7707

Wind Speeds, v [m/s]	f(v)	F(v)
13.0	0.04983	0.7967
13.5	0.04567	0.8206
14.0	0.04160	0.8424
14.5	0.03767	0.8622
15.0	0.03391	0.8801
15.5	0.03035	0.8961
16.0	0.02701	0.9105
16.5	0.02390	0.9232
17.0	0.02103	0.9344
17.5	0.01840	0.9442
18.0	0.01601	0.9528
18.5	0.01385	0.9603
19.0	0.01192	0.9667
19.5	0.01020	0.9722
20.0	0.008688	0.9770
20.5	0.007358	0.9810
21.0	0.006198	0.9843
21.5	0.005194	0.9872
22.0	0.004330	0.9896
22.5	0.003590	0.9915
23.0	0.002962	0.9932
23.5	0.002431	0.9945
24.0	0.001984	0.9956
24.5	0.001612	0.9965
25.0	0.001302	0.9972

Appendix C

Results From the Load Point Consideration Example

C.1 Negative Load Consideration

The Radial System

WTG1			
	λ [failures/ year]	Unavailability [hours/year]	Repair time [hours/failure]
L1	0.0094	13.536	1440
L2	0.0094	0.0094	1
L3	0.0094	0.0094	1
L4	0.0094	0.0094	1
L5	0.0094	0.0094	1
Sum/Average	0.0470	13.574	288.81
Energy not delivered from WTG1 [MWh/year]			27.147

WTG2			
	λ [failures/ year]	Unavailability [hours/year]	Repair time [hours/failure]
L1	0.0094	13.536	1440
L2	0.0094	13.536	1440
L3	0.0094	0.0094	1
L4	0.0094	0.0094	1
L5	0.0094	0.0094	1
Sum/Average	0.0470	27.100	576.60
Energy not delivered from WTG2 [MWh/year]			54.200

WTG3			
	λ [failures/ year]	Unavailability [hours/year]	Repair time [hours/failure]
L1	0.0094	13.536	1440
L2	0.0094	13.536	1440
L3	0.0094	13.536	1440
L4	0.0094	0.0094	1
L5	0.0094	0.0094	1
Sum/Average	0.0470	40.627	864.40
Energy not delivered from WTG3 [MWh/year]			81.254

WTG4			
	λ [failures/ year]	Unavailability [hours/year]	Repair time [hours/failure]
L1	0.0094	13.536	1440
L2	0.0094	13.536	1440
L3	0.0094	13.536	1440
L4	0.0094	13.536	1440
L5	0.0094	0.0094	1
Sum/Average	0.0470	54.153	1152.2
Energy not delivered from WTG4 [MWh/year]			108.31

WTG5			
	λ [failures/ year]	Unavailability [hours/year]	Repair time [hours/failure]
L1	0.0094	13.536	1440
L2	0.0094	13.536	1440
L3	0.0094	13.536	1440
L4	0.0094	13.536	1440
L5	0.0094	13.536	1440
Sum/Average	0.0470	67.680	1440.0
Energy not delivered from WTG5 [MWh/year]			135.36

	END [MWh/year]
WTG 1	27.147
WTG 2	54.200
WTG 3	81.254
WTG 4	108.31
WTG 5	135.36
Total END radial system	406.27

The Radial Loop System

WTG1			
	λ [failures/ year]	Unavailability [hours/year]	Repair time [hours/failure]
L1	0.0094	0.0094	1
L2	0.0094	0.0094	1
L3	0.0094	0.0094	1
L4	0.0094	0.0094	1
L5	0.0094	0.0094	1
Sum/Average	0.047	0.047	1
Energy not delivered from WTG1 [MWh/year]			0.094

WTG2			
	λ [failures/ year]	Unavailability [hours/year]	Repair time [hours/failure]
L1	0.0094	0.0094	1
L2	0.0094	0.0094	1
L3	0.0094	0.0094	1
L4	0.0094	0.0094	1
L5	0.0094	0.0094	1
Sum/Average	0.047	0.047	1
Energy not delivered from WTG2 [MWh/year]			0.094

WTG3			
	λ [failures/ year]	Unavailability [hours/year]	Repair time [hours/failure]
L1	0.0094	0.0094	1
L2	0.0094	0.0094	1
L3	0.0094	0.0094	1
L4	0.0094	0.0094	1
L5	0.0094	0.0094	1
Sum/Average	0.047	0.047	1
Energy not delivered from WTG3 [MWh/year]			0.094

WTG4			
	λ [failures/ year]	Unavailability [hours/year]	Repair time [hours/failure]
L1	0.0094	0.0094	1
L2	0.0094	0.0094	1
L3	0.0094	0.0094	1
L4	0.0094	0.0094	1
L5	0.0094	0.0094	1
Sum/Average	0.047	0.047	1
Energy not delivered from WTG4 [MWh/year]			0.094

WTG5			
	λ [failures/ year]	Unavailability [hours/year]	Repair time [hours/failure]
L1	0.0094	0.0094	1
L2	0.0094	0.0094	1
L3	0.0094	0.0094	1
L4	0.0094	0.0094	1
L5	0.0094	0.0094	1
Sum/Average	0.047	0.047	1
Energy not delivered from WTG5 [MWh/year]			0.094

	END [MWh/year]
WTG 1	0.094
WTG 2	0.094
WTG 3	0.094
WTG 4	0.094
WTG 5	0.094
Total END radial loop system	0.47

C.2 Lumped Load Consideration

Radial System

	λ [failures/ year]	Unavailability [hours/year]	Repair time [hours/failure]	Fraction of lost production [%]	Lost production [MW]	END [MWh/year]
L1	0.0094	13.536	1440	100	10	135.36
L2	0.0094	0.0094/13.563	1/1440	100/80	10/8	108.60
L3	0.0094	0.0094/13.563	1/1440	100/60	10/6	81.472
L4	0.0094	0.0094/13.563	1/1440	100/40	10/4	54.346
L5	0.0094	0.0094/13.563	1/1440	100/20	10/2	27.220
Total energy not delivered [MWh/year]						407.00

Radial Loop System

	λ [failures/ year]	Unavailability [hours/year]	Repair time [hours/failure]	Fraction of lost production [%]	Lost production [MW]	ENS [MWh/year]
L1	0.0094	0.0094	1	100	10	0.094
L2	0.0094	0.0094	1	100	10	0.094
L3	0.0094	0.0094	1	100	10	0.094
L4	0.0094	0.0094	1	100	10	0.094
L5	0.0094	0.0094	1	100	10	0.094
Total energy not supplied [MWh/year]						0.47

Appendix D

Submarine Cable Data Sheets Nexans, 132kV and 33 kV

The data sheets on the next four pages show data for both a 132 kV single core submarine cable, and a 33 kV three core submarine cable. They are used to find the capacities in the cables, which are important parameters in the power flow analysis. The data sheets for the 132 kV and the 33 kV cables are retrieved from:

http://www.nexans.de/eservice/Germany-en/navigate_218098/2XS_FL_2Y_RM_76_132_145_kV.html

and

http://www.nexans.ro/eservice/Romania-en/navigate_222837/2XS_FL_2YRAA_RM_19_33_36_kV.html

Nexans

Contact
High Voltage Cables and Systems
110-500kV
Phone: +49 511 676 3364
hv-team.nd@nexans.com

Cu 132kV Al-PE sheath

76/132 (145)kV XLPE Cable, Cu-Screen, Al-laminated PE sheath

Single core XLPE insulated cable, screen area longitudinally and radially watertight

Description

Stranded copper conductor class 2 according to IEC 60228, semi conducting conductor screen, insulation of cross-linked polyethylene (XLPE), semi conducting insulation screen, semi conducting swellable bedding, copper screen, swellable bedding, aluminium tape bonded to PE sheath.

Application in ground, outdoors, in tubes, in water, indoors and in cable ducts.

Optionally aluminium and/or watertight conductor, semiconductive layer on PE sheath, embossed marking or Fiber Optics in screen area for temperature measurement available.

All high voltage cables are manufactured on the basis of specifications and can be adapted to the requirements of the customer. Therefore, all technical information are purely for information purposes and the electrical characteristics are calculated for values which are specified in the data sheets. For your specific requirements and laying arrangements please don't hesitate to contact us.

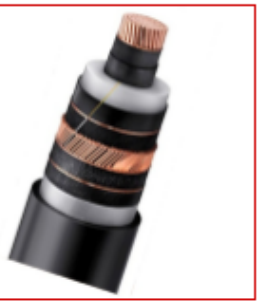

Standards

International IEC 60840

National DIN VDE 0276 part 632

Characteristics

Construction characteristics	
Conductor material	Copper
Insulating material	XLPE
Screen	Copper wire
Outer sheath	HDPE
Lead free	Yes
Halogen free	Yes
Electrical characteristics	
Frequence	50 Hz
Usage characteristics	
Minimum installation temperature	-20 °C
Bending factor when installed	15 (xD)
Bending factor when laying	30 (xD)
Longitudinal water tightness	Yes

Nexans

Contact
High Voltage Cables and Systems
110-500kV
Phone: +49 511 676 3364
hv-team.nd@nexans.com

Cu 132kV Al-PE sheath

Usage characteristics

Max. conductor temperature in service	90 °C

Product List

=Make to order, =In stock

Nexans ref.	Cross section (mm^2)	Nom. insulation thick. (mm)	Screen section (mm^2)	Nom. outer sheath thick. (mm)	Outer Diameter (mm)	Approx. weight (kg/m)	Current rating, buried (A)	Transm. capacity, buried (MVA)
V13224050	240	18.0	50	4.0	70	6	522	119
V13230050	300	18.0	50	4.0	72	7	582	133
V13240050	400	17.0	50	4.0	73	8	654	150
V13250050	500	16.0	50	4.0	74	9	730	167
V13263050	630	15.0	50	4.0	76	10	802	183
V13280050	800	15.0	50	4.0	80	12	889	203
V132100050	1000	15.0	50	4.0	84	14	959	219

= Make to order, = In stock

Lead free
Yes

Halogen free
Yes


Minimum installation temperature
-20 °C


Bending factor installed
15 (xD)


Bending factor when laying
30 (xD)


Longitudinal water tightness
Yes


Max.conductor temp.in service
90 °C

Nexans

Contact
Contact Nexans Romania
Phone: +40 21 206 6020
bogdan.dumitrascu@nexans.com

Submarine cable 33kV

19/33 (36)kV 3 core Copper XLPE cable, Cu-screen, Al/PE-sheath, Armouring

3 core XLPE-insulated cables with PE sheath and armouring, longitudinally and radially watertight

Description

Stranded copper conductor class 2 according to IEC 60228, semi conducting conductor screen, insulation of cross-linked polyethylene (XLPE), semi conducting insulation screen, semi conducting bedding, copper screen with swellable powder, aluminium tape bonded to PE sheath, 3 core layed up, polypropylene yarn bedding, armouring of galvanized steel, hessian tape and polypropylene yarn serving.

Application in water, for example internal and external cabling of offshore windparks, power supply of islands, lighthouses and offshore plattforms.

Optionally watertight conductor with sealing compound, lead sheath and Fiber Optics or Control Cables in the interstices available. Other voltages and EPR insulated cables on request.

All medium voltage submarine cables are manufactured on the basis of specifications and can be adapted to the requirements of the customer. Therefore, all technical information are purely for information purposes and the electrical characteristics are calculated for water saturated seabeds and values which are specified in the data sheets. For your specific requirements and laying depths please don't hesitate to contact us.

Standards

International IEC 60502-2

Characteristics

Construction characteristics	
Number of conductors	3
Type of conductor	Circular compacted stranded
Screen	Copper wire
Armour type	Galvanised round steel wires
Material used for longitudinal water tightness	Swelling powder
Lead free	Yes
Halogen free	Yes
Dimensional characteristics	
Nominal insulation thickness	8.0 mm
Electrical characteristics	
Operating voltage	33 kV
Maximum operating voltage	36 kV
Grounding type	Solid bonding
Load factor	1

Lead free Yes | Halogen free Yes | Ope. volt. 33 kV | Bending factor installed 10 (xD) | Bending factor when laying 15 (xD) | Longitudinal water tightness Yes | Water proof Radial

Nexans

Contact
Contact Nexans Romania
Phone: +40 21 206 6020
bogdan.dumitrascu@nexans.com

Submarine cable 33kV

Electrical characteristics	
Thermal soil resistivity wet zone	0.7 K*m/W
Usage characteristics	
Number of systems	1
Laying depth, center of system	1000 mm
Ambient ground temperature	15 °C
Bending factor when installed	10 (xD)
Bending factor when laying	15 (xD)
Longitudinal water tightness	Yes
Water proof	Radial
Mechanical Resistance	Good mechanical resistance

Product List

=Make to order, =In stock

Nexans ref.	Cross section (mm²)	Screen section (mm²)	Nom. outer sheath thick. (mm)	Outer Diameter (mm)	Approx. weight (kg/m)	Maximum pulling force by laying (kN)	Current rating, buried (A)	Transm. capacity, buried (MVA)
V333x09516	95	16	2.5	100	14.2	81.2	352	20
V333x12016	120	16	2.5	104	15.5	85.5	399	23
V333x15025	150	25	2.5	108	17.3	88.3	446	25
V333x18525	185	25	2.5	111	18.6	91.1	502	28
V333x24025	240	25	2.5	116	21	95.4	581	33
V333x30025	300	25	2.5	121	23.8	106.8	652	37
V333x40035	400	35	2.5	130	28.3	120.8	726	41
V333x50035	500	35	2.6	137	33.4	75.6	811	46
V333x63035	630	35	2.7	145	39.1	151.3	904	52
V333x80035	800	35	2.9	157	48.9	198.6	993	57

= Make to order, = In stock

Lead free
Yes

Halogen free
Yes


Ope. volt.
33 kV


Bending factor installed
10 (xD)


Bending factor when laying
15 (xD)


Longitudinal water tightness
Yes


Water proof
Radial

Appendix E

The IA Cables in the Sheringham Shoal Offshore Wind Farm

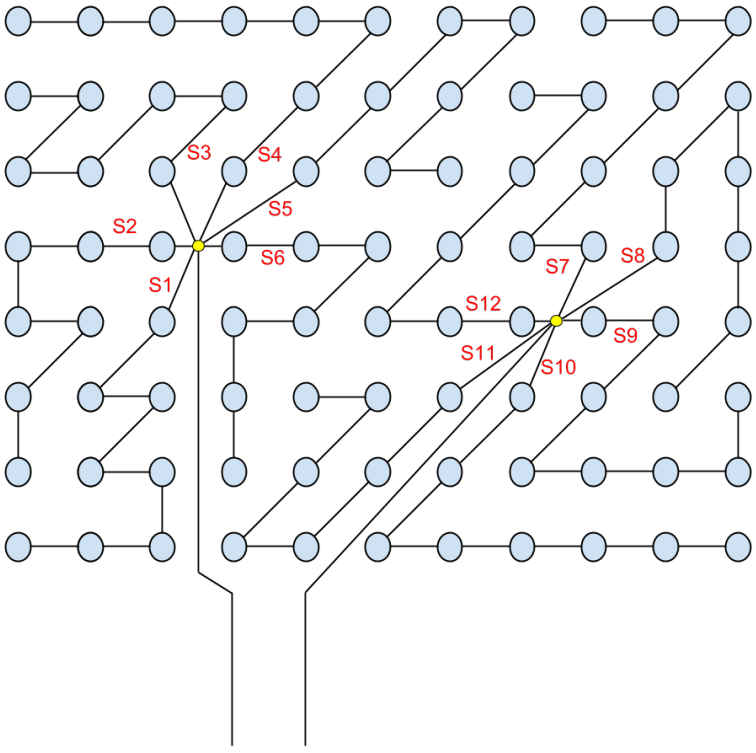

Figure E.1: Illustration of the IA radials, S1-S12.

		L1	L2	L3	L4	L5	L6	L7	L8
String	S1	0.7099	0.8127	0.8980	0.8127	0.8980	1.055	0.8980	0.8980
	S2	0.6102	0.8980	0.8980	1.055	0.8980	0.8127	1.055	
	S3	1.504	0.8127	0.8980	0.8127	0.8980	0.8127	0.8980	
	S4	0.9786	0.8127	0.8127	0.8980	0.8980	0.8980	0.8980	0.8980
	S5	1.020	0.8127	0.8127	0.8980	0.8127	0.8127	0.8980	
	S6	0.4179	0.8980	0.8980	0.8127	0.8980	1.055	1.055	
	S7	0.7518	0.8980	0.8127	0.8127	0.8127	0.8980	0.8180	
	S8	0.8888	1.055	0.8127	1.055	1.055	1.055	0.8127	
	S9	0.4914	0.8980	0.8127	0.8127	0.8980	0.8980	0.8980	1.055
	S10	0.9367	0.8127	0.8127	0.8980	0.8980	0.8980	0.8980	0.8980
	S11	1.084	0.8127	0.8127	0.8980	0.8127	0.8127	0.2980	
	S12	0.5347	0.8980	0.8980	0.8127	0.8127	0.8127	0.8980	

Table E.1: The length of each cable in the strings S1-S12. L1 is the cable closest to the OSP.

Appendix F

Power Flow Calculations

F.1 Layout 1

$P_{gen} = 100$ %:

Faulty connection	Reserve connection	Type of connection	P_{load} (MW)	P_{loss} (MW)	Cables with exceeding power	S_{cap} (MVA)	$P_{ex.cable}$ (MW)
OSP1 - D3	A1 - A2	End	310.5	5.33	OSP1 - C3	41	51.6
					C3 - D2	41	48.2
					D2 - C2	28	45.1
					C2 - B3	28	41.8
					B3 - A3	28	38.6
					A3 - B2	28	35.2
					B2 - A2	28	31.8
					A1 - A2 (res.)	28	28.2
OSP1 - C5	A7 - A8	End	310.5	5.18	OSP1 - C4	41	50.8
					C4 - B4	41	47.4
					B4 - A4	28	44.2
					A4 - A5	28	41.1
					A5 - B5	28	37.8
					B5 - A6	28	34.4
					A6 - A7	28	31.1
					A7 - A8 (res.)	28	27.7

Faulty connection	Reserve connection	Type of connection	P_{load} (MW)	P_{loss} (MW)	Cables with exceeding power	S_{cap} (MVA)	$P_{ex.cable}$ (MW)
OSP1 - E3	G3 - F4	Split	312.5	3.82	OSP1 - D4	41	49.3
					D4 - E4	41	45.9
					E4 - F4	28	42.7
OSP2 - I4	K1 - K2	Split	312.5	3.78	OSP2 - J4	41	49.2
					J4 - J3	41	45.9
					J3 - K2	28	42.7
OSP2 - I5	K7 - K8	Split	311	5.36	OSP2 - H6	41	55.0
					H6 - G7	41	51.7
					G7 - F8	41	48.3
					F8 - G8	28	45.1
					G8 - H8	28	41.9
					H8 - I8	28	38.7
					I8 - J8	28	35.3
					J8 - K8	28	32.0
					K7 - K8 (res.)	28	28.5
OSP2 - H5	E6 - F5	Split	311.5	4.64	OSP2 - G6	41	48.7
					G6 - F7	41	45.2
					F7 - E8	28	42.0
					E8 - D8	28	38.7
					D8 - E7	28	35.4
					E7 - F6	28	32.0
					F6 - E6	28	28.6

P_{gen} = 70 %:

Faulty connection	Reserve connection	Type of connection	P_{load} (MW)	P_{loss} (MW)	Cables with exceeding power	S_{cap} (MVA)	$P_{ex.cable}$ (MW)
OSP1 - D3	A1 - A2	End	217.5	3.73	D2 - C2	28	31.5
					C2 - B3	28	29.3
					B3 - A3	28	27.0
OSP1 - C5	A7 - A8	End	217.5	3.66	B4 - A4	28	31.2
					A4 - A5	28	29.0
					A5 - B5	28	26.7
OSP1 - E3	G3 - F4	Split	218.5	2.68	E4 - F4	28	29.9
OSP2 - I4	K1 - K2	Split	218.5	2.63	J3 - K2	28	29.7
OSP2 - I5	K7 - K8	Split	217.5	3.75	OSP2 - H6	41	38.5
					H6 - G7	41	36.2
					F8 - G8	28	31.6
					G8 - H8	28	29.3
					H8 - I8	28	27.1
OSP2 - H5	E6 - F5	Split	218	3.24	F7 - E8	28	29.4
					E8 - D8	28	27.1

P_{gen} = 60 %:

Faulty connection	Reserve connection	Type of connection	P_{load} (MW)	P_{loss} (MW)	Cables with exceeding power	S_{cap} (MVA)	$P_{ex.cable}$ (MW)
OSP1 - D3	A1 - A2	End	186.5	3.20	OSP1 - C3	41	31.0
					C3 - D2	41	28.9
					D2 - C2	28	27.0
					C2 - B3	28	25.1
					B3 - A3	28	23.1
					A3 - B2	28	21.1
					B2 - A2	28	19.1
					A1 - A2 (res.)	28	16.9

Faulty connection	Reserve connection	Type of connection	P_{load} (MW)	P_{loss} (MW)	Cables with exceeding power	S_{cap} (MVA)	$P_{ex.cable}$ (MW)
OSP1 - C5	A7 - A8	End	186.5	3.13	OSP1 - C4	41	30.6
					C4 - B4	41	28.5
					B4 - A4	28	26.6
					A4 - A5	28	24.8
					A5 - B5	28	22.8
					B5 - A6	28	20.8
					A6 - A7	28	18.8
					A7 - A8 (res.)	28	16.7
OSP1 - E3	G3 - F4	Split	187.5	2.29	OSP1 - D4	41	29.6
					D4 - E4	41	27.6
					E4 - F4	28	25.6
OSP2 - I4	K1 - K2	Split	187.5	2.26	OSP2 - J4	41	29.5
					J4 - J3	41	27.4
					J3 - K2	28	25.5
					K1 - K2 (res.)	28	14.8
OSP2 - I5	K7 - K8	Split	186.5	3.21	OSP2 - H6	41	33.0
					H6 - G7	41	31.0
					G7 - F8	41	29.0
					F8 - G8	28	27.1
					G8 - H8	28	25.2
					H8 - I8	28	23.2
					I8 - J8	28	21.2
					J8 - K8	28	19.2
					K7 - K8 (res.)	28	17.1
OSP2 - H5	E6 - F5	Split	187	2.78	OSP2 - G6	41	29.2
					G6 - F7	41	27.2
					F7 - E8	28	25.2
					E8 - D8	28	23.2
					D8 - E7	28	21.2
					E7 - F6	28	19.2
					F6 - E6	28	17.2

F.2 Layout 2

$P_{gen} = 100$ %:

Faulty connection	Reserve connection	Type of connection	P_{load} (MW)	P_{loss} (MW)	Cables with exceeding power	S_{cap} (MVA)	$P_{ex.cable}$ (MW)
OSP1 - D3	A1 - A2	End	310.5	5.33	OSP1 - C3	41	51.6
					C3 - D2	41	48.2
					D2 - C2	28	45.1
					C2 - B3	28	41.8
					B3 - A3	28	38.6
					A3 - B2	28	35.2
					B2 - A2	28	31.8
					A1 - A2 (res.)	28	28.2
OSP1 - C5	A7 - A8	End	310.5	5.18	OSP1 - C4	41	50.8
					C4 - B4	41	47.4
					B4 - A4	28	44.2
					A4 - A5	28	41.1
					A5 - B5	28	37.8
					B5 - A6	28	34.4
					A6 - A7	28	31.1
					A7 - A8 (res.)	28	27.7
OSP2 - I4	H2 - I1	End	311.5	4.67	OSP2 - H5	41	48.2
					H5 - G5	41	44.8
					G5 - F5	28	41.6
					F5 - G4	28	38.3
					G4 - H3	28	34.9
					H3 - I2	28	31.5
					I2 - H2	28	28.1
OSP2 - I5	J6 - K6	End	311	5.42	OSP2 - J4	41	51.4
					J4 - J3	41	48.0
					J3 - K2	28	44.8
					K2 - K3	28	41.7
					K3 - K4	28	38.5
					K4 - K5	28	35.2
					K5 - J6	28	31.8
					K6 - K7 (res.)	28	28.2

$P_{gen} = 70$ %:

Faulty connection	Reserve connection	Type of connection	P_{load} (MW)	P_{loss} (MW)	Cables with exceeding power	S_{cap} (MVA)	$P_{ex.cable}$ (MW)
OSP1 - D3	A1 - A2	End	217.5	3.73	D2 - C2	28	31.5
					C2 - B3	28	29.3
					B3 - A3	28	27.0
OSP1 - C5	A7 - A8	End	217.5	3.66	B4 - A4	28	31.2
					A4 - A5	28	29.0
					A5 - B5	28	26.7
OSP2 - I4	H2 - I1	End	218.0	3.27	G5 - F5	28	29.1
					F5 - G4	28	26.8
OSP2 - I5	J6 - K6	End	217.5	3.80	J3 - K2	28	31.4
					K2 - K3	28	29.2
					K3 - K4	28	26.9

$P_{gen} = 60$ %:

Faulty connection	Reserve connection	Type of connection	P_{load} (MW)	P_{loss} (MW)	Cables with exceeding power	S_{cap} (MVA)	$P_{ex.cable}$ (MW)
OSP1 - D3	A1 - A2	End	186.5	3.20	OSP1 - C3	41	31.0
					C3 - D2	41	28.9
					D2 - C2	28	27.0
					C2 - B3	28	25.1
					B3 - A3	28	23.1
					A3 - B2	28	21.1
					B2 - A2	28	19.1
					A1 - A2 (res.)	28	16.9
OSP1 - C5	A7 - A8	End	186.5	3.13	OSP1 - C4	41	30.6
					C4 - B4	41	28.5
					B4 - A4	28	26.6
					A4 - A5	28	24.8
					A5 - B5	28	22.8
					B5 - A6	28	20.8
					A6 - A7	28	18.8
					A7 - A8 (res.)	28	16.7
OSP2 - I4	H2 - I1	End	187	2.80	OSP2 - H5	41	28.9
					H5 - G5	41	26.9
					G5 - F5	28	25.0
					F5 - G4	28	23.0
					G4 - H3	28	21.0
					H3 - I2	28	18.9
					I2 - H2	28	16.9
OSP2 - I5	J6 - K6	End	186.5	40.08	OSP2 - J4	41	30.8
					J4 - J3	41	28.8
					J3 - K2	28	26.9
					K2 - K3	28	25.0
					K3 - K4	28	23.1
					K4 - K5	28	21.1
					K5 - J6	28	19.1
					J6 - K6 (res.)	28	16.9

F.3 Layout 3

$P_{gen} = 100$ %:

Faulty connection	Reserve connection	Type of connection	P_{load} (MW)	P_{loss} (MW)	Cables with exceeding power	S_{cap} (MVA)	$P_{ex.cable}$ (MW)
OSP1 - C5	A7 - B7	Split	311	4.99	OSP1 - C4	41	51.3
					C4 - B4	41	47.9
					B4 - A4	28	44.8
					A4 - A5	28	41.6
					A5 - B5	28	38.3
					B5 - A6	28	35.0
					A6 - A7	28	31.6
					A7 - B7 (res.)	28	28.2
OSP1 - D3	C2 - D1	Split	312	4.02	OSP1 - C3	41	52.9
					C3 - D2	41	49.5
					D2 - C2	28	46.4
					C2 - D1 (res.)	28	28.5
OSP1 - E3	G3 - F4	Split	312.5	3.82	OSP1 - D4	41	49.3
					D4 - E4	41	45.9
					E4 - F4	28	42.7
OSP2 - I4	K1 - K2	Split	312.5	3.78	OSP2 - J4	41	49.2
					J4 - J3	41	45.9
					J3 - K2	28	42.7
OSP2 - I5	I7 - H8	Split	312.0	4.46	OSP2 - H6	41	55.9
					H6 - G7	41	52.6
					G7 - F8	41	49.2
					F8 - G8	28	46.1
					G8 - H8	28	42.9
					H8 - I7	28	28.7
OSP2 - H5	E6 - F5	Split	311.5	4.64	OSP2 - G6	41	48.7
					G6 - F7	41	45.2
					F7 - E8	28	42.0
					E8 - D8	28	38.7
					D8 - E7	28	35.4
					E7 - F6	28	32.0
					F6 - E6	28	28.6

$P_{gen} = 70$ %:

Faulty connection	Reserve connection	Type of connection	P_{load} (MW)	P_{loss} (MW)	Cables with exceeding power	S_{cap} (MVA)	$P_{ex.cable}$ (MW)
OSP1 - C5	A7 - B7	Split	217.5	3.47	B4 - A4	28	31.2
					A4 - A5	28	29.0
					A5 - B5	28	26.7
OSP1 - D3	C2 - D1	Split	218.5	2.82	D2 - C2	28	32.5
OSP1 - E3	G3 - F4	Split	218.5	2.68	E4 - F4	28	29.9
OSP2 - I4	K1 - K2	Split	218.5	2.63	J3 - K2	28	29.7
OSP2 - I5	H8 - I7	Split	218.0	3.12	OSP2 - H6	41	39.2
					F8 - G8	28	32.3
					G8 - H8	28	30.0
OSP2 - H5	E6 - F5	Split	218	3.24	F7 - E8	28	29.4
					E8 - D8	28	27.1

$P_{gen} = 60$ %:

Faulty connection	Reserve connection	Type of connection	P_{load} (MW)	P_{loss} (MW)	Cables with exceeding power	S_{cap} (MVA)	$P_{ex.cable}$ (MW)
OSP1 - C5	A7 - B7	Split	186.5	2.97	OSP1 - C4	41	30.6
					C4 - B4	41	28.5
					B4 - A4	28	26.6
					A4 - A5	28	24.8
					A5 - B5	28	22.8
					B5 - A6	28	20.8
					A6 - A7	28	18.8
					A7 - B7 (res.)	28	16.7
OSP1 - D3	C2 - D1	Split	187.5	2.41	OSP1 - C3	41	31.8
					C3 - D2	41	29.7
					D2 - C2	28	27.9
					C2 - D1 (res.)	28	17.1
OSP1 - E3	G3 - F4	Split	187.5	2.29	OSP1 - D4	41	29.6
					D4 - E4	41	27.6
					E4 - F4	28	25.6
OSP2 - I4	K1 - K2	Split	187.5	2.26	OSP2 - J4	41	29.5
					J4 - J3	41	27.4
					J3 - K2	28	25.5
					K1 - K2 (res.)	28	14.8
OSP2 - I5	I7 - H8	Split	187.0	2.68	OSP2 - H6	41	33.6
					H6 - G7	41	31.6
					G7 - F8	41	29.5
					F8 - G8	28	27.6
					G8 - H8	28	25.7
					H8 - I7	28	17.2
OSP2 - H5	E6 - F5	Split	187.0	2.78	OSP2 - G6	41	29.2
					G6 - F7	41	27.2
					F7 - E8	28	25.2
					E8 - D8	28	23.2
					D8 - E7	28	21.2
					E7 - F6	28	19.2
					F6 - E6	28	17.2

F.4 Layout 4

$P_{gen} = 100$ %:

Faulty connection	Reserve connection	Type of connection	P_{load} (MW)	P_{loss} (MW)	Cables with exceeding power	S_{cap} (MVA)	$P_{ex.cable}$ (MW)
OSP1 - D3	A1 - A2	End	310.5	5.33	OSP1 - C3	41	51.6
					C3 - D2	41	48.2
					D2 - C2	28	45.1
					C2 - B3	28	41.8
					B3 - A3	28	38.6
					A3 - B2	28	35.2
					B2 - A2	28	31.8
					A1 - A2 (res.)	28	28.2
OSP1 - C5	A7 - A8	End	310.5	5.18	OSP1 - C4	41	50.8
					C4 - B4	41	47.4
					B4 - A4	28	44.2
					A4 - A5	28	41.1
					A5 - B5	28	37.8
					B5 - A6	28	34.4
					A6 - A7	28	31.1
					A7 - A8 (res.)	28	27.7
OSP2 - I4	K1 - K2	Split	312.5	3.78	OSP2 - J4	41	49.2
					J4 - J3	41	45.9
					J3 - K2	28	42.7
OSP2 - I5	K7 - K8	Split	311	5.36	OSP2 - H6	41	55.0
					H6 - G7	41	51.7
					G7 - F8	41	48.3
					F8 - G8	28	45.1
					G8 - H8	28	41.9
					H8 - I8	28	38.7
					I8 - J8	28	35.3
					J8 - K8	28	32.0
					K7 - K8 (res.)	28	28.5

$P_{gen} = 70$ %:

Faulty connection	Reserve connection	Type of connection	P_{load} (MW)	P_{loss} (MW)	Cables with exceeding power	S_{cap} (MVA)	$P_{ex.cable}$ (MW)
OSP1 - D3	A1 - A2	End	217.5	3.73	D2 - C2	28	31.5
					C2 - B3	28	29.3
					B3 - A3	28	27.0
OSP1 - C5	A7 - A8	End	217.5	3.66	B4 - A4	28	31.2
					A4 - A5	28	29.0
					A5 - B5	28	26.7
OSP2 - I4	K1 - K2	Split	218.5	2.63	J3 - K2	28	29.7
OSP2 - I5	K7 - K8	Split	217.5	3.75	OSP2 - H6	41	38.5
					H6 - G7	41	36.2
					F8 - G8	28	31.6
					G8 - H8	28	29.3
					H8 - I8	28	27.1

$P_{gen} = 60$ %:

Faulty connection	Reserve connection	Type of connection	P_{load} (MW)	P_{loss} (MW)	Cables with exceeding power	S_{cap} (MVA)	$P_{ex.cable}$ (MW)
OSP1 - D3	A1 - A2	End	186.5	3.20	OSP1 - C3	41	31.0
					C3 - D2	41	28.9
					D2 - C2	28	27.0
					C2 - B3	28	25.1
					B3 - A3	28	23.1
					A3 - B2	28	21.1
					B2 - A2	28	19.1
					A1 - A2 (res.)	28	16.9
OSP1 - C5	A7 - A8	End	186.5	3.13	OSP1 - C4	41	30.6
					C4 - B4	41	28.5
					B4 - A4	28	26.6
					A4 - A5	28	24.8
					A5 - B5	28	22.8
					B5 - A6	28	20.8
					A6 - A7	28	18.8
					A7 - A8 (res.)	28	16.7
OSP2 - I4	K1 - K2	Split	187.5	2.26	OSP2 - J4	41	29.5
					J4 - J3	41	27.4
					J3 - K2	28	25.5
					K1 - K2 (res.)	28	14.8
OSP2 - I5	K7 - K8	Split	186.5	3.21	OSP2 - H6	41	33.0
					H6 - G7	41	31.0
					G7 - F8	41	29.0
					F8 - G8	28	27.1
					G8 - H8	28	25.2
					H8 - I8	28	23.2
					I8 - J8	28	21.2
					J8 - K8	28	19.2
					K7 - K8 (res.)	28	17.1

F.5 Layout 5

$P_{gen} = 100$ %:

Faulty connection	Reserve connection	Type of connection	P_{load} (MW)	P_{loss} (MW)	Cables with exceeding power	S_{cap} (MVA)	$P_{ex.cable}$ (MW)
OSP1 - D3	A1 - A2	End	310.5	5.33	OSP1 - C3	41	51.6
					C3 - D2	41	48.2
					D2 - C2	28	45.1
					C2 - B3	28	41.8
					B3 - A3	28	38.6
					A3 - B2	28	35.2
					B2 - A2	28	31.8
					A1 - A2 (res.)	28	28.2
OSP1 - C5	A7 - A8	End	310.5	5.18	OSP1 - C4	41	50.8
					C4 - B4	41	47.4
					B4 - A4	28	44.2
					A4 - A5	28	41.1
					A5 - B5	28	37.8
					B5 - A6	28	34.4
					A6 - A7	28	31.1
					A7 - A8 (res.)	28	27.7
OSP2 - I4	H2 - I1	End	311.5	4.67	OSP2 - H5	41	48.2
					H5 - G5	41	44.8
					G5 - F5	28	41.6
					F5 - G4	28	38.3
					G4 - H3	28	34.9
					H3 - I2	28	31.5
					I2 - H2	28	28.1
OSP2 - I5	J6 - K6	End	311	5.42	OSP2 - J4	41	51.4
					J4 - J3	41	48.0
					J3 - K2	28	44.8
					K2 - K3	28	41.7
					K3 - K4	28	38.5
					K4 - K5	28	35.2
					K5 - J6	28	31.8
					K6 - K7 (res.)	28	28.2

$P_{gen} = 70$ %:

Faulty connection	Reserve connection	Type of connection	P_{load} (MW)	P_{loss} (MW)	Cables with exceeding power	S_{cap} (MVA)	$P_{ex.cable}$ (MW)
OSP1 - D3	A1 - A2	End	217.5	3.73	D2 - C2	28	31.5
					C2 - B3	28	29.3
					B3 - A3	28	27.0
OSP1 - C5	A7 - A8	End	217.5	3.66	B4 - A4	28	31.2
					A4 - A5	28	29.0
					A5 - B5	28	26.7
OSP2 - I4	H2 - I1	End	218.0	3.27	G5 - F5	28	29.1
					F5 - G4	28	26.8
OSP2 - I5	J6 - K6	End	217.5	3.80	J3 - K2	28	31.4
					K2 - K3	28	29.2
					K3 - K4	28	26.9

$P_{gen} = 60$ %:

Faulty connection	Reserve connection	Type of connection	P_{load} (MW)	P_{loss} (MW)	Cables with exceeding power	S_{cap} (MVA)	$P_{ex.cable}$ (MW)
OSP1 - D3	A1 - A2	End	186.5	3.20	OSP1 - C3	41	31.0
					C3 - D2	41	28.9
					D2 - C2	28	27.0
					C2 - B3	28	25.1
					B3 - A3	28	23.1
					A3 - B2	28	21.1
					B2 - A2	28	19.1
					A1 - A2 (res.)	28	16.9
OSP1 - C5	A7 - A8	End	186.5	3.13	OSP1 - C4	41	30.6
					C4 - B4	41	28.5
					B4 - A4	28	26.6
					A4 - A5	28	24.8
					A5 - B5	28	22.8
					B5 - A6	28	20.8
					A6 - A7	28	18.8
					A7 - A8 (res.)	28	16.7
OSP2 - I4	H2 - I1	End	187	2.80	OSP2 - H5	41	28.9
					H5 - G5	41	26.9
					G5 - F5	28	25.0
					F5 - G4	28	23.0
					G4 - H3	28	21.0
					H3 - I2	28	18.9
					I2 - H2	28	16.9
OSP2 - I5	J6 - K6	End	186.5	40.08	OSP2 - J4	41	30.8
					J4 - J3	41	28.8
					J3 - K2	28	26.9
					K2 - K3	28	25.0
					K3 - K4	28	23.1
					K4 - K5	28	21.1
					K5 - J6	28	19.1
					J6 - K6 (res.)	28	16.9

Appendix G

Calculations of the Income Used in the Sensitivity Analysis

G.1 Varying the Failure Rate

Failure rate [1/year/km]	Income Layout 1 [M£]	Income Layout 2 [M£]	Income Layout 3 [M£]	Income Layout 4 [M£]	Income Layout 5 [M£]
0.0008	1.138	0.8121	1.174	1.859	1.774
0.0051	2.207	1.613	2.149	6.545	6.131
0.0094	3.276	2.415	3.125	11.23	10.49
0.0137	4.345	3.216	4.100	15.92	14.85
0.0180	5.415	4.017	5.076	20.60	19.20

Table G.1: The income for all layouts with varying failure rate.

G.2 Varying the MTTR

MTTR [h]	Income Layout 1 [M£]	Income Layout 2 [M£]	Income Layout 3 [M£]	Income Layout 4 [M£]	Income Layout 5 [M£]
720/360	2.088	1.524	2.074	5.948	5.577
1440/720	3.276	2.415	3.125	11.23	10.49
2160/1080	4.465	3.305	4.176	16.51	15.40

Table G.2: The income for all layouts with varying MTTR.

G.3 Varying the Manual Disconnecting Time

Manual Disconnecting Time [h]	Income Layout 1 [M£]	Income Layout 2 [M£]	Income Layout 3 [M£]	Income Layout 4 [M£]	Income Layout 5 [M£]
12	3.340	2.442	3.125	11.41	10.65
24	3.276	2.415	3.125	11.23	10.49
36	3.212	2.387	3.124	11.05	10.32
48	3.148	2.360	3.124	10.87	10.16
60	3.085	2.332	3.123	10.69	9.993
72	3.021	2.305	3.123	10.51	9.827

Table G.3: The income for all layouts with varying manual disconnecting time.

G.4 Varying the Cost of Disconnector Switches

Cost per breaker [£]	Total cost DSs [£]
1,000	164,000
2,000	328,000
3,000	492,000
4,000	656,000
5,000	820,000
6,000	984,000
7,000	1,148,000
8,000	1,312,000
9,000	1,476,000
10,000	1,640,000

Table G.4: The total cost of the installed DSs with varying DS cost.